

Functional and structural analysis of
carbonic anhydrases from the filamentous ascomycete
Sordaria macrospora

Dissertation

for the award of the degree

“Doctor rerum naturalium”

of the Georg-August-Universität Göttingen

within the doctoral program *Molecular Biology of Cells*

of the Georg-August University School of Science (GAUSS)

submitted by

Ronny Lehneck

from Jena

Göttingen, 2014

Member of the Thesis Committee:

Prof. Stefanie Pöggeler

Department of Genetics of Eukaryotic Microorganisms
Institute of Microbiology and Genetics

Prof. Gerhard Braus

Department of Microbiology and Genetics
Institute of Microbiology and Genetics

Prof. Heinz Neumann

Department of Applied Synthetic Biology
Institute of Microbiology and Genetics

Members of the Examination Board:

Prof. Ralf Ficner

Department for Molecular Structural Biology
Institute of Microbiology and Genetics

Prof. Kai Heimes

Department of Microbial Cell Biology
Institute of Microbiology and Genetics

PD Dr. Michael Hoppert

Department of General Microbiology
Institute of Microbiology and Genetics

Date of oral examination: 09.04.2014

Affirmation

I hereby declare that this thesis was written independently and with no other sources and aids than quoted.

Göttingen, 20.02.2014

Ronny Lehneck

This doctoral study was performed in the group of Prof. Stefanie Pöggeler in the Department of Genetics of Eukaryotic Microorganisms at Institute of Microbiology and Genetics, Georg-August-University Göttingen

Some parts of the results section of this doctoral study were peer-reviewed and published in the “The FEBS Journal” and some results are currently under revision for publication in the journal “Molecular Microbiology”.

Ronny Lehneck, Piotr Neumann, Daniela Vullo, Skander Elleuche, Claudiu T. Supuran, Ralf Ficner and Stefanie Pöggeler (2014). Crystal structures of two tetrameric β -carbonic anhydrases from the filamentous ascomycete *Sordaria macrospora*. FEBS J DOI: 10.1111/febs.12738, Accepted manuscript online: 7. February 2014

Author contributions to this publication:

Planned experiments: SP, RL, SE, CS, PN

Performed experiments: RL, PN, DV, SE

Analyzed data: RL, PN, RF, SP, CS

Contributed reagents or other essential material: SP, RF, CS, SE

Wrote the paper: RL, SP, PN, CS

Ronny Lehneck, Skander Elleuche, Stefanie Pöggeler (2014). The filamentous ascomycete *Sordaria macrospora* can survive in ambient air without carbonic anhydrases. Mol Microbiol (in revision)

Author contributions to this publication:

Planned experiments: SP, RL, SE

Performed experiments: RL

Analyzed data: RL, SP

Contributed reagents or other essential material: SP, SE

Wrote the paper: RL, SP, SE

I. Table of Contents

| | | |
|-------------|--|-------------|
| I. | Table of Contents..... | i |
| II. | List of figures | v |
| III. | List of Tables..... | vii |
| IV. | List of Abbreviations..... | viii |
| | Summary | 1 |
| | Zusammenfassung | 3 |
| 1. | Introduction | 5 |
| 1.1 | The enzyme carbonic anhydrase | 6 |
| 1.2 | The α-class of carbonic anhydrases | 8 |
| 1.3 | The β-class of carbonic anhydrases | 12 |
| 1.4 | Carbonic anhydrases in the fungal kingdom | 17 |
| 1.5 | <i>Sordaria macrospora</i>: a model organism for fruiting-body development..... | 19 |
| 1.6 | Aim of this thesis..... | 22 |
| 2. | Materials and Methods | 23 |
| 2.1 | Materials..... | 23 |
| 2.1.1 | Strains | 23 |
| 2.1.2 | Plasmids | 26 |
| 2.1.3 | Primers | 27 |
| 2.1.4 | Chemicals and materials | 32 |
| 2.1.5 | Kits..... | 34 |
| 2.1.6 | Enzymes | 34 |
| 2.1.7 | Buffers and solutions | 35 |
| 2.1.8 | Cultivation media..... | 37 |
| 2.2 | Methods | 39 |
| 2.2.1 | Cultivation of organisms..... | 39 |
| 2.2.2 | Preparation and transformation of competent microorganisms | 39 |

| | | |
|------------|---|----|
| 2.2.3 | Crossing of <i>S. macrospora</i> | 41 |
| 2.2.4 | Molecular biology methods | 41 |
| 2.2.4.1 | Preparation of DNA | 41 |
| 2.2.4.1.1 | Isolation of plasmid DNA from <i>E. coli</i> | 41 |
| 2.2.4.1.2 | Isolation of plasmid DNA from <i>S. cerevisiae</i> | 42 |
| 2.2.4.1.3 | Isolation of genomic DNA and RNA from <i>S. macrospora</i> | 42 |
| 2.2.4.2 | Hydrolysis and ligation of nucleic acids | 42 |
| 2.2.4.3 | Purification of nucleic acids..... | 43 |
| 2.2.4.4 | Polymerase chain reaction (PCR) | 43 |
| 2.2.4.5 | Gelelectrophoresis of nucleic acids..... | 44 |
| 2.2.4.6 | Southern blotting and hybridisation | 44 |
| 2.2.4.7 | Synthesis of cDNA and quantitative real-time PCR | 44 |
| 2.2.4.8 | Oligonucleotide synthesis, sequencing and sequence analysis | 45 |
| 2.2.4.9 | Isolation of the <i>S. macrospora</i> gene <i>cas4</i> | 45 |
| 2.2.4.10 | Generation of a <i>S. macrospora cas4</i> deletion strain..... | 45 |
| 2.2.4.11 | Generation of <i>S. macrospora</i> double, triple and quadruple <i>cas</i> deletion strains | 46 |
| 2.2.4.12 | Generation of a <i>S. macrospora cas4</i> complementation strain..... | 47 |
| 2.2.4.13 | Complementation of a haploid Δ nce103 yeast deletion mutant..... | 47 |
| 2.2.4.14 | Morphological investigation of <i>S. macrospora</i> | 48 |
| 2.2.4.15 | Light and fluorescence microscopic investigations | 49 |
| 2.2.4.16 | Localization analysis of CAS4 in <i>S. macrospora</i> | 49 |
| 2.2.4.17 | Deglycosylation of CAS4-GFP..... | 50 |
| 2.2.4.18 | Overexpression of <i>cas</i> genes in <i>E. coli</i> | 50 |
| 2.2.4.18.1 | Construction of <i>E. coli</i> overexpression vectors | 50 |
| 2.2.4.18.2 | Expression of <i>cas</i> genes in <i>E. coli</i> | 51 |
| 2.2.4.18.3 | Purification of CAS proteins..... | 51 |

| | | |
|------------|--|-----------|
| 2.2.5 | Proteinchemistry methods..... | 52 |
| 2.2.5.1 | Determination of protein concentration | 52 |
| 2.2.5.2 | Denaturing polyacrylamide gel electrophoresis (SDS-PAGE) and staining of polyacrylamide-gels | 52 |
| 2.2.5.3 | Western-blot | 53 |
| 2.2.5.4 | Size-exclusion chromatography and MALLS | 53 |
| 2.2.5.5 | Crystallization, data collection and structure determination | 53 |
| 2.2.5.6 | CA activity and inhibition measurements | 54 |
| 2.3 | Measures of safety | 55 |
| 3. | Results..... | 56 |
| 3.1 | Characterization of a putative α-class carbonic anhydrase from <i>S. macrospora</i> | 56 |
| 3.1.1 | Identification of the <i>S. macrospora</i> α -class carbonic anhydrase CAS4 | 56 |
| 3.1.2 | Analysis of the transcriptional expression of <i>cas4</i> during sexual development in ambient air and in 5% CO ₂ | 58 |
| 3.1.3 | Analysis of the N-terminal CAS4 signal peptide and the CAS4 glycosylation pattern | 60 |
| 3.1.4 | Construction of a homokaryotic <i>cas4</i> deletion strain | 63 |
| 3.1.4.1 | Morphological characterization of the <i>S. macrospora</i> Δ <i>cas4</i> strain..... | 65 |
| 3.2 | Construction of double <i>cas</i> gene deletion mutants | 66 |
| 3.3 | Generation of triple <i>cas</i> gene-deletion mutants | 69 |
| 3.4 | Construction of a quadruple <i>cas</i> gene-deletion mutant | 72 |
| 3.5 | Functional characterization of CAS1, CAS2, CAS3 and CAS4..... | 77 |
| 3.5.1 | Complementation of a CA-deficient <i>S. cerevisiae</i> Δ <i>nce103</i> deletion mutant... | 77 |
| 3.5.2 | Analysis of the <i>in-vitro</i> activity and inhibition of CAS1 and CAS2 | 78 |
| 3.6 | Structural characterization of CAS1 and CAS2..... | 80 |
| 3.6.1 | Analysis of the oligomerization state of the plant-type β -CAs CAS1, CAS2 and cab-type β -CA CAS3 by SEC-MALLS..... | 80 |

| | | |
|------------|---|------------|
| 3.6.2 | Analysis of the crystal structure of the plant-like β -CAs CAS1 and CAS2 | 82 |
| 3.6.2.1 | Structural comparison of CAS1 and CAS2..... | 84 |
| 3.6.2.2 | Analysis of the active site organization of CAS1 and CAS2..... | 85 |
| 4. | Discussion | 88 |
| 4.1 | <i>S. macrospora</i> encodes an α-class carbonic anhydrase..... | 88 |
| 4.1.1 | The <i>S. macrospora</i> α -CA is posttranslationally glycosylated and secreted..... | 89 |
| 4.1.2 | The α -CA <i>cas4</i> is expressed mainly during sexual development in ambient air and at day five in 5% CO ₂ | 91 |
| 4.1.3 | CAS4 is involved in vegetative growth and ascospore germination | 92 |
| 4.2 | <i>S. macrospora</i> survives in ambient air without CA | 93 |
| 4.3 | The plant-type β-CAs CAS1 and CAS2 are active enzymes..... | 94 |
| 4.4 | The plant-type β-CAs CAS1 and CAS2 are tetrameric enzymes in crystal and solution..... | 95 |
| 5. | References | 103 |
| 6. | Appendix | 119 |
| 7. | Acknowledgment – Danksagung | 122 |
| 8. | Curriculum vitae | 124 |

II. List of figures

| | |
|--|----|
| Fig. 1: Crystal structure of human CA II..... | 9 |
| Fig. 2: Catalytic and inhibition mechanisms of α -CAs. | 11 |
| Fig. 3: The different oligomeric forms of β -CAs.. | 13 |
| Fig. 4: Typical crystal structure of a β -class CA. | 14 |
| Fig. 5: Organization of the active site of type-I and type-II β -CAs. | 16 |
| Fig. 6: Schematic illustration of CO ₂ sensing and CA regulation in fungi. | 18 |
| Fig. 7: Schematic illustration of the life cycle of <i>Sordaria macrospora</i> | 21 |
| Fig. 8: Multiple sequence alignment of the zinc ion coordinating domain of CAs of the α - class..... | 57 |
| Fig. 9: Expression analysis of the <i>cas4</i> gene by quantitative real-time PCR.. | 59 |
| Fig. 10: Expression analysis of the <i>cas4</i> gene in ambient air and 5% CO ₂ by quantitative real-time PCR.. | 60 |
| Fig. 11: Fluorescence localization of CAS4SS-EGFP-KDEL in <i>S. macrospora</i> | 61 |
| Fig. 12: Western-blot analysis of the localization and glycosylation of CAS4 in <i>S. macrospora</i> | 62 |
| Fig. 13: Construction of a $\Delta cas4$ strain. | 63 |
| Fig. 14: PCR and Southern blot verification of the successful construction of a $\Delta cas4$ strain. | 64 |
| Fig. 15: Phenotypic analysis of wild type and the $\Delta cas4$ strain. | 65 |
| Fig. 16: Comparison of vegetative growth and ascospore germination rate of wild type and the $\Delta cas4$ strain..... | 66 |
| Fig. 17: Comparison of the sexual development of wt and double knock outs..... | 67 |
| Fig. 18: Comparison of vegetative growth and ascospore germination rate of wt and double- deletion mutants..... | 68 |
| Fig. 19: Microscopic analysis of the sexual development of triple knock outs compared to the wt..... | 70 |
| Fig. 20: Comparison of the vegetative growth rate of wt with $\Delta cas1/2$ and triple knock outs. | 71 |
| Fig. 21: Analysis of the germination efficiency of triple knock outs compared to wt.. | 71 |
| Fig. 22: Genetic analysis of the quadruple knockout strain to confirm the gene deletion. | 73 |
| Fig. 23: Vegetative growth rate of <i>S. macrospora</i> wild type and quadruple mutant compared on fructification (SWG) and complete medium (BMM) in ambient air and at 5% CO ₂ | 74 |

| | |
|---|-----|
| Fig. 24: Comparison of the fruiting-body development of the quadruple knock out strain and wt. | 75 |
| Fig. 25: Investigation of the vegetative growth of wild type and quadruple knock out strain in air and in 5% CO ₂ atmosphere.. | 76 |
| Fig. 26: Functional complementation of the haploid <i>S. cerevisiae</i> CA deletion mutant Δ nce103 with <i>cas1</i> , <i>cas2</i> , <i>cas3</i> and <i>cas4</i> of <i>S. macrospora</i> | 77 |
| Fig. 27: Purification of His-CAS1, CAS2-His and CAS3-His..... | 79 |
| Fig. 28: Size-exclusion chromatography of His-CAS1, CAS2-His and CAS3-His..... | 81 |
| Fig. 29: Crystal structures of carbonic anhydrase CAS1 and CAS2. | 83 |
| Fig. 30: Superposition of the monomeric ribbon representation for CAS1 and CAS2 | 84 |
| Fig. 31: Illustration of the active center of CAS1..... | 85 |
| Fig. 32: Illustration of the active center of CAS2..... | 86 |
| Fig. 33: Overlay of the active site of CAS1 and CAS2..... | 87 |
| Fig. 34: Schematic illustration of the putative bicarbonate metabolism in <i>S. macrospora</i> | 90 |
| Fig. 35: Amino-acid sequence alignment of β -CAs from different species. | 97 |
| Fig. 36: Superposition of the active site of type-I and type-II plant-like β -CAs..... | 99 |
| Fig. 37: Detailed view on the C-terminal loop-helix-loop extension of CAS2 and polar contacts to the adjacent subunit..... | 100 |
| Fig. 38: Structure-based sequence alignment of CAS2 with nine other β -CAs.. | 101 |

III. List of Tables

| | |
|--|-----|
| Table 1: Overview of strains used and constructed in this study. | 23 |
| Table 2: Overview of the used and generated plasmids in this study..... | 26 |
| Table 3: Overview of the used oligonucleotides. | 27 |
| Table 4: Composition of PCR reactions for Phusion and Taq-polymerases | 43 |
| Table 5: Composition of SDS-gels..... | 52 |
| Table 6: Overview about the kinetic parameters of different α - and β -class carbonic anhydrases. | 79 |
| Table S1: Data collection and refinement statistics..... | 119 |
| Table S2: Inhibition constants of anionic inhibitors against α -CA isozymes as well as β -CAs. | 120 |

IV. List of Abbreviations

| | |
|-----------|--|
| Å | Ångström |
| aa | amino acids |
| bp | base pair |
| BMM | biomalt maize medium |
| BLAST | basic local alignment search tool |
| BSA | bovine serum albumin |
| CA | carbonic anhydrase |
| cDNA | complementary DNA |
| DIC | differential interference contrast |
| DsRED | encodes red fluorescence protein of <i>Discosoma</i> sp |
| ER | endoplasmic reticulum |
| EGFP | enhanced green fluorescence protein of <i>Aequorea Victoria</i> |
| HCR | high CO ₂ requiring |
| gDNA | genomic DNA |
| kDa | kilo Dalton |
| MTS | mitochondrial target sequence |
| ORF | open-reading frame |
| PAGE | polyacrylamide gel electrophoresis |
| PBS | phosphate buffered saline |
| PCR | polymerase chain reaction |
| qRT-PCR | quantitative real-time PCR |
| RMSD | root-mean-square deviation |
| SD | synthetic dextrose |
| SDS | sodium dodecyl sulfate |
| SEC-MALLS | size exclusion chromatography multi-angle laser light scattering |
| SG | synthetic galactose |
| ssi | single spore isolate |
| SWG | Sordaria Westergaards medium |
| YPD | yeast extract, peptone, dextrose |
| wt | wild type |

Common used abbreviations and units of measurement are not enlisted.

Summary

Carbonic anhydrases (CAs) are metalloenzymes catalyzing the rapid and reversible hydration of carbon dioxide to bicarbonate (hydrogen carbonate) and protons. CAs have been identified in archaea, bacteria and eukaryotes and can be classified into five groups (α , β , γ , δ , ζ) that are unrelated in sequence and structure. The function of the mammalian, prokaryotic and plant α -CAs has been intensively studied but the function of α -CAs in filamentous ascomycetes is mostly unknown. The filamentous ascomycete *Sordaria macrospora* encodes four CAs, three of the β -class (*cas1*, *cas2* and *cas3*) and one of the α -class (*cas4*). The CAS4 protein exhibits a functional N-terminal signal peptide for translocation into the endoplasmic reticulum and is posttranslationally glycosylated and targeted to the supernatant. The knockout strain $\Delta cas4$ had a significantly reduced rate of ascospore germination but showed no significant involvement into sexual development and vegetative growth. The expression of the respective *cas4* gene was up-regulated during early stages of sexual development and differently regulated by elevated CO₂ concentrations (5%).

To determine which *cas* genes are required for *S. macrospora* growth under ambient air conditions, double and triple mutations of the four *cas* genes in all possible combinations and a quadruple mutant were constructed. Vegetative growth rate of the quadruple mutant lacking all *cas* genes was drastically reduced compared to the wild type and the mutant invaded the agar under normal air conditions. Likewise, the fruiting bodies that were formed only after elongated incubation time were embedded in the agar and completely devoid of mature ascospores. The phenotypic defects could only be partially restored by elevated CO₂-levels and the fruiting bodies that were formed after prolonged incubation were immature without ascospores. Intracellular β -class CAs and the secreted α -CA contributed differently to the vegetative growth and sexual development of *S. macrospora*.

The two β -class CA proteins CAS1 and CAS2 representing the major CA proteins of *S. macrospora* and were biochemically and structurally characterized. In an *in-vivo* assay, CAS1 and CAS2 could substitute for the *S. cerevisiae* β -CA Nce103p. Both proteins could be easily produced in *E. coli* and purified to high purity (5-10 mg of CAS1 and 10-20 mg of CAS2 per L of culture) and exhibited noticeable *in-vitro* CO₂ hydration activity (k_{cat}/K_m of CAS1: $1.30 \times 10^6 \text{ M}^{-1} \text{ s}^{-1}$; CAS2: $1.21 \times 10^6 \text{ M}^{-1} \text{ s}^{-1}$). In addition, CAS1 and CAS2 were only weakly inhibited by the widely used sulfonamide drug acetazolamide, with inhibition constants of 445 nM and 816 nM against CAS1 and CAS2, respectively. The best anionic inhibitors for both enzymes were sulfamide, sulfamate, phenylboronic acid and phenylarsonic acid, with

inhibition constants from 84 to 9 μM . In contrast, the activity of both CAs was only weakly inhibited by nitrite and nitrate anions and some other anions making them good candidates for industrial applications. To further investigate the structural properties of CAS1 and CAS2 their crystal structures were determined to a resolution of 2.7 Å and 1.8 Å, respectively. The oligomeric state of both proteins is tetrameric. With exception of the active site composition, no further major differences could be observed. In both enzymes the Zn^{2+} ion is tetrahedrally coordinated. In CAS1 the zinc ion is coordinated by Cys45, His101 and Cys104 and a water molecule and in CAS2 by the side chains of Cys56, His112, Cys115 and Asp58. The active site organization of CAS1, that is designated as type-I (“accessible”), and of CAS2, belonging to type-II (“blocked”), is mainly characterized by a conformational change of a aspartic acid residue.

In contrast to other organisms, the filamentous ascomycete *S. macrospora* appears to be able to use traces of HCO_3^- for growth without CA genes in a standard CO_2 atmosphere. With no functional CAs, *S. macrospora* switched from preferred growth at the air/medium interface to submerged growth. This work provides for the first time crystal structures of two β -CA enzymes from a filamentous ascomycete that form tetrameric assemblies, unlike other fungal β -CAs.

Zusammenfassung

Carboanhydrasen (CAs) sind Metalloenzyme, die eine schnelle und reversible Hydrierung von Kohlenstoffdioxid zu Bikarbonat (Hydrogencarbonat, HCO_3^-) und einem Wasserstoffatom katalysieren. CAs wurden in Eukaryoten, Bakterien und Archaeen identifiziert und werden in fünf Gruppen unterteilt (α , β , γ , δ , ζ), die keine Sequenz- oder Strukturähnlichkeiten aufweisen. Die Funktion von menschlichen, bakteriellen und pflanzlichen α -CAs wurde intensiv erforscht, während die Funktion von α -CAs aus filamentösen Pilzen bisher weitgehend unbekannt ist. Das Genom des filamentösen Schlauchpilzes *S. macrospora* codiert für vier CAs von denen drei zur Gruppe der β -CAs (*cas1*, *cas2* und *cas3*) gehören und eine zur Gruppe der α -CAs (*cas4*). Das CAS4 Protein besitzt ein funktionales N-terminales Signalpeptid für den Import in das Endoplasmatische Retikulum und wird als glykosyliertes Protein vom Pilz in die Umgebung sekretiert. Die $\Delta cas4$ Deletionsmutante besitzt eine signifikant reduzierte Keimungsrate der Ascosporen sowie eine geringfügige Reduzierung des vegetativen Wachstums und einer damit einhergehenden leicht verzögerten sexuellen Entwicklung. Die Transkriptionsrate des *cas4* Gens war signifikant erhöht in der frühen sexuellen Entwicklung während die Expressionsrate unter erhöhten CO_2 Bedingungen an verschiedenen Tagen unterschiedlich reguliert war.

Um herauszufinden, welche der vier *cas* Gene für das Überleben von *S. macrospora* unter normalen atmosphärischen Bedingungen wichtig sind, wurden Doppel- und Dreifachmutanten in allen Kombinationen sowie eine Vierfachmutante konstruiert. Das vegetative Wachstum der Vierfachmutante, die keine *cas* Gene mehr besitzt, war im Vergleich zum Wildtyp drastisch reduziert und die Mutante wuchs ausschließlich innerhalb des Agarsmediums. Die Fruchtkörper, die nur nach längerer Inkubationszeit unter normaler Luft gebildet wurden, waren ebenfalls im Agarmedium eingeschlossen und enthielten keine Ascosporen. Die phenotypischen Defekte der Vierfachmutante konnten nur teilweise durch Inkubation in 5% CO_2 wiederhergestellt werden. Intrazelluläre und sekretierte CAs tragen im unterschiedlichen Maß zum vegetativen Wachstum und zur sexuellen Entwicklung von *S. macrospora* bei.

Die beiden zur Gruppe der β -CAs gehörenden Enzyme CAS1 und CAS2 wurden als die wichtigsten CAs von *S. macrospora* beschrieben und wurden deshalb biochemisch und strukturell charakterisiert. Beide Enzyme konnten *in-vivo* eine *S. cerevisiae* CA-Mutante komplementieren und ließen sich einfach und in großen Mengen in *E. coli* produzieren (5-10 mg von CAS1 und 10-20 mg von CAS2 je L Zellkultur). Zudem besaßen sie deutliche *in-vitro* Aktivität (k_{cat}/K_m of CAS1: $1,30 \times 10^6 \text{ M}^{-1} \text{ s}^{-1}$; CAS2: $1,21 \times 10^6 \text{ M}^{-1} \text{ s}^{-1}$). Die Enzymaktivität

beider Proteine wurde nur schwach durch die als Medikament verwendete Chemikalie Acetazolamid inhibiert (Inhibierungskonstanten von 445 nM und 816 nM gegen CAS1 beziehungsweise CAS2). Es wurde auch die Inhibierung durch Anionen untersucht, wobei die deutlichste Inhibierung mit Sulfonamiden, Sulfamaten, Benzolboronsäure und Phenylarsonsäure erreicht wurde. Im Gegensatz dazu wurden beide Enzyme nur schwach von Nitrit und Nitrat sowie von einigen anderen Anionen gehemmt. Das schwache Inhibierungsprofil, insbesondere gegen Nitrit und Nitrat, macht beide Enzyme zu geeigneten Kandidaten für die Anwendung in der Industrie.

Außerdem wurden beide Proteine auch strukturell charakterisiert. Die Kristallstruktur von CAS1 wurde mit einer Auflösung von 2,7 Å und die von CAS2 mit 1,8 Å bestimmt. Beide Proteine sind Tetramere und bis auf das aktive Zentrum sehr ähnlich. In beiden Enzymen ist das Zn^{2+} Ion tetrahedral koordiniert. In CAS1 wird das Zn^{2+} Ion von den Seitenketten dreier Aminosäuren und einem Wassermolekül als vierten Liganden koordiniert. In CAS2 sind ausschließlich die Seitenketten von vier Aminosäuren an der Koordinierung des Zn^{2+} Ions beteiligt. Diese beiden verschiedenen Koordinierungsumgebungen werden als „type-I“ oder zugänglich bzw. „type-II“ oder blockiert beschrieben und sind hauptsächlich durch die konformationelle Änderung einer Aminosäure (Asparaginsäure) in der Nähe des aktiven Zentrums bestimmt.

Im Gegensatz zu allen anderen Organismen kann *S. macrospora* vollständig ohne CAs unter Luft leben und scheint in der Lage zu sein geringste Spuren von HCO_3^- zu nutzen. Ohne CAs wechselte der Pilz vom bevorzugten Wachstum auf dem Agar zu einem Wachstum innerhalb des Agarmediums.

In dieser Arbeit konnte zum ersten Mal gezeigt werden, dass β -CAs eines filamentösen Ascomyceten eine homotetramere Oligomerisierung aufweisen.

1. Introduction

The greenhouse gas carbon dioxide (CO₂) is naturally present in earth's atmosphere and composed of two oxygen atoms each covalently double bonded to a single carbon atom. It plays an eminent role in earth's ecosystems and can be considered a key molecule in the life of all organisms. It is the raw material for the biosynthesis of carbohydrates by autotrophic organisms and the end product of respiration in heterotrophic organisms. In addition to its metabolic functions, CO₂ acts also as a mediator triggering animal behavior, virulence and the growth of pathogenic organisms (Nijhout and Carter 1978; Bahn *et al.* 2005; Klengel *et al.* 2005; Hall *et al.* 2010; Cummins *et al.* 2013; Cottier *et al.* 2013). With an average concentration of about 400 parts per million by volume (0.04%) (Keeling *et al.* 2011), CO₂ can be designated as a trace gas in earth's atmosphere that can reach concentrations of 5% or more in patches where large amounts of CO₂ are released due to enhanced cellular respiration or geological processes (Cummins *et al.* 2013). In nature, CO₂ is reversibly hydrated in the reaction $\text{CO}_2 + \text{H}_2\text{O} \leftrightarrow \text{HCO}_3^- + \text{H}^+$. Bicarbonate (hydrogen carbonate; HCO₃⁻), the hydration product of CO₂, is an important biological molecule involved in many biosynthetic reactions such as arginine-, fatty acid-, uracil- or purine-biosynthesis (Aguilera *et al.* 2005; Supuran 2008b; Elleuche and Pöggeler 2009b). In addition, bicarbonate was described as an important cofactor for different enzymatic reactions such as detoxification of poisonous cyanate or the formation of menaquinone in *Escherichia coli* (Elleuche and Pöggeler 2008a; Jiang *et al.* 2010; Qian *et al.* 2011). In living cells more than 90% of the CO₂ is transported as HCO₃⁻ (Jones 2008). In contrast to CO₂, it cannot easily pass membranes of living cells by diffusion but rather has to be actively transported (Sterling and Casey 2002; Cordat and Casey 2009). The spontaneous and balanced interconversion of CO₂ and bicarbonate is slow, but can be accelerated up to 10⁶ reactions per second by a group of metalloenzymes called carbonic anhydrases (CA) (Lindskog 1997).

Since the CO₂ concentration in the atmosphere significantly increased over the past two hundred years (Crowley 2000), CO₂ and its biological role attracted interdisciplinary attention. Understanding the different mechanism of CO₂ assimilation and release in the biosphere will be of great importance when challenging the continuous increase of the atmospheric CO₂ levels in the future (Falkowski *et al.* 2000).

1.1 The enzyme carbonic anhydrase

Carbonic anhydrases (CAs) are metalloenzymes that can be divided into five classes (α , β , γ , δ , and ζ) unrelated in amino acid sequence and structure. The five classes are thought to be the result of convergent evolution (Hewett-Emmett and Tashian 1996; Tripp *et al.* 2001; Supuran 2008b).

CAs are important enzymes that contribute to a broad range of biological processes by providing high amounts of CO_2 or HCO_3^- to anaplerotic or biosynthetic reactions (Raven and Newman 1994; Giordano *et al.* 2003; Kumar and Ferry 2014). In cyanobacteria, CAs are associated with the enzyme ribulose-bisphosphate carboxylase/oxygenase (RuBisCO) within an organelle called carboxysome. In this association CAs concentrate and supply CO_2 to the RuBisCO and thereby enable the high photosynthetic activity of cyanobacteria (So *et al.* 2004; Sawaya *et al.* 2006; Kinney *et al.* 2012). This so called “carbon concentrating mechanism” (CCM) has been described to be of fundamental importance for inorganic carbon assimilation (Moroney *et al.* 2011). However, in other organisms CAs have other various functions. They are involved in fatty acid-, amino-acid- and DNA-synthesis and have been connected with proliferation, survival and differentiation of many pathogenic organisms inside and outside of their respective host (Bahn *et al.* 2005; Innocenti *et al.* 2008; Elleuche and Pöggeler 2009b; Cummins *et al.* 2013; Tobal and Balieiro 2014).

A long time it was believed that CAs are exclusively Zn^{2+} -dependent metalloenzymes but in 2000, the first functional CA with cadmium at the active site was reported from the marine diatom *Thalassiosira weissflogii* (Lane and Morel 2000). The Cd^{2+} ion is typically incorporated under conditions of zinc limitation and can fully maintain CA activity. The anaerobic methane producing bacteria *Methanosarcina thermophila* contains two CAs, Cam and CamH, which both contain ferrous iron at their active site when heterologously purified from *E. coli* in an atmosphere void of oxygen (Tripp *et al.* 2004; MacAuley *et al.* 2009; Zimmerman *et al.* 2010). The CA activity of the iron enzyme is increased by 3-fold over the zinc enzyme, that is only formed in air. The ferrous iron is rapidly oxidized to ferric iron accompanied by a loss of CA activity when the enzyme is exposed to normal air conditions. Furthermore, a variety of other divalent metal ions (Co^{2+} , Mn^{2+} , Ni^{2+} , Cu^{2+}) can replace the zinc in bacterial and mammalian CAs *in-vitro* without loss of activity (Lindskog 1963; Bertini *et al.* 1982; Hoffmann *et al.* 2011).

CAs have been identified in all three domains of life but despite their importance for many cellular processes in ambient air, some prokaryotes can live with no CA encoding genes

(Smith *et al.* 1999). These microorganisms are adapted to environmental niches where CO₂ is available at high concentrations. In ambient air, their growth depends on HCO₃⁻ or CO₂ produced by other organisms (Morotomi *et al.* 2012). Genomic and phylogenetic analyses of CA-deficient microorganisms reveal that genes coding for CAs have been lost during evolution (Nishida *et al.* 2009; Ueda *et al.* 2012). Hence, the lack of CA genes might explain why many microorganisms cannot be cultivated under normal CO₂ conditions. Many experiments have shown that CAs are essential enzymes for growth in ambient air, therefore, most prokaryotes and all eukaryotes encode at least one CA. The crucial role of CAs was furthermore demonstrated by deletion studies in bacteria including *E. coli* (Hashimoto and Kato 2003), *Ralstonia eutropha* (Kusian *et al.* 2002), *Haemophilus influenzae* (Langereis *et al.* 2013) and *Corynebacterium glutamicum* (Mitsuhashi *et al.* 2004) which showed that CA activity is essential for growth in ambient air. Bacterial CA deletion mutants grow only at elevated CO₂ concentrations (5%), when provided with HCO₃⁻ or when co-cultured with other bacteria (Watsuji *et al.* 2006).

Since their discovery, CAs are also of pharmacological interest, as their activity has not only been connected to a broad range of human diseases but has also been shown to be crucial for bacterial and fungal pathogenicity (McKenna and Supuran 2014). Intensive research identified a large group of competent CA inhibitory agents (CAI) of that anions, sulfonamides and dithiocarbamates have been described as the most effective (Nishimori *et al.* 2010; Monti *et al.* 2012). These CAIs have been used to treat human diseases such as glaucoma, convulsion, obesity and especially cancer with a long pharmacological history (Supuran 2008b). To explore the possibilities of CAIs as a therapeutic approach in bacterial related human diseases, several *in-vivo* studies have already been initiated (Shahidzadeh *et al.* 2005). The mode of action of the majority of CAIs is well understood: Typically, the inhibitor interacts in its deprotonated form with the metal ion at the active site and thereby inactivating the enzyme (Alterio *et al.* 2012). Other mechanisms for CA inactivation that do not involve the binding to the zinc ion were reported for polyamines that bind to the zinc-coordinated water/hydroxide ion and for coumarins that bind to and thereby closing the active site entrance (Maresca *et al.* 2009; Carta *et al.* 2010; Maresca *et al.* 2010).

To discover more efficient and selective anti-CA agents, the so called structure-based drug discovery, a modern and emerging new research field, has been introduced (Supuran 2012b). CAs of pathogenic organisms or of mammalian origin are crystallized in complex with known or putative inhibitors so that the molecular details of the CA and inhibitor interaction can be accessed easily. The obtained results are used as a foundation for the chemically design of

novel anti-CA drugs but also to enhance the efficiency and selectivity of existing anti-CA agents.

In addition, CAs are also proposed as biocatalysts for industrial applications such as CO₂ capture and sequestration, generation of biofuel but also for cheap CO₂ production for industrial purposes (González and Fisher 2014). The importance of this research field increased in the last years since cheap and fast techniques are needed to reduce the anthropogenic CO₂ release into the atmosphere. Current techniques to extract CO₂ from air or industrial fumes are very expensive and require harsh chemical conditions and elevated temperatures (Benson and Surles 2006). The usage of CAs as biocatalysts offers a very attractive approach to solve these problems as they are renewable, selective and relatively inexpensive (Bond *et al.* 2001). The most advanced results in industrial research were achieved with mammalian α -CAs as they can be easily overproduced in *E. coli* and represent the fastest kinetics for such applications (Banerjee *et al.* 2004; Supuran 2010b).

1.2 The α -class of carbonic anhydrases

The first active CA was discovered in red blood cells of bovine origin (Meldrum and Roughton 1933a; Meldrum and Roughton 1933b). Since that time sixteen α -CA isoforms, which is the only class found in mammals, have been described (Supuran 2008a). In humans (h) eight of them are cytosolic isoforms (hCA I to hCA III, hCA VII and hCA XIII), five are membrane localized (hCA IV, hCA IX, hCA XII, hCA XIV and hCA XV), two are mitochondrial proteins (hCA VA and hCA VB) and one α -CA is secreted (hCA VI) (Frost 2014). Three of the cytosolic CAs are inactive and are designated as CA-related proteins (CARP's). The human isozymes are involved in many different vital physiological processes such as gas exchange, transport of CO₂ and HCO₃⁻, acid-base balance and oncogenesis (Dodgson and Forster 1986; Esbaugh and Tufts 2006; Frost 2014). Of all isoforms, hCA II is the physiologically most relevant enzyme. It exhibits the greatest kinetics and is connected to pH-regulation and transport of CO₂ in erythrocytes (Frost 2014). Deficiency of hCA II is a rare autosomal recessive syndrome that manifests itself as renal tubular acidosis and cerebral calcification (Sly *et al.* 1983; Shah *et al.* 2004). In addition, the membrane localized hCA IX has also drawn attention because its expression is strongly connected to hypoxia, a condition of inadequate oxygen supply that is often associated with tumor formation (Supuran *et al.* 2004; Supuran 2008b). As for all α -CAs, hCA IX is susceptible to inhibition by CAIs providing possibilities of developing both diagnostic tools for the non-invasive imaging of

these tumors, as well as therapeutic agents that probably perturb the extratumoral acidification in which CA IX is involved (Supuran 2008b; Sedlakova *et al.* 2014; Akurathi *et al.* 2014).

The available three-dimensional structures of human α -CA isozymes I, II, III, IV, V, VI, IX, XII, XIII, and XIV revealed a high degree of structural similarity (Whittington *et al.* 2001; Alterio *et al.* 2009; Pilka *et al.* 2012). The typical fold of human α -CAs is characterized by a central antiparallel β -sheet harboring the active site, which is located in a large cone-shaped cavity that reaches the center of the protein molecule (Fig. 1). The Zn^{2+} ion, essential for catalysis, is located close to the bottom of the cavity. It is coordinated by three conserved histidine residues in a tetrahedral geometry with H_2O or OH^- as the fourth ligand. Another important histidine residue (His64 of CA II) that exists as two rotamers has been described as the major proton shuttling residue in mammalian α -CAs (Fig. 1). The two forms of His64 are designated as the “in” and the “out” conformations relative to the Zn^{2+} (Nair and Christianson 1991; Fisher *et al.* 2007). Furthermore, the histidine residue at this position seems to be the reason for the high catalytic efficiency of the some mammalian α -CAs. Mammalian isoforms such as hCA III or the murine CA V display a lower activity and the only difference is that they contain a lysine and tyrosine residue instead of the histidine at position 64 (Boone *et al.* 2014).

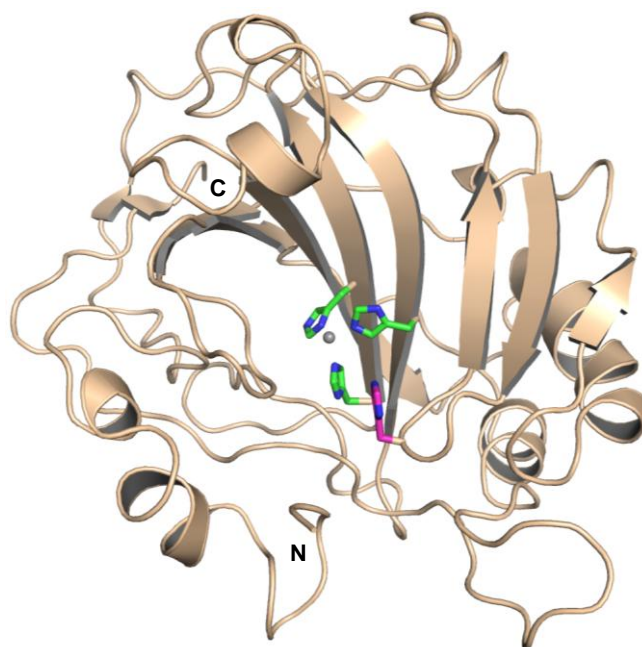
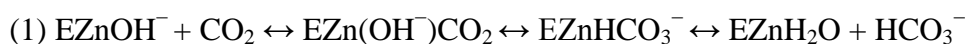


Fig. 1: Crystal structure of human CA II. The Zn^{2+} -ion is presented as a grey sphere. Histidine residues important for zinc binding are shown as green sticks. His64 is depicted as a purple stick. The first and the last residue are labeled N and C (PDB ID: 1AC2).

The catalytic mechanism of CAs has been extensively studied over last years, using mainly hCA I and hCA II as models (Fig. 2). It is proposed that all α -class CAs employ the same general CO₂ hydration reaction scheme: a nucleophilic attack of the ZnOH⁻ on the carbon atom of CO₂ by a two-step, ping-pong mechanism (equation 1 and 2) (Steiner *et al.* 1975; Christianson and Fierke 1996; Lindskog 1997; Rowlett 2010).



(E, enzyme; B, solution buffer)

CO₂ is concentrated to a hydrophobic pocket at the active site close to the zinc metal, which promotes the nucleophilic attack by the ZnOH⁻ and leads to the formation of HCO₃⁻ which is then displaced from the zinc by a water molecule (Fig. 2). The zinc-bound OH⁻ is regenerated for a subsequent round of catalysis by the transfer of H⁺ from the zinc-bound water molecule to the solution buffer. This proton transfer involves residue His64 and occurs on the order of 10⁶ s⁻¹ (hCA II) and is proposed to be the rate-limiting step of the overall velocity.

Major research on the α -class CA was performed mostly with the mammalian isoforms. However, many bacteria contain α -CAs as well (Supuran 2012a). They were identified in many pathogenic species, such as *Neisseria gonorrhoeae*, *Helicobacter pylori*, *E. coli*, *Mycobacterium tuberculosis*, *Streptococcus pneumoniae*, *H. influenzae*, and *Pseudomonas aeruginosa*. Amino-acid sequence and structural comparison of the *N. gonorrhoeae* α -CA with the human isoforms hCA I and II suggested that secondary structures are essential identical, although, some loops are much shorter (Chirica *et al.* 1997; Elleby *et al.* 2001). The active-site residues are almost identical to those of the hCA II. The crucial zinc ion is placed at a bottom of a rather deep and large active site and coordinated by three histidine residues and a water molecule/hydroxide ion. The bacterial enzyme exhibits a high CO₂ hydrase activity (k_{cat} of $1.1 \times 10^6 \text{ s}^{-1}$ and K_{m} of 20 mM (at pH 9 and 25 °C); hCA I: k_{cat} of $2.0 \times 10^5 \text{ s}^{-1}$ and $k_{\text{cat}}/K_{\text{m}}$ of $5.0 \times 10^7 \text{ M}^{-1} \text{ s}^{-1}$; hCA II: k_{cat} of 1.4×10^6 and $k_{\text{cat}}/K_{\text{m}}$ of 1.5×10^8) and showed also esterase activity for the hydrolysis of 4-nitrophenyl acetate, similarly to the mammalian isoforms hCA I and II (Chirica *et al.* 1997).

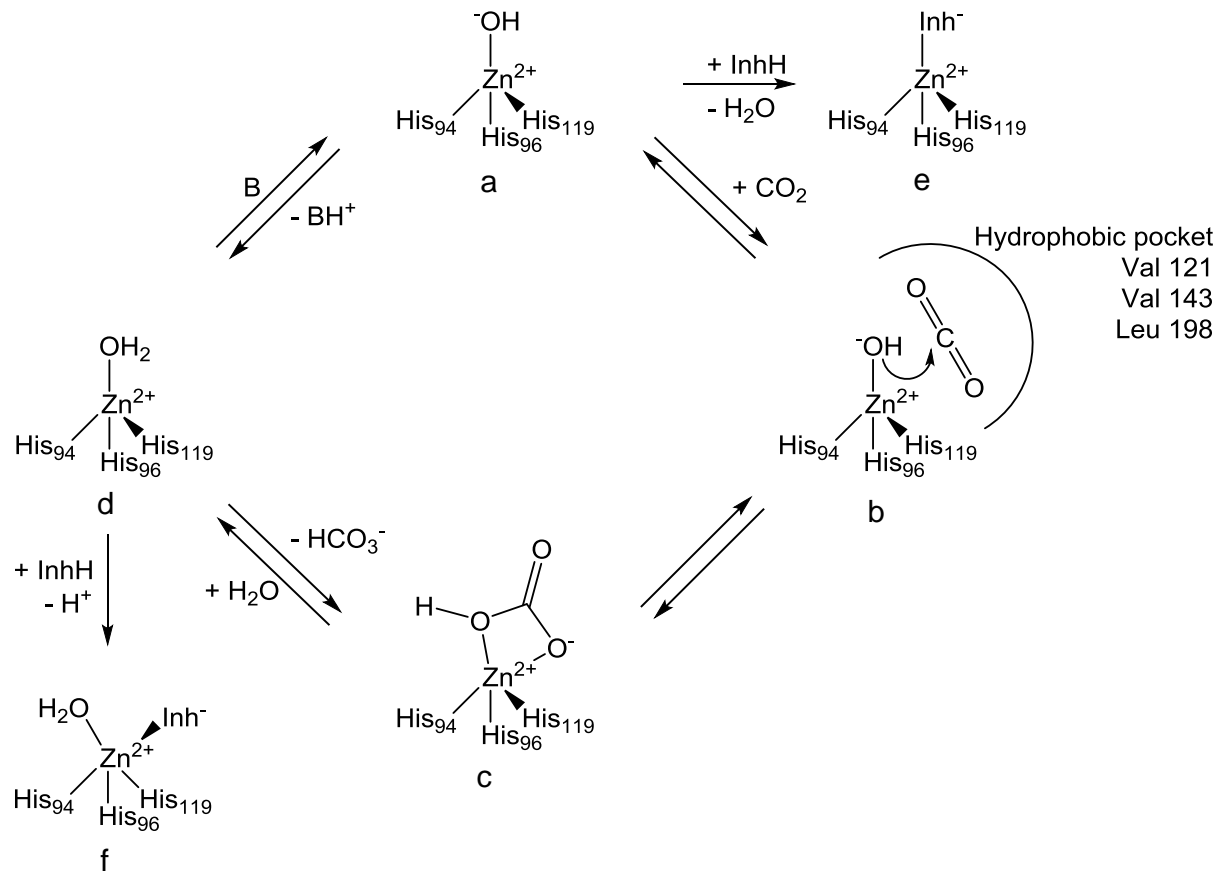


Fig. 2: Catalytic and inhibition mechanisms of α -CAs (amino-acid numbering according to hCA I). (a) The metal hydroxide species is generated from water, coordinated to the zinc ion. (b) The substrate CO_2 is bound in a hydrophobic pocket, defined by residues Val121, Val143, and Leu198. (c) In this position CO_2 is transformed by a nucleophilic attack into bicarbonate that is bound bidentately to the zinc ion. The formed intermediate is rather instable and quickly transformed into d by a reaction with water that releases the bicarbonate into solution. (d) The regeneration of the zinc bound hydroxyl species is achieved by a proton transfer from the zinc-bound water to the buffer that is the rate determining step of the reaction. (e and f) Binding of the inhibitor to the zinc ion in a tetrahedrally or trigonal geometry (modified according to McKenna and Supuran 2014).

The best studied bacterial α -class CA is the periplasmic *hpaCA* of the human pathogen *H. pylori* (Chirica *et al.* 2001; Chirica *et al.* 2002) that causes chronic active gastritis, ulcer disease, and gastric cancer (Sachs *et al.* 2011). The bacterial enzyme was shown to be indispensable for urease-dependent colonization of the gastric environment and the *hpaCA* deletion mutant of the mouse adapted *H. pylori* strain X47-2AL exhibited a strongly reduced colonization rate compared to the wild type (wt) (Bury-Mone *et al.* 2008). Current treatment modalities use a proton pump inhibitor and two antibiotics but the success rate of this triple therapy is less than 80%, below the cutoff for efficacious eradication (Sachs *et al.* 2011). Since the *H. pylori* enzyme is highly inhibited by many CAIs *in-vitro* and in cell cultures

(Nishimori *et al.* 2008) an alternative therapeutic approach for patients with *H. pylori* infection can be applied by using CAIs (Shahidzadeh *et al.* 2005).

In contrast to the large number of mammalian and bacterial α -CAs, only a single fungal α -CA has been structurally, but not functionally, characterized (Cuesta-Seijo *et al.* 2011). The α -CA AoCA of the filamentous ascomycete *Aspergillus oryzae* has a functional N-terminal signal peptide and is highly glycosylated. The protein is targeted to the supernatant in its soluble form. The crystal structure revealed that AoCA is a dimeric protein with a monomeric fold known from other α -CAs. Mammalian α -CAs use a His residue (His64 in human CA II) as a proton shuttle for enzyme regeneration. This residue is replaced by phenylalanine in the α -CA of *A. oryzae*.

1.3 The β -class of carbonic anhydrases

The second most prominent subgroup of CAs is the β -class which was unwittingly discovered only a few years after the α -class in 1939 as a constituent of plant leaf chloroplasts (Neish 1939). Since then, it was discovered that the β -class of CAs is present in many organisms in all domains of life but is absent in the mammalian family. This fact led to intensive research on the β -class CAs in the last years.

The first complete cDNA sequence of a plant β -CA from *Spinacia oleracea* was published in 1990 (Burnell *et al.* 1990). Shortly thereafter, the first bacterial β -CA gene was discovered in *E. coli* (Guilloton *et al.* 1992) and the first fungal β -CA in *Saccharomyces cerevisiae* (Götz *et al.* 1999). Since then, many more β -CAs have been identified in pathogenic and non-pathogenic bacteria, archaea, algae, plants and fungi (Smith *et al.* 1999; Rowlett 2010; Elleuche and Pöggeler 2010; Elleuche 2011).

The β -class can be further subdivided into plant-type and cab-type sub-classes that are named after the β -CA CAB (carbonic anhydrase beta) from the archaeon *Methanobacterium thermoautotrophicum* (Smith and Ferry 1999; Kimber and Pai 2000). The plant-type sub-class is characterized by three conserved residues close to the active site (Gln151, Phe179 and Tyr205; numbering according to the *Pisum sativum* β -CA) that are variable in the cab-type sub-class. Originally, it was thought that there is a third sub-group of β -CAs which was discovered in the chemolithoautotrophic bacterium *Halothiobacillus neapolitanus*. This β -CA had such a unique structure compared to members of the other sub-groups that it was designated as a member of a novel ϵ -class. When the crystal structure of this enzyme became

available it was obvious that this enzyme indeed belongs to β -class and not to a separated subgroup (So *et al.* 2004; Sawaya *et al.* 2006).

The physiological role of the β -class has been studied intensively: β -CAs have been described as accessory enzymes for CO_2 or HCO_3^- utilizing enzymes such as cyanases (Guilloton *et al.* 1993), RuBisCO, ureases (Nishimori *et al.* 2008) or bicarbonate-dependent carboxylases (Mitsuhashi *et al.* 2004). Furthermore, the enzymes of the β -class were shown to be involved in growth under ambient air and in photosynthesis, as they are part of the carboxysome in cyanobacteria. Although, they catalyze the same reaction, the structure and sequence of β -CAs exhibits only minor homologies to α -class CAs. Like CAs of the α -class, all known β -CAs utilize a Zn^{2+} as the active metal species for catalysis that is coordinated in a pseudo-tetrahedral manner by two cysteine and one histidine residue and an exchangeable fourth ligand. Almost all structurally analyzed β -CAs have one zinc ion per monomer. In contrast to α -class CAs, that are mainly monomeric enzymes, β -CAs are described to appear as dimeric, tetrameric or octameric proteins (Fig. 3).

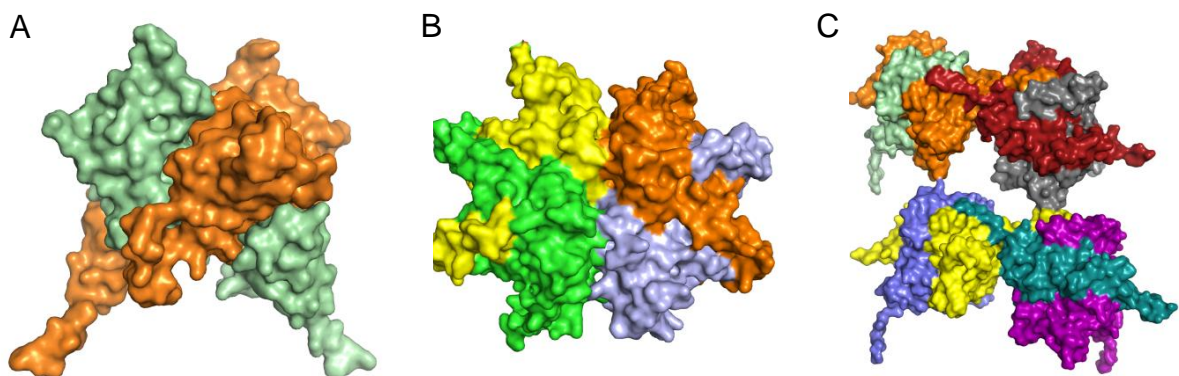


Fig. 3: The different oligomeric forms of β -CAs. (A) Dimeric Can2 of *C. neoformans* with monomers labeled in pale green and orange (PDB ID: 2W3Q). (B) Tetrameric β -CA of *H. influenzae* (2A8C). One fundamental dimer is green and yellow, the other light blue and orange. (C) Octameric β -CA of *P. sativum* (1EKJ). The fundamental dimers are pale green/orange, gray/red, cyan/purple and yellow/blue.

The first structurally characterized β -CA was the tetrameric enzyme of the red algae *Porphyridium purpureum*, quickly followed by the tetrameric β -CA of *E. coli* (Fig. 4) and the octameric β -CA of *P. sativum*. (Kimber and Pai 2000; Mitsuhashi *et al.* 2000; Cronk *et al.* 2001). The fundamental structural unit of all β -CAs appears to be a dimer (Rowlett 2010). The monomers have a unique α/β fold in common that is not found in any other protein. It consists of an N-terminal arm composed of one or more α -helices and the central β -sheet that is composed of four parallel strands in a $\beta 2-\beta 1-\beta 3-\beta 4$ arrangement. Some structures have an

additional antiparallel fifth β -strand connected to β 4. Numerous C-terminal α -helices flanking on one side the convex surface of the β -sheet while the other side is involved in dimer and tetramer formation (Fig. 4) (Rowlett 2010). The N-terminal arm was shown to be important for activity but not for dimerization (Teng *et al.* 2009; Schlicker *et al.* 2009). With the exception of the unique dimeric β -CA of *H. neapolitanus*, this structure applies for all β -CAs. The β -CA of *H. neapolitanus* has evolutionarily diverged because one of the monomers has lost all zinc ligands (Sawaya *et al.* 2006). The enzyme is composed of three domains: An N-terminal part that consists of four α -helices, the catalytic domain that shares structural similarities with other β -CAs and the C-terminal domain that has the classic β 2- β 1- β 3- β 4 arrangement but without any properly constituted active site or zinc ligands (Rowlett 2010). It is proposed that this defunct and somewhat diminished monomer may have evolved a new function, specific to its carboxysomal environment.

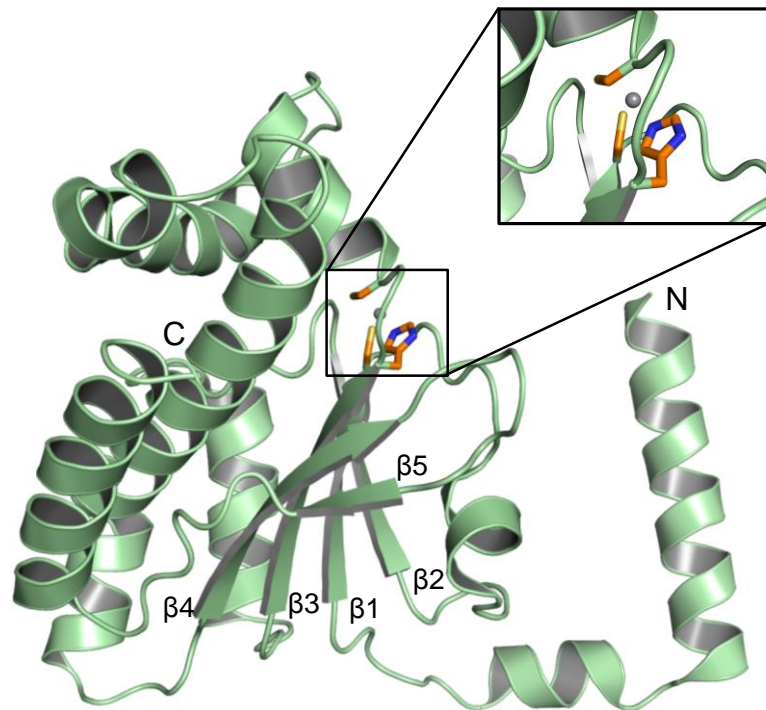


Fig. 4: Typical crystal structure of a β -class CA. Depicted is the monomer of the *E. coli* β -CA to illustrate to core elements of β -CAs (an N-terminal arm, a conserved α/β core and a C-terminal subdomain). The first and the last residue are labeled N and C. The zinc ion is presented as a grey sphere and residues binding the zinc are colored as orange sticks (PDB ID: 1I6P).

The oligomerization of β -CAs is proposed to be the result of surface extensions or unique elaborations of the secondary structure of the basic β -CA fold (Rowlett 2010). Dimeric β -CAs have been reported from the fungi *S. cerevisiae* and *Cryptococcus neoformans* and from the

prokaryotes *M. thermoautotrophicum* and *M. tuberculosis* (Strop *et al.* 2001; Covarrubias *et al.* 2005; Teng *et al.* 2009; Schlicker *et al.* 2009). Except of the *S. cerevisiae* protein all dimeric β -CAs can also form higher oligomerization states in solution and crystals. The oligomerization of the dimeric β -CAs seems to depend either on the pH or on salt bridges induced by complex formation of the enzymes with small molecules (Smith and Ferry 1999; Smith *et al.* 2000; Covarrubias *et al.* 2006; Rowlett 2010). The octameric arrangement of β -CAs has been reported exclusively from plant β -CAs and has been structurally confirmed only for the *P. sativum* CA (Kimber and Pai 2000), while the octameric oligomerization state for the *S. oleraceae* and the *A. thaliana* β -CA has only been confirmed by size exclusion chromatography and non-denaturing gel electrophoresis (Pocker and Joan 1973; Rowlett *et al.* 2002). Tetramers seem to be the most common arrangement of β -CAs and have been reported from bacteria (*E. coli* and *H. influenzae*) and algae (*Cocomyxa spp.* and *P. purpureum*) but yet not from fungi (Cronk *et al.* 2000; Mitsuhashi *et al.* 2000; Cronk *et al.* 2006; Huang *et al.* 2011).

All reported three-dimensional structures of β -CAs can be divided into two distinct classes depending on the organization of their active site (Rowlett 2010). The principal difference between the two classes, which are designated as type-I and type-II, can be reduced to the zinc-coordination environment and the conformation of nearby residues (Fig. 5). The active site of type-I β -CAs depicts the “accessible” conformation with the zinc ion coordinated by three residues (two cysteine residues and one histidine residue) and an exchangeable ligand (Rowlett 2010). This ligand can either be water as in the case of the β -CA of *M. thermoautotrophicum*, Can2 of *C. neoformans* and the β -CA of *H. neapolitanus* or acetic acid or an acetate ion as in the *P. sativum* β -CA (Kimber and Pai 2000; Schlicker *et al.* 2009; Rowlett 2010). In addition, a hydrogen bond is formed between the exchangeable ligand, directly bound to the zinc, and an aspartic acid residue in type-I β -CAs. The Asp is oriented in the right position by an arginine residue with which it forms hydrogen bonds (Fig. 5A). Both residues are part of a dyad and conserved in all β -CAs independent of the subgroup. The final characteristic of type-I β -CAs is that the exchangeable ligand donates a hydrogen bond to the zinc-bound bicarbonate ion (Rowlett 2010).

Type-II β -CAs are characterized by a zinc ion coordinated by four amino-acid ligands coordinating the zinc ion with no other ligands involved. This organization state is designated as the “closed” conformation. The exchangeable ligand position is occupied by the aspartic acid of the Asp/Arg dyad that is broken in type-II CAs. The arginine is rotated away from the active site causing the loss of hydrogen bonds (Fig. 5B). The same conformational change

was observed for the hydrogen-bond donor of the zinc-bound bicarbonate ion. However, at $\text{pH} > 8$ the observed “closed” state may convert to an “accessible” state when the conserved Arg residue forms a salt bridge with the Asp residue and thereby liberating the fourth zinc coordination position, which is then occupied by an incoming water molecule (Covarrubias *et al.* 2005).

Despite all differences, both types have a small, hydrophobic active site cleft in common that lies along the dimer interface and leads to the zinc ion.

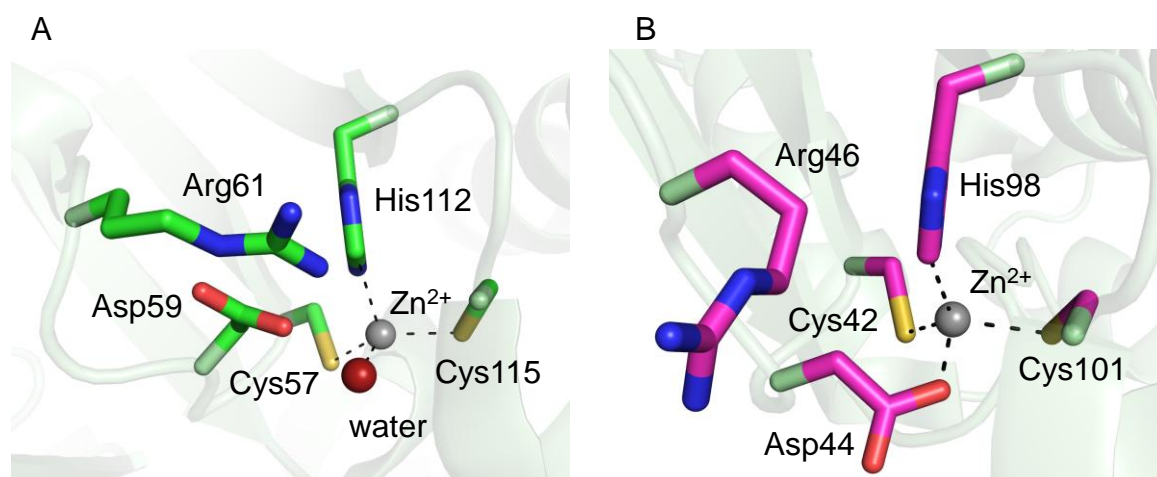


Fig. 5: Organization of the active site of type-I and type-II β -CAs. (A) Active site of the *S. cerevisiae* type-I β -CA (PDB ID: 3EXY). The zinc ion (grey sphere) is coordinated by Cys57, His112, Cys115 (green sticks) and a water molecule (red sphere) as the fourth ligand. (B) Active site of the *H. influenzae* type-II β -CA (2A8C). The zinc ion (grey sphere) is coordinated by four amino-acid ligands (Cys42, His98, Cys101 and Asp44; shown as purple sticks).

Like α -class CAs, β -class CAs are targets for inhibition with CAIs. However, the β -class CAs are of special interest in the CAI research, as it is the main group of most fungal organisms (Elleuche and Pöggeler 2010; Elleuche 2011). Furthermore, the research on β -CAs is of more relevance since they are not encoded by mammals. Many pathogenic fungi such *Candida albicans* or *Aspergillus fumigatus* depend on at least one or more β -CAs for infection of their mainly mammalian hosts. A selective inhibition only of β -class CAs offers an excellent possibility for a gently treatment of fungal-related diseases. Despite the large number of fungal β -CAs known, only two have been structurally and functionally characterized to date: the N-terminally truncated *S. cerevisiae* CA Nce103, and the full length CA Can2 from the basidiomycete *C. neoformans* (Teng *et al.* 2009; Schlicker *et al.* 2009). As mentioned before, both enzymes are dimeric and have an active site organization reflecting type-I β -CAs.

1.4 Carbonic anhydrases in the fungal kingdom

Fungal genome inspection shows that hemiascomycetous and basidiomycetous yeasts encode one or two β -CAs, while most filamentous ascomycetes encode multiple β -CAs with some also possessing genes encoding α -class CAs (Elleuche and Pöggeler 2009a). Various gene-duplication and gene-loss events during evolution seem to be the cause for the multiplicity of CAs in fungi. In filamentous ascomycetes, a gene encoding a plant-type β -CA was duplicated, resulting in two closely related isoforms differing in the presence or absence of an N-terminal mitochondrial target sequence (MTS) (Elleuche and Pöggeler 2009a).

The yeasts *C. albicans*, *Candida glabrata* and *S. cerevisiae* encode only single plant-type β -CAs and the growth of the corresponding CA-deletion mutants is inhibited in ambient air, similar to prokaryotic CA-deletion strains (Götz *et al.* 1999; Klengel *et al.* 2005; Cottier *et al.* 2013). In contrast, the pathogenic basidiomycete *C. neoformans* has two β -class CA-encoding genes (*can1* and *can2*), although, only the deletion of *can2* inhibits growth under regular CO₂ conditions (Bahn *et al.* 2005). As shown for the prokaryotic CA-deletion strains, the so called HCR (high CO₂-requiring) phenotype, can be unspecifically restored either by incubation at 5% CO₂ or by addition of end products (arginine or fatty acids) of CO₂ and HCO₃⁻-dependent biosynthetic pathways (Aguilera *et al.* 2005; Bahn *et al.* 2005).

The transcript levels of the *S. cerevisiae*, *C. albicans* and *C. glabrata* β -CA genes are regulated by the CO₂ concentration. In normal CO₂ conditions, the expression of CA-genes is up regulated but drastically reduced at elevated CO₂ levels (Götz *et al.* 1999; Amoroso *et al.* 2005; Cottier *et al.* 2013). Moreover, low CO₂ concentrations induce filamentous growth and promote white to opaque switch, thus, facilitating mating in the human pathogenic yeast *C. albicans*. In addition, it has been shown that *C. albicans* depends on CA activity for pathogenesis on the skin of its host during epithelial invasion (Klengel *et al.* 2005). Likewise in *C. neoformans*, bicarbonate produced by Can2 is required for later mating steps, including production of potentially infectious spores. The *in-vivo* proliferation and virulence at high CO₂ levels in the host was not affected in the *C. neoformans* and *C. albicans* CA mutants (Klengel *et al.* 2005; Bahn *et al.* 2005).

Only recently it was uncovered how fungi sense different CO₂ concentrations and regulate CA expression (Fig. 6).

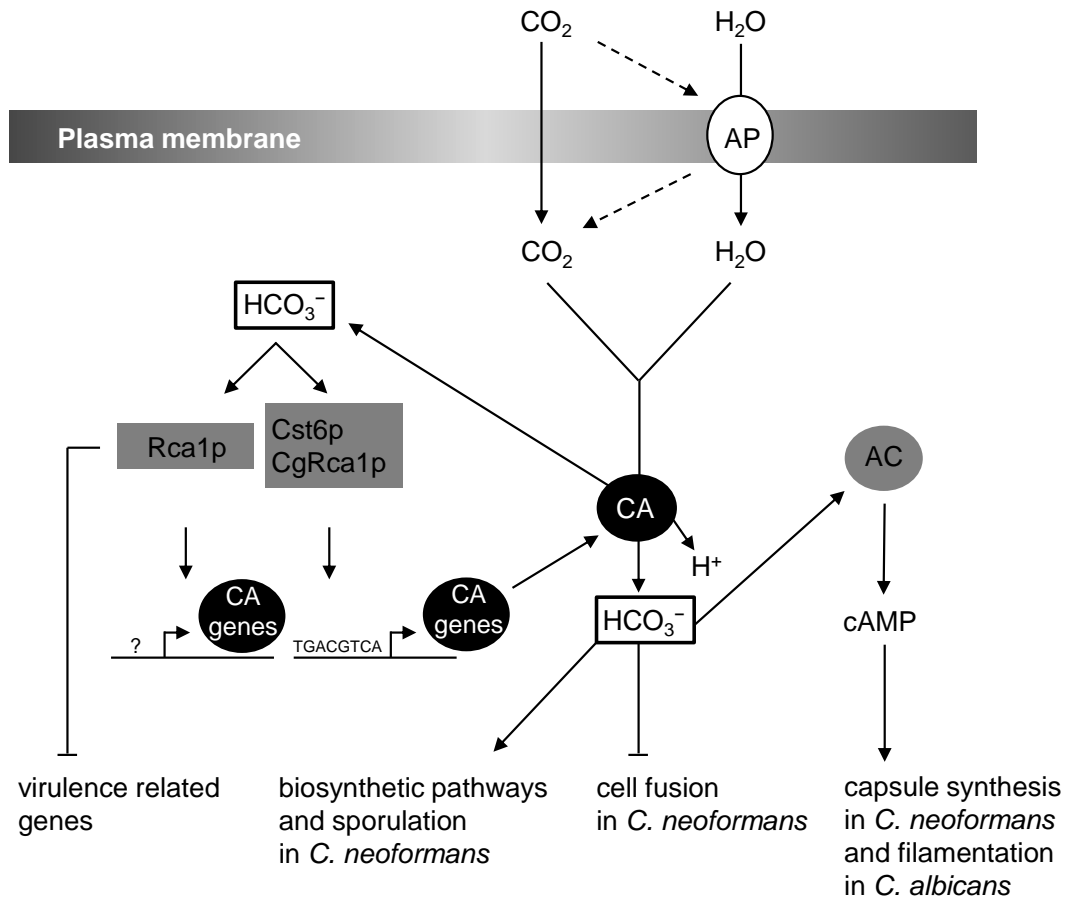


Fig. 6: Schematic illustration of CO₂ sensing and CA regulation in fungi. CO₂ enters the cell mainly via diffusion or via aquaporins (AP). In the cell, CO₂ is quickly and reversibly hydrated to bicarbonate (HCO₃⁻) which contributes to several biosynthetic pathways. In addition, HCO₃⁻ activates sporulation and represses at the same time cell fusion in *C. neoformans*. High concentrations of HCO₃⁻ stimulate the enzyme adenylyl cyclase that induces capsule synthesis in *C. neoformans* and filamentation in *C. albicans* via the second messenger cAMP. Additionally, HCO₃⁻ also induces expression of CA genes by activation of transcription factors Rca1p (*C. albicans*), Cst6p (*S. cerevisiae*) and CgRca1p (*C. glabrata*). The latter two proteins bind to a conserved TGACGTCA motif at the promoter region (modified from Bahn and Mühlischlegel 2006; Cottier *et al.* 2013).

In *C. albicans* and *C. neoformans* a bicarbonate-dependent adenylyl cyclase was described (Klengel *et al.* 2005; Mogensen *et al.* 2006; Hall *et al.* 2010) that is activated by bicarbonate and is homologous to prokaryotic adenylyl cyclases (Chen *et al.* 2000). These enzymes produce the important second messenger cAMP and are essential for pathogenicity-related morphogenesis such as capsule synthesis in *C. neoformans* or filamentation in *C. albicans*. A *C. albicans* mutant without a functional adenylyl cyclase is not able to grow filamentously anymore and loses its pathogenicity (Klengel *et al.* 2005). Surprisingly, the expression of CA-genes seems not to be regulated by adenylyl cyclases (Cottier *et al.* 2012). In *C. albicans*, the novel transcription factor Rca1p was discovered and described as the first direct CO₂

regulator of CA-genes in yeast. Rca1p activates CA-gene expression at low CO₂ concentrations, independent of the adenylyl cyclase and also seems to repress virulence-related genes, confirming the existence of an additional cAMP-independent CO₂ signaling pathway (Cottier *et al.* 2012). Orthologs of Rca1p were also discovered in the yeasts *S. cerevisiae* (Cst6p) and *C. glabrata* (CgRca1p) (Cottier *et al.* 2013). In the deletion mutants of the respective transcription factor genes, CA-gene expression was no longer induced in ambient air. It has been shown that the transcription factor Cst6p in *S. cerevisiae* controls CA-gene expression through a conserved TGACGTCA motif in the promoter of the yeast CA-gene *nce103* (Fig. 6) (Garcia-Gimeno and Struhl 2000; Cottier *et al.* 2012). An identical sequence can also be found in the promoter of the *C. glabrata* CA-gene but not in the promoter of the *C. albicans nce103* gene (Cottier *et al.* 2013). Deletion of the TGACGTCA motif in the promoter of both CA genes led to the loss of CA-gene induction at 0.04% CO₂.

As described for the basidiomycete *C. neoformans*, a major and minor β -CA have been also observed in filamentous ascomycetes (Elleuche and Pöggeler 2009b; Han *et al.* 2010). *Aspergillus nidulans* has two β -CA class genes (*canA* and *canB*) and *A. fumigatus* has four (*cafA*, *cafB*, *cafC* and *cafD*). In *A. fumigatus*, *cafA* and *cafB*, are constitutively and strongly expressed, while *cafC* and *cafD* are weakly expressed and are induced by low CO₂ concentrations. In *A. nidulans*, only deletion of *canB* inhibits growth in ambient air conditions; in *A. fumigatus*, single deletion mutants are not growth inhibited in ambient air and only the Δ cafA Δ cafB mutant is unable to grow in regular CO₂ conditions (Han *et al.* 2010). Furthermore, the CA-deletion affects *A. fumigatus* conidiation, which is in accord with results shown in *S. cerevisiae*, where the CA Nce103p seems to be involved in spore formation (Jungbluth *et al.* 2012). The virulence of single and double CA mutants of *A. fumigatus* were not affected in a low-dose murine infection model similar to CA mutants of *C. albicans* and *C. neoformans*. While both β -CA genes of *A. nidulans* rescue a CA-deficient *S. cerevisiae* mutant (Δ nce103), only the *A. fumigatus cafB* gene complements the yeast deletion strain (Han *et al.* 2010).

1.5 *Sordaria macrospora*: a model organism for fruiting-body development

Lower eukaryotes, like unicellular yeasts and filamentous fungi, are attractive organisms to study the complex eukaryotic cell biology. Compared to animals and plants, fungi offer the advantages of simple cultivation under laboratory conditions with short generation times and

easy accessibility towards molecular and classical genetics. Filamentous fungi have the ability to form complex sexual structures from a simple two dimensional mycelium. This process is driven by a highly regulated and dynamic molecular-machinery whose principles seem to be conserved from fungi to higher eukaryotes. The fact that fungi are closer related to animals than to plants underlines their value as favorable models for human cells (van der Klei and Veenhuis 2006; Pace 2009).

The filamentous ascomycete *Sordaria macrospora* is a coprophytic fungus that naturally lives on herbivore dung. For many years *S. macrospora* served as a model organism to study fruiting-body development because it offers many advantages: *S. macrospora* is not infective, easy cultivable under laboratory conditions and has a short sexual life cycle of seven days (Kück *et al.* 2009; Engh *et al.* 2010) (Fig. 7). The genome size (40 Mb) is relatively small and is completely sequenced (Nowrousian *et al.* 2012). Furthermore, many molecular techniques are well established and allow an easy and fast manipulation of *S. macrospora*. In addition, *S. macrospora* produces only large meiotic ascospores, asexual spores (conidia) are absent. The fungus is homothallic (self-fertile) and can complete its life cycle without a mating partner. Thus, recessive mutations that affect the sexual development are directly observable as alterations of the phenotype.

The life cycle of *S. macrospora* starts with a germinating ascospore (Fig. 7). After germination, *S. macrospora* grows as a two-dimensional mycelium. The sexual cycle starts at day 3 of development with the formation of ascogonial coils representing female gametangia. At day 4, ascogonia are enclosed completely by sterile hyphae, forming a globular premature structure, called the prefruiting body (protoperithecium). Consecutive cell differentiation generates an outer, pigmented peridial tissue and initial ascus at day 5. After self-fertilization, karyogamy, meiosis, and postmeiotic mitosis, mature perithecia are formed containing asci with eight sexual ascospores that are forcibly discharged at day 7 (Read 1983; Read and Beckett 1985; Engh *et al.* 2010; Lord and Read 2011).

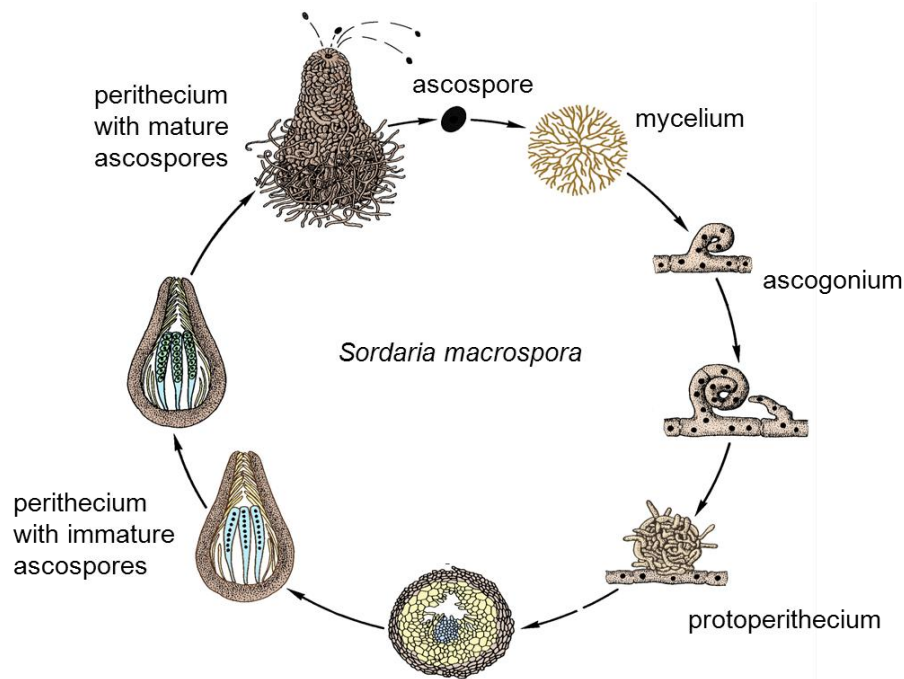


Fig. 7: Schematic illustration of the life cycle of *Sordaria macrospora*. The cycle starts with a single ascospore that germinates to a two-dimensional mycelium that develops ascogonia coils. Ascogonia form protoperithecia and later mature fruiting bodies (perithecia) that discharge the mature and melanized ascospores. After seven days, the life cycle is completed in the laboratory (modified according to Kück *et al.* 2009).

Previous studies identified four CA genes in the genome of *S. macrospora* (Elleuche and Pöggeler 2009b) that are designated as *cas1*, *cas2*, *cas3* and *cas4* (Elleuche and Pöggeler 2009a; Elleuche and Pöggeler 2009b; Elleuche 2011). No additional CAs with known primary structures or typical domains were found in the genome. The β -CA genes *cas1* and *cas2* have high sequence identity and encode enzymes with the characteristics of the plant-like sub-class of β -CAs (Elleuche and Pöggeler 2009a). The β -CA *cas3* belongs to the cab-like sub-class and *cas4* to the α -class. CAS1 and CAS3 are cytoplasmic enzymes while CAS2 is located to the mitochondria and CAS4 is proposed to be secreted (Elleuche and Pöggeler 2009b; Elleuche and Pöggeler 2010).

The function of the three β -CAs *cas1*, *cas2* and *cas3* in sexual development has been studied intensively (Elleuche and Pöggeler 2009b). When single-deletion mutants of *S. macrospora* β -CA genes are compared to wt, only the $\Delta cas2$ strain has a significantly reduced vegetative growth and ascospore germination rate. All mutants grow in ambient air (Elleuche and Pöggeler 2009b). Double-deletion mutants $\Delta cas1/3$ and $\Delta cas2/3$ grow and form fruiting bodies similar to wt in regular CO₂ concentrations; however, $\Delta cas1/2$ has a drastically reduced vegetative growth rate and produces sterile fruiting bodies only after elevated incubation time of 20 days. The impairment of sexual development and vegetative growth are

fully restored by elevating CO₂ to 5% (Elleuche and Pöggeler 2009b). However, the reduced ascospore germination rate is not rescued by incubation at 5% CO₂.

1.6 Aim of this thesis

Most fungal CAs analyzed so far belong to the β -class and to date only a single fungal α -CA was structurally and functionally analyzed (Cuesta-Seijo *et al.* 2011). Still nothing is known about their regulation and involvement in fungal developmental processes. The objective of this study was the functional analysis of the *S. macrospora* α -CA gene *cas4*. By means of qRT-PCR, the regulation under different atmospheric CO₂ concentrations and during sexual development should be analyzed. In addition, the role during sexual development, vegetative growth and sporulation should be accessed by generation of a $\Delta cas4$ deletion mutant. All known fungal CA mutants exhibited a growth inhibition in ambient air (Elleuche and Pöggeler 2010). In contrast, single- and double-deletion mutants of the three β -class CAs of *S. macrospora*, constructed so far were still able to grow in ambient air (Elleuche and Pöggeler 2009b). The strongest alteration of the phenotype was observed for the $\Delta cas1/2$ mutant that formed fruiting bodies devoid of ascospores only after elongated time in ambient air. To further investigate the contribution of the four *cas* genes on vegetative and sexual development of *S. macrospora* in ambient air, double, triple CA-mutants in all possible combinations as well as a quadruple mutant should be generated. All mutants will be analyzed in detail with regard to their growth abilities in ambient air and to their impact on sexual development and germination.

Another aim of this work was the biochemical and structural characterization of the two major CA proteins from *S. macrospora*, CAS1 and CAS2. Despite the large number of fungal β -CAs known, only two have been structurally characterized to date: the N-terminally truncated *S. cerevisiae* CA Nce103, and the full length CA Can2 from the basidiomycete *C. neoformans* (Teng *et al.* 2009; Schlicker *et al.* 2009). To biochemically characterize CAS1 and CAS2 both proteins should be heterologously produced in *E. coli* as His-tagged fusion proteins. After purification, β -CAs CAS1 and CAS2 should be crystallized to elucidate their structural details and solve their three-dimensional structures. To functionally prove that both proteins exhibit CA activity both enzymes should be tested for their catalytic efficiency in an *in-vitro* stopped-flow CO₂ hydration assay. In addition, the enzymes should be used to demonstrate their ability to functionally restore the *S. cerevisiae* $\Delta nce103$ deletion mutant *in-vivo* (Götz *et al.* 1999).

2. Materials and Methods

2.1 Materials

2.1.1 Strains

Table 1: Overview of strains used and constructed in this study.

| Strain | Genotype | Source |
|--|--|-----------------------------|
| <i>ESCHERICHIA COLI</i> | | |
| Mach1 | $\Delta recA139\ endA1\ tonA\ \Phi80(lacZ)\Delta M15$ $\Delta lacX74\ hsdR(r_K^- m_K^+)$ | Invitrogen, Germany |
| BL21 (DE3) | $F^- ompT\ dcm^+ lon\ hsdS_B(r_B^- m_B^-) gal$ (DE3) | Invitrogen, Germany |
| Rosetta (DE3) | $F^- ompT\ dcm^+ hsdS_B(r_B^- m_B^-) gal$ (DE3) pRARE (<i>cam</i> ^R) | Invitrogen, Germany |
| <i>SACCHAROMYCES CEREVISIAE</i> | | |
| PJ69-4A | <i>MATa trp1-901 leu2-3_112 ura3-52</i> <i>his3_200 gal14Δ gal18OΔ LYS2::GAL1-</i> <i>HIS3 GAL2-ADE2 met2::GAL7-lacZ</i> | James <i>et al.</i> 1996 |
| CEN.HE28 | <i>CEN.PK Mat α/a ura3-52/ura3-52</i> <i>his3Δ1/his3Δ1 leu2-3_112/leu2-3_112</i> <i>trp1-289/trp1-289 (YNL036w::KAN/</i> <i>YNL036w)</i> | EUROSCARF, Frankfurt |
| CEN.HE28-h | <i>CEN.PK ura3-52 his3Δ1 leu2-3_112</i> <i>trp1-289 (YNL036w::KAN)</i> (haploid) | This study |
| CEN.HE28 + p426GAL1 | <i>CEN.PK Mat α/a ura3-52/ura3-52</i> <i>his3Δ1/his3Δ1 leu2-3_112/leu2-3_112</i> <i>trp1-289/trp1-289 (YNL036w::KAN/</i> <i>YNL036w)</i> + p426GAL1 | This study |
| CEN.HE28-h + p426GAL1 | <i>CEN.PK ura3-52 his3Δ1 leu2-3_112</i> <i>trp1-289 (YNL036w::KAN)</i> + p426GAL1 (haploid) | This study |

| | | |
|-----------------------------------|--|--------------------------------|
| CEN.HE28-h + p426-CAS1-His | <i>CEN.PK ura3-52 his3Δ1 leu2-3_112 trp1-289 (YNL036w::KAN)</i> + p426-CAS1-RGSHis ₆ under the <i>GAL1</i> promoter (haploid) | This study |
| CEN.HE28-h + p426-CAS2-His | <i>CEN.PK ura3-52 his3Δ1 leu2-3_112 trp1-289 (YNL036w::KAN)</i> + p426-CAS2-RGSHis ₆ under the <i>GAL1</i> promoter (haploid) | This study |
| CEN.HE28-h + p426-CAS3-His | <i>CEN.PK ura3-52 his3Δ1 leu2-3_112 trp1-289 (YNL036w::KAN)</i> + p426-CAS3-RGSHis ₆ under the <i>GAL1</i> promoter (haploid) | This study |
| CEN.HE28-h + p426-CAS4-His | <i>CEN.PK ura3-52 his3Δ1 leu2-3_112 trp1-289 (YNL036w::KAN)</i> + p426-CAS4-RGSHis ₆ under the <i>GAL1</i> promoter (haploid) | This study |
| <i>SORDARIA MACROSPORA</i> | | |
| S48977 | wild type | U. Kück, Bochum |
| S66001 | $\Delta ku70::nat^R$; fertile | Pöggeler and Kück 2006 |
| S23442 | mutation in <i>fus1-1</i> gene; brownish ascospores | Nowrousian <i>et al.</i> 2012 |
| S67813 | mutation in gene <i>r</i> ; pink ascospores | U. Kück, Bochum |
| $\Delta cas1$ | $\Delta cas1::hyg^R$; ssi; fertile | Elleuche and Pöggeler 2009b |
| $\Delta cas2$ | $\Delta cas2::hyg^R$; ssi; fertile | Elleuche and Pöggeler 2009b |
| $\Delta cas3$ | $\Delta cas3::hyg^R$; ssi; fertile | Elleuche and Pöggeler 2009b |
| $\Delta cas1/2$ | $\Delta cas1::hyg^R, \Delta cas2::hyg^R$; ssi from crossing of $\Delta cas1$ and $\Delta cas2$; sterile | Elleuche and Pöggeler 2009b |

| | | |
|---|--|-----------------------------|
| $\Delta cas1/3$ | $\Delta cas1::hyg^R, \Delta cas3::hyg^R$; ssi; fertile | Elleuche and Pöggeler 2009b |
| $\Delta cas2/3$ | $\Delta cas2::hyg^R, \Delta cas3::hyg^R$; ssi; fertile | Elleuche and Pöggeler 2009b |
| $\Delta cas4$ | $\Delta cas4::hyg^R$; ssi; fertile | This study |
| $\Delta cas1/4$ | $\Delta cas1::hyg^R, \Delta cas4::hyg^R$; ssi; fertile | This study |
| $\Delta cas2/4$ | $\Delta cas2::hyg^R, \Delta cas4::hyg^R$; ssi; fertile | This study |
| $\Delta cas3/4$ | $\Delta cas3::hyg^R, \Delta cas4::hyg^R$; ssi; fertile | This study |
| $\Delta cas1/2/3$ | $\Delta cas1::hyg^R, \Delta cas2::hyg^R, \Delta cas3::hyg^R$; ssi from crossing of $\Delta cas1/4$ and $\Delta cas2/3$; sterile | This study |
| $\Delta cas1/2/4$ | $\Delta cas1::hyg^R, \Delta cas2::hyg^R, \Delta cas4::hyg^R$; ssi from crossing of $\Delta cas2/4$ and $\Delta cas2/3$; sterile | This study |
| $\Delta cas2/3/4$ | $\Delta cas2::hyg^R, \Delta cas3::hyg^R, \Delta cas4::hyg^R$; ssi; fertile | This study |
| $\Delta cas1/3/4$ | $\Delta cas1::hyg^R, \Delta cas3::hyg^R, \Delta cas4::hyg^R$; ssi; fertile | This study |
| $\Delta cas1/2/3/4$ | $\Delta cas1::hyg^R, \Delta cas2::hyg^R, \Delta cas3::hyg^R, \Delta cas4::hyg^R$; ssi from crossing of $\Delta cas1/3/4$ and $\Delta cas2/3/4$; sterile | This study |
| S23442::pDS23-eGFP | S23442 + <i>egfp</i> ^{ect} , <i>nat</i> ^R ; fertile | This study |
| S23442::pDS23-CAS4-eGFP | S23442 + <i>cas4-egfp</i> ^{ect} , <i>nat</i> ^R ; fertile | This study |
| S23442::pRSnat-CAS44SS-eGFP | S23442 + <i>cas4</i> secretion signal (aa1-20)- <i>egfp</i> ^{ect} , <i>nat</i> ^R ; fertile | This study |
| S48977::pDS23-CAS4SS-eGFP-KDEL | S48977 + <i>cas4</i> secretion signal (aa 1-20)- <i>egfp</i> -KDEL ^{ect} , <i>hyg</i> ^R ; fertile | This study |
| S48977::pDS23-CAS4SS-eGFP-KDEL + pDsREDKDEL | S48977 + <i>cas4</i> secretion signal (aa1-20)- <i>egfp</i> -KDEL ^{ect} + <i>DsRED</i> -KDEL ^{ect} , <i>hyg</i> ^R , <i>nat</i> ^R ; fertile | This study |

hyg^R, hygromycin resistance; *nat*^R, nourseothricin resistance; *cam*^R, chloramphenicol resistance; ssi, single spore isolate; ect, ectopic

2.1.2 Plasmids

Table 2: Overview of the used and generated plasmids in this study.

| Plasmids | Characteristics | Source |
|------------------------------|---|---------------------------------|
| VECTOR BACKBONES | | |
| pRS426 | <i>URA3</i> | Christianson <i>et al.</i> 1992 |
| pRSnat | <i>URA3</i> , <i>nat</i> -cassette | Klix <i>et al.</i> 2010 |
| KNOCKOUT | | |
| pCB1003 | <i>hph</i> , <i>amp</i> ^R | Carroll <i>et al.</i> 1994 |
| p1783-1 | <i>egfp</i> under control of <i>gpd</i> promoter and <i>trpC</i> terminator of <i>A. nidulans</i> , <i>hph</i> -cassette | Pöggeler <i>et al.</i> 2003 |
| pRS426-Δ <i>cas4</i> | 1036 bp of the 5'-ORF region and 737 bp of 3'-ORF region of <i>cas4</i> interrupted by the <i>hph</i> -cassette in pRS426 | This study |
| YEAST COMPLEMENTATION | | |
| p426GAL1 | <i>GAL1</i> promoter, <i>URA3</i> , <i>amp</i> ^R | Mumberg <i>et al.</i> 1994 |
| p426-CAS1-His | <i>cas1</i> under the control of the <i>GAL1</i> promoter, <i>URA3</i> , <i>amp</i> ^R , C-His ₆ | This study |
| p426-CAS2-His | <i>cas2</i> under the control of the <i>GAL1</i> promoter, <i>URA3</i> , <i>amp</i> ^R , C-His ₆ | This study |
| p426-CAS3-His | <i>cas3</i> under the control of the <i>GAL1</i> promoter, <i>URA3</i> , <i>amp</i> ^R , C-His ₆ | This study |
| p426-CAS4-His | <i>cas4</i> under the control of the <i>GAL1</i> promoter, <i>URA3</i> , <i>amp</i> ^R , C-His ₆ | This study |

CAS4 LOCALIZATION

| | | |
|------------------------|--|-------------------------------|
| pDS23-eGFP | <i>egfp</i> under control of the <i>gpd</i> promoter and <i>trpC</i> terminator of <i>A. nidulans</i> , <i>URA3</i> ; <i>nat</i> -cassette | Nowrousian unpublished |
| pDsREDKDEL | <i>pro41</i> secretion signal- <i>DsRED</i> ^{ect} , <i>nat</i> ^R ; fertile | Nowrousian <i>et al.</i> 2007 |
| pDS23-CAS4-eGFP | Full-length <i>cas4-egfp</i> ^{ect} , <i>nat</i> ^R | This study |
| pRSnat-CAS4SS-eGFP | <i>cas4</i> secretion signal (aa 1-20)- <i>egfp</i> ^{ect} , <i>nat</i> ^R | This study |
| pDS23-CAS4SS-eGFP-KDEL | <i>cas4</i> secretion signal (aa 1-20)- <i>egfp</i> -KDEL ^{ect} , <i>hyg</i> ^R ; | This study |

PROTEIN EXPRESSION

| | | |
|------------|---|-----------------|
| pQE30 | N-His ₆ expression vector, <i>P</i> _{T5} / <i>O</i> _{lac} , ColEI ori, <i>amp</i> ^R | Qiagen, Germany |
| pET22b(+) | <i>P</i> _{T7} , <i>amp</i> ^R , <i>ori</i> _{pBR322} , <i>lacI</i> , C-His ₆ | Novagen, USA |
| pQE30-CAS1 | <i>cas1</i> in pQE30, <i>amp</i> ^R | This study |
| pET-CAS2 | <i>cas2</i> in pET22b(+), <i>amp</i> ^R | This study |
| pET-CAS3 | <i>cas3</i> in pET22b(+), <i>amp</i> ^R | This study |
| pET-CAS4 | <i>cas4</i> in pET22b(+), <i>amp</i> ^R | This study |

hyg^R, hygromycin resistance; *nat*^R, nourseothricin resistance; *amp*^R, ampicillin resistance; ect, ectopic; C-His₆ and N-His₆, C- and N-terminally 6 × histidine tag

2.1.3 Primers

Table 3: Overview of the used oligonucleotides.

| Oligomer name | Sequence (5' – 3') | Binding position |
|-------------------|----------------------|---------------------|
| SEQUENCING | | |
| CAS1Seqf | ACCGCAACATCGCCAACATT | <i>cas1</i> 197-216 |
| CAS1Seqr | AAGGACACCGCCGATGCGGC | <i>cas1</i> 360-343 |
| CAS2-f | ACCCCTGGCTGCGCAACATC | <i>cas2</i> 392-411 |
| CAS2-r | TTCTCGGCATACGACTGCTG | <i>cas2</i> 557-538 |
| CAS3Seqf | ACCTTCGACAAAGGCCATCT | <i>cas3</i> 64-83 |

| | | |
|------------|------------------------|---------------------|
| CAS3Seqr | CATAAGCATCCTCATTCTTG | <i>cas3</i> 322-303 |
| CAS4Seqf | GGTTCCGCATCAGGAGAGCC | <i>cas4</i> 563-582 |
| CAS4Seqr | CGACGTCAATGTAAGTGCCG | <i>cas4</i> 445-426 |
| CAS4Seq1-f | ATGACCCTCGGCGAGAAGCA | <i>cas4</i> 289-308 |
| pRS_seq_F | GGCCTCTTCGCTATTACGCCAG | pRS426 1859-1880 |
| pRS_seq_R | CACTCATTAGGCACCCCAGG | pRS426 2262-2243 |

KNOCKOUT

| | | |
|-------------|---|--|
| CAS4_5f | <u>GTAACGCCAGGGTTTTCCAGTCA</u> <u>CGACGCGGTTGGGAATCGTGACGG</u> C | pRS426 1920-1948 <i>cas4</i> -1043-(-)1023 |
| CAS4_5r | <u>CAAAAAATGCTCCTTCAATATCAG</u> <u>TTAACCGACGGGAGGAAGATGTGT</u> G | <i>hph</i> (-)337-(-)366 <i>cas4</i> -25-(-)6 |
| CAS4_3f | <u>GAGTAGATGCCGACCGGGAACCA</u> <u>GTTAACGGTGCGCCACGGTCCTC</u> CT | <i>hph</i> 1386-1414 <i>cas4</i> 799-818 |
| CAS4_3r | <u>GCGGATAACAATTTACACAGGAA</u> <u>ACAGCGCATCGTTAGGCACTGCTC</u> C | pRS426 2197-2169 <i>cas4</i> 1536-1517 |
| 5f-f | CAAGTTCCAACCGTTCTTCT | <i>cas4</i> -1067-(-)1048 |
| 3r-r | CCTTCCCCTCGTCACTCTT | <i>cas4</i> 1563-1544 |
| tC1-o | CCTGGACGACTAAACCAAAA | <i>hph</i> (-)273-(-)292 |
| h3-o | GATGGCTGTGTAGAAGTACT | <i>hph</i> 955-974 |
| hph-f | GTAACTGATATTGAAGGAGCATT TTTTGG | <i>hph</i> 1-29 |
| hph-r | GTAACTGGTTCCCGGTCGGCATC TACTC | <i>hph</i> 1414-1386 |
| cynT1-GFP-f | CCATGGTTTCTCCCGAGAACACCT TCCAC | <i>cas1</i> 4-21 |
| cynT1-r | GTCGACCCATGGCCTGCGCAGCAG CAATCTCCGC | <i>cas1</i> 701-686 |

| | | |
|-------------|---|---------------------|
| cynT2-GFP-f | CCATGGAATTTAGCACACGTCTGG GTCCTTC | <i>cas2</i> 4-23 |
| cynT2-r | AAGCTTCCATGGCGGCGGTCAGGT TATAGATCTTC | <i>cas2</i> 674-653 |
| cynT3-GFP-f | CCATGGAACCCGTCACCAACGAAG ACATCG | <i>cas3</i> 4-25 |
| cynT3-r | GTCGACCCATGGCAACAACCCTCA CCGTCTTGCCCCG | <i>cas3</i> 521-499 |

YEAST COMPLEMENTATION

| | | |
|-------------------------------|---|--|
| p426RGS _{HIS} CAS1-r | <u>GACGGTATCGATAAAGCTTGATATC</u> <u>GAATTCTAGTGATGGTGATGGTGAT</u> <i>GCGATCCTCTCTGCGCAGCAGCAA</i> TCT | <u>p426GAL1 4142-4114</u> <i>cas1</i> 702-686 italic: RGS6xHis |
| p426RGS _{HIS} CAS2-r | <u>GACGGTATCGATAAAGCTTGATATC</u> <u>GAATTTTAGTGATGGTGATGGTGAT</u> <i>GCGATCCTCTGGCGGTCAGGTTATA</i> GA | <u>p426GAL1 4142-4114</u> <i>cas2</i> 674-658 italic: RGS6xHis |
| p426RGS _{HIS} CAS3-r | <u>GACGGTATCGATAAAGCTTGATATC</u> <u>GAATTTCAAGTGATGGTGATGGTGAT</u> <i>GCGATCCTCTAACAACCCTCACCGT</i> CT | <u>p426GAL1 4142-4114</u> <i>cas3</i> 522-506 italic: RGS6xHis |
| p426RGS _{HIS} CAS4-r | <u>GACGGTATCGATAAAGCTTGATATC</u> <u>GAATTTTAGTGATGGTGATGGTGAT</u> <i>GCGATCCTCTCTGCGCCGGCTGAG</i> ACG | <u>p426GAL1 4142-4114</u> <i>cas4</i> 1044-1028 italic: RGS6xHis |
| p426CAS1-f | <u>TAGAACTAGTGATCCCCGGGCT</u> <u>GCAGGATGTCTCCCGAGAACACCT</u> T | <u>p426GAL1 4084-4113</u> <i>cas1</i> 1-20 |
| p426CAS2-f | <u>TAGAACTAGTGATCCCCGGGCT</u> <u>GCAGGATGGAAAAAGACCGCAAG</u> AA | <u>p426GAL1 4084-4113</u> <i>cas2</i> 181-201 |

| | | |
|---------------------|--|---|
| p426CAS3-f | <u>TAGAACTAGTGGATCCCCCGGGCT</u> <u>GCAGGATGCCCCGTCACCAACGAAG</u> A | <u>p426GAL1 4084-4113</u> <i>cas3</i> 1-20 |
| p426CAS4-f | <u>TAGAACTAGTGGATCCCCCGGGCTG</u> <u>CAGGATGCTCTGCTCGCACAAATAC</u> | <u>p426GAL1 4084-4113</u> <i>cas4</i> 1-20 |
| LOCALIZATION | | |
| pDS23Cas4eGFP-f | <u>CACTTCATCGCAGCTTGACTAACA</u> <u>GCTACATGGCCAGGATGCTCAAGT</u> C | <u>pDS23-eGFP 2778-</u> <u>2806</u> <i>cas4</i> 1-20 |
| pDS23Cas4eGFP-r | <u>GTGAACAGCTCCTCGCCCTTGCTC</u> <u>ACCATCTGCGCCGGCTGAGACGCA</u> G | <u>pDS23-eGFP 2847-</u> <u>2819</u> <i>cas4</i> 4081-4061 |
| pRS426GPDf2 | <u>GTAACGCCAGGGTTTTCCAGTCA</u> <u>CGACGGTACAGTGACCGGTGACTC</u> T | <u>pRS426 1920-1948</u> <i>Pgpd</i> 2748-2767 |
| GPDCAS4-r | <u>ACCATCAACGACTTGAGCATCCTG</u> <u>GCCATGTAGCTGTTAGTCAAGCTG</u> CG | <i>cas4</i> 29-1 <i>Pgpd</i> 858-838 |
| cas4ssgfp-f | <u>ATGGCCAGGATGCTCAAGTCGTTG</u> <u>ATGGTGGTAGCGGCCGCGTCTGTG</u> <u>ACGCCCCTCTGGTCGGTGAGCAAG</u> GGCGAGGAGCT | <i>cas4</i> 1-63 <i>egfp</i> 3-23 |
| pRS426GFPprev | <u>GCGGATAACAATTTACACAGGAA</u> <u>ACAGCTCGAGTGGAGATGTGGAGT</u> G | <u>pRS426 2197-2169</u> TtrpC 5137-5118 |
| CAS4GFP-f | <u>CACTTCATCGCAGCTTGACTAACA</u> <u>GCTACATGGCCAGGATGCTCAAGT</u> C | <u>pDS23-eGFP 2778-</u> <u>2806</u> <i>cas4</i> 1-20 |
| GFP-r | CTTGTACAGCTCGTCCATGCCGAG AGTG | <i>egfp</i> 4343-4316 without stop codon |

| | | |
|------------|--|---|
| TrpCKDEL-f | <u>TGGACGAGCTGTACAAGGACGAG</u> <u>CTCTAAGATCCACTTAACGTTACT</u> <u>GA</u> | <i>egfp</i> 4327-4343 bold: KDEL <i>TtrpC</i> 4369-4388 |
| pDS23GFP-r | <u>CAAACGACGAGCGTGACACCACG</u> <u>ATGCCTTCGAGTGGAGATGTGGAG</u> TG | <i>TtrpC</i> 766-749 <u>pDS23</u> 5621-5593 |

OVEREXPRESSION

| | | |
|-------------|---|---|
| CynT1-pQE_f | <i>GGATCCTCTCCCGAGAACACCTTCC</i> AC | <i>cas1</i> 3-24 |
| CynT1_r | <i>GTCGACCCATGGCCTGCGCAGCAG</i> CAATCTCCGC | <i>cas1</i> 702-682 |
| CAS2pET22-f | <u>GGAGATATACATATGATGGAAAA</u> AGACCGCAAGAA | <u>pET22b(+)</u> 5193-5207 <i>cas2</i> 181-200 |
| CAS2pET22-r | <u>GGTGGTGGTGCTCGAGGGCGGTCA</u> GGTTATAGATCT | <u>pET22b(+)</u> 5346-5331 <i>cas2</i> 675-656 |
| Cas3-pet-f | <u>GGAGATATACATATGATGCCCGTC</u> ACCAACGAAGA | <u>pET22b(+)</u> 5193-5207 <i>cas3</i> 1-20 |
| Cas3-pet-r | <u>GGTGGTGGTGCTCGAGAACAACCC</u> TCACCGTCTTGC | <u>pET22b(+)</u> 5346-5331 <i>cas3</i> 522-503 |
| Cas4-pet-f | <u>GGAGATATACATATGATGCTCTGC</u> TCGCACAATAC | <u>pET22b(+)</u> 5193-5207 <i>cas4</i> 61-80 |
| Cas4-pet-r | <u>GGTGGTGGTGCTCGAGCTGCGCCG</u> GCTGAGACGCAG | <u>pET22b(+)</u> 5346-5331 <i>cas4</i> 1044-1025 |
| T7Prom | TAATACGACTCACTATAGGG | <u>pET22b(+)</u> 5117-5135 |
| T7Term | CCGCTGAGCAATAACTAGC | <u>pET22b(+)</u> 5425-5407 |

REAL-TIME PCR

| | | |
|-----------|----------------------|-----------------------------------|
| cas4-RT-f | TGTCGACGCAGACGCTAAGG | <i>cas4</i> 869-888 |
| cas4-RT-r | GCAGCCCCAGAAGAAGCAAA | <i>cas4</i> 1028-1009 |
| SSU-f | ATCCAAGGAAGGCAGCAGGC | <i>Nc</i> gDNA SC8 93867-93886 |

| | | |
|------------|---|-----------------------------------|
| SSU-r | TGGAGCTGGAATTACCGCG | <i>Nc</i> gDNA SC8 94028-94046 |
| Act2In-f | AAGGAGAAGCTCTGCTACGT | <i>SMAC_04416</i> 1119- 1138 |
| Act2In-r | GAACCACCGATCCAGACGGA | <i>SMAC_04416</i> 1577- 1558 |
| CAS4-pQE-f | <i>GCATGCGCCAGGATGCTCAAGTCGT</i> TG | <i>cas4</i> 3-24 |
| CAS4-pQE-r | <i>AAGCTTTACTGCGCCGGCTGAGAC</i> GCAG | <i>cas4</i> 1278-1256 |

Underlined: Overhangs for homologous recombination or In-fusion

Italic: restriction sites

2.1.4 Chemicals and materials

Acetic acid (Roth GmbH, 3738.2), acrylamide (Rotiphorese[®] Gel 40 37,5:1) (Roth GmbH, 3029.1), adenine (Sigma-Aldrich, 01830-50G), agar-agar (Roth GmbH, 5210.2), agar-agar SERVA high gel-strength (SERVA, 11396.03), agarose (Biozym Scientific GmbH, 840004), albumin bovine (Sigma-Aldrich, A9647-50G), ammonium chloride (VWR International, BDH0208-500G), ammonium sulfate (AppliChem, A1032,1000), ammonium iron (II) sulfate (Roth GmbH, 203505-5G), ampicillin (Sigma-Aldrich, A9518-25G), arginine (AppliChem, A3709,0250), ammonium persulfate (APS) (Roth GmbH, 9592.3), bacto-yeast-extract (Oxoid LTD., LP0021), bio malt maize extract (Brau-Partner Kling, 115), biotin (Sigma-Aldrich, B4501-1G), boric acid (Roth GmbH, 6943.1), bromophenol blue (AppliChem, A3640,0005), calcium chloride (Roth GmbH, CN92.1), calcium chloride dihydrate (Roth GmbH, 5239.1), carbonic anhydrase from bovine erythrocytes (Sigma-aldrich, C3934-100MG), chloroform (Merck Millipore, 1024451000), citric acid monohydrate (Roth GmbH, 3958.1), copper (II) sulfate 5-hydrate (Roth GmbH, P024.1), Corning[®] Spin-X[®] UF concentrators (Corning, 431489), coomassie brilliant blue G-250 (Roth GmbH, 9598.1), coomassie brilliant blue R-250 (Roth GmbH, 3862.1) CSM-Ade-His-Leu-Trp-Ura (MP Biomedicals, 4550-122), desoxynucleotid triphosphate (dNTPs) (Thermo Scientific, R0191), Difco[™] skim milk (BD Biosciences, 232100), Difco[™] yeast nitrogen base w/o amino acids and ammonium sulfate (BD Biosciences, 233520), dimethylformamide (Roth GmbH, T921.1), di-sodium hydrogen

phosphate (Merck-Millipore, 1065855000), DMSO (dimethyl sulfoxide) (Merck Millipore, 1029310500), DTT (1,4-Dithiothreitol) (AppliChem, A1101,0025), EDTA (ethylenediamine tetraaceticacid disodium salt dihydrate) (Roth GmbH, 8043.2), electroporation cuvettes (VWR International, 732-1137), ethanol (VWR International, 20821.321), ethidium bromide (Sigma-Aldrich, 46065), “Flat Optical 8-Cap Strip” 0.2 ml (Biozym, 712100), formaldehyde (Roth GmbH, 4979.2), formamide (Sigma-Aldrich, 47670), formic acid (Merck Millipore, 1002641000), galactose (AppliChem, A1131,0500), “Gene Ruler DNA Ladder Mix” (Thermo Scientific, SM0331 or SM0311), geneticindisulfate (G418) (Roth GmbH, CP11.1), “GeneScreen Hybridization Transfer Membrane” (PerkinElmer Lifesciences, NEF988001PK), glass beads Ø 0.25-0.5 mm (Roth GmbH, A553.1), glass beads Ø 2.85-3.45 mm (Roth GmbH, A557.1), glucose (AppliChem, A3617,1000), glycine (Roth GmbH, 0079.1), glycerine (VWR International, 24388.295), HEPES (4-(2-hydroxyethyl)-1-piperazineethanesulfonicacid) (Roth GmbH, 9105.4), histidine (Merck Millipore, 1.04351.0025), hydrochloric acid (Roth GmbH, 4625.2), hydrogen peroxide 30% (H₂O₂) (Merck Millipore, 8.22287.2500), hygromycin B (Merck-Millipore, 400051-10MU), IPTG (isopropyl-β-D-galactopyranoside) (Roth GmbH, 2316.3), iron (II) chloride (Roth GmbH, 231-753-5), iron(II) sulfate heptahydrate (Sigma-Aldrich, 31236), imidazole (Roth GmbH, X998.1), isopropanol (AppliChem, A0900,2500GL), kanamycin sulfate (Sigma-Aldrich, 60615), leucine (AppliChem, A1426,0100), lithium acetate (Roth GmbH, 5447.1), maize flour (Mühle Levers, Bochum, Germany), magnesium chloride hexahydrate (Merck Millipore, 1.05833.1000), magnesium sulfate heptahydrate (Roth GmbH, P027.2), manganese (II) chloride tetrahydrate (Roth GmbH, T881.1), manganese (II) sulfate monohydrate (Roth GmbH, 4487.1), methanol (VWR International, 20864.320), MOPS (3-(N-morpholino)-propane sulfonic acid) (AppliChem, A2947,0500), Ni-NTA agarose (Qiagen, 1018244), nitrocellulose transfer membrane Protran[®] BA (Whatman, 10401196), Nonident[®] P40 (AppliChem A2239,0025), nourseothricin (WernerBioAgents, 5004000), PEG 6000 (Sigma-Aldrich, 81255), phenol (AppliChem, A1153,0500), phosphoric acid (Roth GmbH, 6366.1), PMFS (phenylmethylsulfonyl) fluoride (Sigma-Aldrich, P-7626), potassium acetate (Merck Millipore, 1.04820.1000), potassium chloride (AppliChem, A3582,1000), potassium dihydrogen phosphate (Merck Millipore, 1.04873.1000), potassium hydroxide (Roth GmbH, 6751.1), potassium nitrate (Merck Millipore, 1.05063.1000), RNA loading dye (2x) (Thermo Scientific, R0641), Rotiphorese Gel 40 (Roth GmbH, 3030.2), SDS (sodium dodecyl sulfate) (Roth GmbH, 4360.2), sodium acetate (Roth GmbH, 6773.2), sodium chloride (AppliChem, A3597,1000), sodium dihydrogen phosphate monohydrate (Merck Millipore, 1.06346.1000),

sodium hydroxide (VWR International, 28244.295), sodium molybdate-dihydrate (Sigma-Aldrich, 31439), sorbitol (Roth GmbH, 6213.1), β -mercaptoethanol (Roth GmbH, 4227.1), sterile filter 0.45/0.2 μm (Sarstedt, 83.1826/83.1826.001), sucrose (AppliChem, A4734,1000), TEMED (N,N,N',N'-tetramethylethylenediamine) (Roth GmbH, 2367.3), Tris (tris-hydroxymethyl-aminomethane) (Roth GmbH, AE15.2), Tris/HCl (Roth GmbH, 9090.3), Trizol (Invitrogen,15596026), tryptone/peptone (Roth GmbH, 8952,2), tryptophan (MP Biomedicals, 4061-012), Tween 20[®] (AppliChem, A4974,0100), uracil (MP Biomedicals, 4061-212), urea (Roth GmbH, 2317.3), whatman paper B002 580x600 mm (Schleicher & Schuell, 88-3852), X-ray films (Fujifilm, 4741019236), xylene cyanol (AppliChem, A4976,0005), yeast extract (Roth GmbH, 2904.1), zinc chloride (Sigma-Aldrich, 14424), zinc sulfate heptahydrate (Roth GmbH, K301.1).

2.1.5 Kits

AlkPhos Direct Labelling and Detection Kit (Amersham, GE Healthcare, RPN3680), CloneJET PCR Cloning Kit (Thermo Scientific, K1231), High Prime DNA Labelling and Detection Starter Kit II (Roche, 1585614), HiSpeed Plasmid Midi Kit (Qiagen, 12643), In-Fusion[®] HD Cloning Kit (Clontech, 639648), LumiMax Superoxide Anion Detection Kit (Agilent Technologies, 204525), Protein Deglycosylation Mix (NEB, P6039S), Qiagen PCR Cloning Kit (Qiagen, 231124), QIAprep Spin Miniprep Kit (Qiagen, 27106), QIAquick Gel Extraction Kit (Qiagen, 28704), QIAquick PCR Purification Kit (Qiagen, 28104), qPCR Mastermix for SYBR GreenI (Eurogentec, RT-SN2X-03T), Transcriptor High Fidelity cDNA Synthesis Kit (Roche, 05091284001).

2.1.6 Enzymes

Calf Intestine Alkaline Phosphatase (CIAP) (Thermo Scientific, EF0341), DNase I (Thermo Scientific, EN0521), natuzym (Schliessmann, 5090), HotstarTaq Master Mix (Qiagen, 203443), lysozyme (Serva, 28262.03), MolTaq DNA polymerase (Molzym, P-010-1000), Phusion[®] Hot Start High-Fidelity DNA polymerase (Thermo Scientific, F-549S), restriction endonucleases (Thermo Scientific), RNase A (Roth GmbH, 7164.1), T4 DNA ligase (Thermo Scientific, EL0011), Zymolyase[®] 20T (amsbio, 120491-1)

2.1.7 Buffers and solutions

Amino acid stock solutions

| | |
|----------------------------|------------------------------------|
| Adenine stock solution: | 0.02% (w/v) adenine in A. dest. |
| Leucine stock solution: | 1% (w/v) leucine in A. dest. |
| Histidine stock solution: | 1% (w/v) histidine in A. dest. |
| Uracil stock solution: | 0.02% (w/v) uracil in A. dest. |
| Tryptophan stock solution: | 0.02% (w/v) tryptophan in A. dest. |

Plasmid isolation by Birnboim and Doly (1979)

| | |
|------------------|--|
| BD solution I: | 50 mM glucose, 10 mM EDTA, 25 mM Tris/HCl, 0.2% lysozyme |
| BD solution II: | 0.4 M NaOH, 2% (w/v) SDS (mixed 1:1) |
| BD solution III: | 3 M potassium acetate, 1.8 M formic acid |

Southern Blot solutions

| | |
|------------------------------|---|
| Buffer I: | 0.25 M HCl |
| Buffer II: | 0.5 M NaOH, 1.5 M NaCl |
| Buffer III: | 1.5 M NaCl, 0.5 M Tris |
| First washing buffer: | 2 M Urea, 0.1% SDS, 50 mM NaH ₂ PO ₄ x H ₂ O pH 7, 150 mM NaCl, 1mM MgCl ₂ , 0.2% blocking reagent |
| Second washing buffer (20x): | 1 M Tris pH 10, 2 M NaCl, 1 mM MgCl ₂ |

Transformation of *S. macrospora*

| | |
|------------------------------|--|
| Protoplast buffer (PPP): | 13 mM Na ₂ HPO ₄ , 45 mM KH ₂ PO ₄ , 0.6 M KCl, pH 6.0 |
| Transformation buffer (TPS): | 1 M sorbitol, 80 mM CaCl ₂ , pH 7.4 |
| Topagar: | 0.8 M NaCl, 0.8% agar-agar |

Transformation of *S. cerevisiae*

| | |
|------------------------|-----------------------------------|
| Lithium acetate (10x): | 1 M lithium acetate, pH 7.5 |
| TE(D) (10x): | 10 mM Tris/HCl, 1 mM EDTA, pH 7.2 |
| DTT: | 1M DTT in H ₂ O |
| Sorbitol: | 1M sorbitol in H ₂ O |

| | |
|------------------------------------|--|
| <i>S. macrospora</i> lysis buffer: | 10 mM Tris/HCl pH 8.0, 1 mM EDTA, 100 mM NaCl, 2% SDS |
| Trace-element stock solution: | 5% (w/v) citric acid (C ₆ H ₈ O ₇ monohydrate), 5% (w/v) ZnSO ₄ heptahydrate, 1% (w/v) Fe(NH ₄) ₂ (SO ₄) ₂ hexahydrate, 0.25% (w/v) CuSO ₄ pentahydrate, 0.05% (w/v) MnSO ₄ monohydrate, 0.05% (w/v) H ₃ BO ₃ , 0.05% (w/v) Na ₂ MoO ₄ dihydrate |
| Biotin stock solution: | 0.01% (w/v) biotin, 50% (v/v) ethanol |

DNA methods

| | |
|-----------------------|---|
| dNTP mix (10 mM): | 10 mM dATP, dCTP, dGTP, dTTP each in A. dest. |
| EtBr stock solution: | 10 mg/mL ethidium bromide in A. dest. |
| DNA loading dye (6x): | 0.25% (w/v) xylene cyanol FF, 0.25% (w/v) bromophenol blue, 40% (w/v) sucrose |
| MOPS buffer (10x): | 0.2 M MOPS pH 7.0, 50 mM sodium acetate, 10 mM EDTA |
| TBE (10x): | 1 M Tris/HCl, 1 M boric acid, 20 mM EDTA, pH 8.3 |

Protein methods

| | |
|----------------------------|--|
| Protein loading dye (5x): | 125 mM Tris/HCl pH 6.8, 50% (v/v) glycerine, 2% (w/v) SDS, 0.01% (w/v) bromophenol blue, 0.01% (w/v) β-mercaptoethanol |
| IPTG stock solution: | 1 M in A. dest. |
| Ampicillin stock solution: | 100 mg/mL in A. dest. |
| SDS-PAGE-running buffer: | 1.5% (w/v) Tris pH 8.3, 9.4% (w/v) glycine, 20% (w/v) SDS |
| TBST: | 10 mM Tris/HCl pH 7.5, 150 mM NaCl, 0.1% (v/v) Tween 20 [®] |
| Towbin buffer: | 192 mM glycine, 25 mM Tris, 20% (v/v) methanol |

| | |
|------------------------------|---|
| SDS-gel staining solution: | 0.02% (w/v) coomassie brilliant blue R250, 0.02% (w/v) coomassie brilliant blue G250, 42.5% (v/v) ethanol 0.5% (v/v) methanol 10% (v/v) acetic acid |
| SDS-gel destaining solution: | 45% (v/v) ethanol 10% (v/v) acetic acid |
| PBS (10x): | 1.4 M NaCl, 27 mM KCl, 101 mM Na ₂ HPO ₄ , 17.6 mM KH ₂ PO ₄ , pH 7.4 |
| Elution buffer: | 250 mM imidazole, 300 mM NaCl, 50 mM NaH ₂ PO ₄ |
| Lysis buffer: | 20 mM imidazole, 300 mM NaCl, 50 mM NaH ₂ PO ₄ |
| Bradford-reagent: | 100 mg Coomassie, 50 mL ethanol (96%), 100 mL H ₃ PO ₄ (85%), ad 1L H ₂ O |

2.1.8 Cultivation media

E. coli

LB: 1% (w/v) tryptone/peptone, 0.5% yeast extract, 0.5% NaCl, pH 7.2; 1.5% (w/v) agar-agar for solid medium; addition of ampicillin (100 µg/mL) for selection

TB: 1.86% (w/v) KCl, 0.66% (w/v) MnCl₂ tetrahydrate, 0.3% (w/v) HEPES, 0.22% (w/v) CaCl₂ dihydrate, pH 6.7.

SOB: 2% (w/v) tryptone, 0.5% (w/v) yeast extract, 10 mM MgCl₂, 10 mM MgSO₄, 10 mM NaCl, 2.5 mM KCl, pH 7.5.

S. cerevisiae

YEPD: 2% (w/v) tryptone, 2% (w/v) glucose, 1% (w/v) yeast extract, pH 5.8; 1.5% (w/v) agar-agar SERVA for solid medium.

YEPDA: YEPD + 0.003% (w/v) adenine, pH 6.5; 1.5% (w/v) agar-agar SERVA for solid medium.

SD: 0.17% (w/v) Difco™ Yeast Nitrogen Base w/o amino acids and ammonium sulfate, 2% (w/v) glucose, 0.064% (w/v) CSM-Ade-His-Leu-Trp-Ura (0.002% (w/v) L-methionine, 0.005% (w/v) L-arginine hydrochloride, L-isoleucine, L-lysine hydrochloride, L-phenylalanine, L-tryptophan, L-tyrosine each, 0.008% (w/v) L-aspartic acid, 0.01% (w/v) L-leucine and L-threonine, 0.014% (w/v) L-valine), pH 5.8; 1.5% (w/v) agar-agar SERVA for solid medium. Selection of transformants occurred by exclusion of respective amino acid(s).

SG: SD with 2% (w/v) galactose instead of glucose.

S. macrospora

BMM: 0.8% bio malt maize extract and maize flour (25 g/L), pH 6.5; 1.5% (w/v) agar-agar for solid medium; addition of hygromycin B (110 U/mL) or nourseothricin dihydrogen sulfate (50 µg/mL) for selection; 1.5% agar-agar for solid-medium

BMM sodium acetate: BMM + 0.5% (w/v) sodium acetate (sporulation induction); 1.5% agar-agar for solid-medium

CMS: 1% (w/v) glucose, 0.2% (w/v) tryptone/peptone, 0.2% (w/v) yeast extract, 0.15% (w/v) KH_2PO_4 , 0.05% (w/v) KCl, 0.05% (w/v) MgSO_4 heptahydrate, 0.37% (w/v) NH_4Cl , 10.8% (w/v) sucrose, 0.01% (v/v) trace-element stock solution (10 mg/l ZnSO_4 , 10 mg/l Fe(II)Cl_2 , 10 mg/l MnCl_2), pH 6.5; 1.5% (w/v) agar-agar for solid medium.

SWG: 1x Westergaard's (0.1% (w/v) KNO_3 , 0.1% (w/v) KH_2PO_4 , 0.05% (w/v) MgSO_4 heptahydrate, 0.01% (w/v) NaCl, 0.01% (w/v) CaCl_2 , [0.01% (v/v) trace-element stock solution + 0.1% (v/v) chloroform]), 2% (w/v) glucose, 0.1% (w/v) arginine, 0.1% (v/v) biotin stock solution, pH 6.5; 1.5% (w/v) agar-agar for solid medium; addition of hygromycin B (110 U/ml) or nourseothricin dihydrogen sulfate (50 µg/mL) for selection.

2.2 Methods

2.2.1 Cultivation of organisms

E. coli

Cultivation of *E. coli* strains was done at 37 °C or 30 °C on solid LB medium or in liquid LB medium while shaking at 200 rpm. Selection was carried out by the addition of 100 µg/mL ampicillin.

S. cerevisiae

Yeast strains were inoculated on solid YEPD medium (complete medium) and solid SD- or SG medium (minimal medium) supplemented with appropriate amino acids and incubated at 30 °C either under ambient air or in a 5% CO₂ atmosphere. Liquid cultures were incubated in corresponding liquid medium while shaking at 100 rpm.

S. macrospora

Cultivation of *S. macrospora* strains was conducted on solid corn meal medium (BMM), complex rich medium containing 10.8% sucrose (CMS) and fruiting-body development inducing SWG medium at 27 °C either under ambient air or at 5% CO₂. Liquid cultures were grown in corresponding liquid medium at 27 °C in petri dishes. For analysis of growth velocity, 30 cm long race tubes were filled with 25 mL of solid SWG and inoculated with a mycelia plug of 0.5 cm in diameter from a petri dish at one end of race tubes. The growth front was marked after 7 days and calculated in growth rate per day (Nowrousian and Cebula 2005). To induce sexual development, *S. macrospora* was grown in liquid BMM medium at 27 °C in floating cultures and in Erlenmeyer flasks with 100 mL of liquid BMM medium shaken at 130 rpm to induce vegetative development.

2.2.2 Preparation and transformation of competent microorganisms

E. coli

The preparation of chemical competent *E. coli* cells was done according to Mandel and Higa (1970) and Dagert and Ehrlich (1979) respectively. 20 mL *E. coli* cells were grown at 37°C to an OD₆₀₀ of 0.5. The cells were then harvested and gripped in 8 mL ice cold 0.1 M CaCl₂

solution and incubated for 60 – 90 min on ice. After a centrifugal step (5 min, 4 °C, 13.000 rpm) the cells were again incubated in 0.1 M CaCl₂ for 90 – 120 min. Finally, the cells were shifted with 40 µL 40% glycerol and frozen in 200 µL aliquots. For transformation of chemically competent *E. coli* cells plasmid DNA was added to thawed competent cells and incubated for 30 min on ice (Sambrook and Russell 2001). After a 90 sec heat shock at 42 °C, cells were incubated on ice for 2 min followed by the addition of 800 µL liquid LB and incubation for 1 h at 37 °C and 200 rpm. Cells were plated on solid LB medium with 100 µg/µL ampicillin.

S. cerevisiae

To introduce DNA into *S. cerevisiae* strains the electroporation method was used (Becker and Lundblad 2001). For the preparation of electro-competent *S. cerevisiae* cells, a 50 mL culture was grown to an OD₆₀₀ of 1.0 – 1.2 in YPED and ambient air or in a CO₂ chamber at 5% CO₂, respectively. The cells were subsequently pelleted and washed with LiAc and TE(D). After 45 minutes at 30 °C and 100 rpm, 0.5 mL 1M DTT were added. After additional incubation at 30 °C and 100 rpm for 15 min the cells were washed with A. dest. and 1 M sorbitol and stored in 50 – 200 µL aliquots in 1 M sorbitol for immediate usage.

For the transformation 40 µL competent cells were mixed with 500 ng DNA and electroporated in 0.2 cm electroporation cuvettes in the “Eppendorf Electroporator 2510” (Eppendorf, Germany) at 1.5 kV. After electroporation, 800 µL of 1 M sorbitol were added and 200 µL portions of the yeast suspension were plated on respective solid selection medium.

S. macrospora

For the transformation of *S. macrospora* protoplasts had to be prepared. Therefore, mycelium was inoculated in liquid BMM medium with agar pieces. After three days the mycelium was harvested and transferred into a sterile 250 mL flask and incubated with 0.4 g natuzyme in 20 mL PPP buffer for 2 h at 27 °C and 100 rpm. The next step was the separation of the cell debris from the protoplasts. Therefore, the protoplast solution was transferred on a filter (frit) to remove the debris and collect the protoplasts in falcon tubes. The solution was filled up to 50 mL with PPP buffer and centrifuged (6 min, 4 °C, 4400 rpm). After this step the protoplast solution was washed with 10 mL PPP buffer and consequently centrifuged (6 min, 4 °C, 4.400 rpm). The pelleted protoplasts were resuspended in 100 – 200 µL TPS buffer. Finally, 20 µg DNA was mixed with 100 µl protoplasts and incubated for 10 min on ice. After the addition

of 200 μL PEG 6000 TPS (0.25 g/mL) the solution was incubated for 20 more minutes at room temperature. At the end the mixture was plated on solid CMS medium in 150 μL aliquots. On the next day the plates were covered with 9 ml topagar containing the appropriate antibiotic.

2.2.3 Crossing of *S. macrospora*

Two different *S. macrospora* strains were crossed by placing two agar pieces (0.25 cm²), each containing one strain, directly towards each other on a petri dish with solid BMM medium. After incubation for 8 – 10 days at 27 °C, the crossing front formed in the middle of the petri dish containing the recombinant crossing perithecia. Single spore isolates (ssi) were done by transferring and opening the recombinant perithecia on preparation agar (6% agar-agar in A. dest.). Single spores were placed on solid BMM sodium acetate medium, supplemented with hygromycin B (110 U/mL) or nourseothricin dihydrogen sulfate (50 $\mu\text{g}/\text{mL}$) for selection, with a sterile needle to support germination.

2.2.4 Molecular biology methods

2.2.4.1 Preparation of DNA

2.2.4.1.1 Isolation of plasmid DNA from *E. coli*

For the extraction of plasmid DNA from *E. coli* the QIAprep Spin Miniprep according to the manufacturer's manual or a modified plasmid extraction protocol according to Birnboim and Doly (1979) was used. For this purpose an *E. coli* 5 mL LB culture was grown over night at 37 °C and 200 rpm. The cells were harvested by centrifugation at 5.000 rpm for 5 min. Subsequently the pellet was mixed with 200 μL of BD1, BD2 and BD3, respectively. Following another centrifugal step the obtained supernatant was mixed with 7 μL RNase (1 mg/mL) and incubated for 10 min at 37 °C. For DNA precipitation 750 μL of ice cold isopropanol was added and the mixture was incubated for 20 min at -80 °C. After centrifugation, the DNA was washed with 70% ethanol and dried under the hood. Finally, the DNA was resuspended in 100 – 200 μL distilled water.

2.2.4.1.2 Isolation of plasmid DNA from *S. cerevisiae*

To isolate recombinant plasmid DNA from *S. cerevisiae* transformants, the cells were washed down from selective media plates with 2 ml sterile water. After a centrifugation step the DNA was isolated using the QIAprep Spin Miniprep Kit according to manufacturer's manual except that 0.3 g of glass beads (\emptyset 0.25-0.5 mm) were added to the buffer P1 and cells were disrupted by vortexing.

2.2.4.1.3 Isolation of genomic DNA and RNA from *S. macrospora*

The isolation of genomic DNA from *S. macrospora* was achieved either by the phenol/chloroform extraction method according to Lecellier and Silar (1994) or a modified sodium acetate/isopropanol precipitation: After growth for three days in liquid BMM medium the mycelium was harvested, dried and grinded in liquid nitrogen. After the addition of 600 μ l lysis buffer the cells were incubated for 30 min at 70 °C. Afterwards 400 μ L of a 3 M sodium acetate solution was added followed by incubation for 10 min at -20 °C. The mixture was centrifuged for 10 min at 13.000 rpm and the obtained supernatant was mixed with same volume of ice-cold isopropanol and incubated for 20 min at -80 °C. After a new centrifugation (10 min, 4 °C, 7.000 rpm) the pellet was washed with 70% ethanol and dried under the hood. The genomic DNA was resuspended in 50 – 100 μ L distilled water.

The extraction of RNA was done according to Elleuche and Pöggeler (2009b). In brief, the mycelium was grinded to powder with liquid nitrogen and mixed with 1 mL trizol. After centrifugation for 10 min at 13.000 rpm the supernatant was transferred to a new reaction tube and mixed with 0.2 mL chloroform. Again, the mixture was centrifuged and 500 μ L of the newly obtained supernatant was mixed with the same volume of isopropanol. After incubation for 10 min at RT the RNA was centrifuged, washed with 70% ethanol and dried under the hood. Finally, the RNA was resuspended in 120 μ L water and incubated for 30 min at 1000 rpm and 60 °C.

2.2.4.2 Hydrolysis and ligation of nucleic acids

Nucleic acids were hydrolyzed using specific restriction endonucleases (1 U/1 μ g DNA) according to manufacturer's manual in setups of 10 – 100 μ L. The ligation of nucleic acids was carried out using the T4 DNA ligase as suggested by the manufacturer. To avoid self-

ligation plasmids were treated with “Calf Intestine Alkaline phosphatase” after hydrolysis and prior to ligation.

2.2.4.3 Purification of nucleic acids

Prior to transformation or ligation experiments salts from the PCR or restriction reactions needed to be removed from the aqueous nucleic acid solution. For this purpose up to 10 μL of the solution was applied on a dialysis filter (Merck-Millipore, Germany) placed onto sterile A. dest. at RT and removed after 10 min. Furthermore, DNA could also be loaded on a 1% agarose gel and isolated with the “QIAquick Gel Extraction Kit” as described by the manufacturer.

2.2.4.4 Polymerase chain reaction (PCR)

The PCR technique was used for *in-vitro* amplification of genes or gene fragments from genomic, plasmid or complementary DNA using specific forward and reverse oligonucleotides (Mullis and Faloona 1987; Saiki *et al.* 1988). Two different polymerases were used according to the manufacturer’s description: For PCRs where a low error rate was needed the Phusion[®] Hot Start High-Fidelity DNA polymerase was used while the MolTaq DNA polymerase was used for analytical and colony-PCR. The reactions were carried out in the cycler machines “Eppendorf Mastercycler egradient S” (Eppendorf, Germany) or “iCycler” (BioRad, USA) as suggested by the enzyme manufacturer’s. Components used for the standard 50 μL PCR reactions for Phusion and MolTaq polymerase were as follows:

Table 4: Composition of PCR reactions for Phusion and MolTaq-polymerases

| components | Phusion polymerase | MolTaq polymerase |
|------------------|--------------------|-------------------|
| water | 34 μL | 40 μL |
| reaction buffer | 10 μL | 5 μL |
| dNTPs (10 mM) | 1 μL | 1 μL |
| primer 1 (10 pM) | 1 μL | 1 μL |
| primer 2 (10 pM) | 1 μL | 1 μL |
| template DNA | 50 – 100 ng | 50 – 100 ng |
| DMSO | 1,5 μL | - |
| polymerase | 0,5 μL | 0,2 μL |

2.2.4.5 Gelelectrophoresis of nucleic acids

DNA fragments were mixed with 1x loading dye, then loaded onto a 1% agarose gel (1g agarose in 100 ml 1x TBE buffer) and separated by 70 – 130 V using a horizontal gel chamber (Mupid one, Biozym Scientific GmbH, Germany) in 0.5x TBE buffer. The gel was stained with ethidium bromide for 25 min and the DNA was visualized by UV trans illumination. The “GeneRuler™ Ladder Mix” from Thermo Scientific (Germany) served as standard.

RNA fragments were mixed in a 1:1 ratio with ethidium bromide containing loading dye and incubated for 10 min at 65 °C. Then, the RNA was loaded on a 1.2% 1x MOPS, 5% formaldehyde agarose gel and separated at 80 – 100 V. 1 x MOPS served as electrophoresis buffer.

2.2.4.6 Southern blotting and hybridisation

The “AlkPhos Direct Labelling and Detection Kit” (GE Healthcare, Germany) was used for Southern blotting. First, 30 – 50 µg of gDNA was hydrolyzed in a 50 µL reaction volume. The digested DNA was loaded on a 1% agarose gel and separated for 90 - 120 min at 90 V. After the run, the gel was soaked for 10 min in buffer I (0.25 M HCl), 25 min in buffer II (0.5 M NaOH, 1.5 M NaCl) and 30 min in buffer III (1.5 M NaCl, 0.5 M Tris). Subsequently to denaturation, the DNA was transferred to a Hybond™-N membrane (GE Healthcare, Germany). After 2 – 3 h blotting the membrane was dried for 7 min at 70 °C and the DNA was cross-linked via UV-light exposure of each side for 3 min. The labeling of the probe and the preparation of the membrane as well as the detection was performed according to the manufacturer’s manual.

2.2.4.7 Synthesis of cDNA and quantitative real-time PCR

RNA from *S. macrospora* was isolated as described in 2.2.4.1.3. To remove obsolete gDNA, the isolated RNA was treated with DNaseI according to the manufacturer’s manual. The “Transcriptor High Fidelity cDNA Synthesis Kit” (Roche, Germany) was used for the reverse transcription reaction. Template concentration was 2 µg of RNA. All quantitative real-time PCR experiments were performed for at least three times utilizing three biologically independent replicates. The reactions were carried out in a “Mastercycler® ep *realplex*” (Eppendorf, Germany) using the “qPCR MasterMix for SYBR GreenI” (Eurogentec,

Belgium) (Pöggeler *et al.* 2006). For qRT-PCR of *cas4*, primer pair cas4-RT-f/cas4-RT-r amplified a 159 bp fragment of the *cas4* gene. As a normalization reference of Ct values a 180 bp fragment encoding for the small rRNA subunit of *S. macrospora* was amplified with primer pair SSU-f/SSU-r. The significance of the obtained data was analyzed using the REST application (Pfaffl *et al.* 2002).

For semi-quantitative real-time PCR exact 500 ng of cDNA and the primer pair cas4-pQE-f/cas4-pQE-r were used. The number of cycles during the PCR was limited to 25 and the resulting PCR fragments were analyzed on a 1% agarose gel. A part of the actin gene, amplified with the primer pair Act2In-f/Act2In-r served as loading control while gDNA served as negative control.

2.2.4.8 Oligonucleotide synthesis, sequencing and sequence analysis

The synthesis of oligonucleotide used in this study was done by Eurofins MWG Operon (Ebersberg, Germany). All primer pairs are listed in Table 3. DNA sequencing was performed by the G2L-sequencing service of the “Göttinger Genom Labor” (Georg-August-University Göttingen). DNA and protein sequences as well as sequence alignments were obtained from the public databases BLAST (Altschul *et al.* 1990) (<http://blast.ncbi.nlm.nih.gov/Blast.cgi>). Molecular weights and isoelectric points of proteins were calculated with programs from the ExPASy Proteomics Server (<http://www.expasy.org>). For the prediction of a putative signal sequence of *cas4* the program “SignalP” from the ExPASy Proteomics Server was used (Petersen *et al.* 2011).

2.2.4.9 Isolation of the *S. macrospora* gene *cas4*

For the isolation of the *S. macrospora* putative carbonic anhydrase gene *cas4* (*SMAC_03821*), a TBLASTX search of the *S. macrospora* genomic sequence was performed (Nowrousian *et al.* 2010). The search was conducted using a nucleotide sequence of the *N. crassa* gene *NCU_05653*.

2.2.4.10 Generation of a *S. macrospora cas4* deletion strain

Homologous recombination procedure in *S. cerevisiae* was used to generate the *cas4* deletion cassette (Colot *et al.* 2006). The 5'- (1036 bp) and 3'- (737 bp) regions of the *cas4* open reading frame (ORF) were amplified from wt gDNA with the primer pairs CAS4_5f/CAS4_5r

and CAS4_3f/CAS4_3r carrying 29-bp overhangs for the pRS426 vector (Christianson *et al.* 1992) (Table 2) and the hygromycin resistance (*hyg*) cassette, respectively. The *cas4* deletion cassette consists of the upstream and downstream sequences of the *cas4* ORF interrupted by the 1419 bp *hph* gene amplified from plasmid pCB1003 with the primer pair hph-f/hph-r. The three obtained amplicons and the *EcoRI/XhoI* linearized vector pRS426 were co-transformed into the *S. cerevisiae* strain PJ69-4A as described in 2.2.2 and in Mayrhofer *et al.* (2006). Transformants were selected on SD-Ura medium. The recombinant plasmid pRS426- Δ cas4 was isolated from the *S. cerevisiae* transformants and served as template for the amplification of the 3192 bp deletion cassette with primer pair CAS4_5f/CAS4_3r. Subsequently, the amplicon of the *cas4* deletion cassette was transformed into the *S. macrospora* Δ ku70 strain, which is enhanced in homologous recombination (Pöggeler and Kück 2006). The resulting hygromycin resistant *S. macrospora* primary transformants were analyzed for the successful integration of the deletion cassette at the desired gene locus by PCR with the primer pairs 5f-f/tC1-o and 3r-r/h3-o. *S. macrospora* primary transformants are mainly heterokaryotic, carrying both wt and mutant nuclei. To obtain homokaryotic deletion strains, single-spore isolates were generated from the primary transformants. Additionally, to eliminate the Δ ku70::*nat*^R background the obtained single-spore isolates were crossed with the *S. macrospora* spore-color mutant *fus1-1* (S23442) (Nowrousian *et al.* 2012). To easily identify recombinant hybrid perithecia, the crossing partners always differed in spore color. Spores from hybrid perithecia were isolated and selected on hygromycin containing BMM agar plates (110 U/mL). The resulting homokaryotic deletion strain Δ cas4::*hyg*^R was analyzed by PCR and Southern blotting.

2.2.4.11 Generation of *S. macrospora* double, triple and quadruple *cas* deletion strains

For the generation of double *cas* gene deletion mutants two single *cas* gene deletion mutants were crossed as described in 2.2.3. For triple deletion mutants, the generated double deletion mutants were crossed except that the double deletions had at least one gene deletion in common. The quadruple deletion mutant was generated by crossing two triple deletion mutants which had two gene deletions in common. To easily access recombinant crossing perithecia the two crossing partners should differ in their spore color. To verify the deletion mutants, the spores from the crossing perithecia were isolated and their genomic DNA was analyzed by PCR with the primer pairs cynT1-GFP-f/cynT1-r and cynT1-GFP-f/tC1-o for

cas1, *cynT2-GFP-f/cynT2-r* and *cynT2-GFP-f/tC1-o* for *cas2*, *cynT3-GFP-f/cynT3-r* and *cynT3-GFP-f/tC1-o* for *cas3* and *5f-f/cas4seq-r* and *5f-f/h3-o* for *cas4*.

2.2.4.12 Generation of a *S. macrospora cas4* complementation strain

The complementation of the $\Delta cas4$ phenotype was achieved by transformation of plasmid pDS23-CAS4-eGFP, consisting of the full-length *cas4* gene C-terminally fused to *egfp* under the control of the constitutive *gpd* promoter of *A. nidulans*. The cloning procedure was done as described in 2.2.4.16. The pDS23-CAS4-eGFP was transformed into the $\Delta cas4$ strain as described in 2.2.2. Complemented transformants were selected on medium containing nourseothricin and hygromycin. The integration of the ectopic *cas4-egfp* copy was confirmed by PCR using the primer pair pRS_seq_F/CAS4Seqr.

2.2.4.13 Complementation of a haploid $\Delta nce103$ yeast deletion mutant

For heterologous complementation of *S. cerevisiae* with carbonic anhydrase genes of *S. macrospora* we used the haploid yeast strain CEN.HE28-h (CEN.HE28, EUROSCARF). This strain cannot grow in ambient air conditions because the yeast carbonic anhydrase gene *nce103* is replaced by a kanamycin resistance cassette. The heterozygotes diploid yeast deletion strain was incubated on sporulation medium (8.2 g/L sodium acetate, 1.9 g/L KCl, 0.35 g/L MgSO₄, 1.2 g/L NaCl, 15 g/L agar) for 2 – 4 days at 30 °C. For separation of single spores the tetrads were resuspended in Zymolyase solution (100 mg/mL). After 5 min the solution is spread as single lane on a YPD plate. The spores were isolated with a Micromanipulator (Singer Instruments, MSM System) and transferred to a new YPD plate. Only spores able to germinate at 5% CO₂ on plates containing 200 µg/mL G418 sulfate (Roth, Germany) were used for the complementation assay.

For the complementation of the haploid yeast mutant, the ORF of all four *cas* genes were amplified using the primer pairs p426CAS1-f/p426RGSHISCAS1-r for *cas1*, p426CAS2-f/p426RGSHISCAS2-r for *cas2*, p426CAS3-f/p426RGSHISCAS3-r for *cas3* and p426CAS4-f/p426RGSHISCAS4-r for *cas4*. Using the homologous recombination mechanism of *S. cerevisiae* (Colot *et al.* 2006) the PCR fragments (*cas1*: 790 bp, *cas2*: 763 bp, *cas3*: 610 bp, *cas4*: 1132 bp) consisting of the corresponding ORF, a 27 bp sequence coding for the RGS6xHis-tag and two 29 bp overhangs to the plasmid, were cloned into the *EcoRI* linearized vector p426GAL1 (Mumberg *et al.* 1994). The respective genes are

expressed under the control of a galactose inducible promoter. The obtained plasmids were named p426-CAS1-His, p426-CAS2-His, p426-CAS3-His and p426-CAS4-His. After transformation into the haploid yeast mutant (CEN.HE28-h), transformants were incubated in the “Inkubator C42” (Labotect, Germany) at 5% CO₂ on SD-Ura plates containing 200 µg/mL G418 sulfate as described under 2.2.2. For the complementation assay the cells were grown over night in liquid SD-Ura medium and plated in 50 µL aliquots in concentrations lasting from 10⁶ to 10¹ cells on solid SD- and SG-Ura medium, respectively. The cells were incubated in ambient air and 30 °C and to demonstrate viability of all cells also at 5% CO₂. The haploid yeast mutant transformed with the empty vector (CEN.HE28-h + p426GAL1) was used as a negative control. The heterozygous diploid yeast deletion strain transformed with the empty vector (CEN.HE28 + p426GAL1) served as a positive control. To confirm the production of the proteins western blotting with an anti-His antibody (Qiagen, Germany, 1:4000, 1x PBS + 0.5% BSA) was performed as described in 0. For protein preparation, the respective yeast strains were inoculated in liquid YPD medium (5 mL) over night. The cells were harvested by centrifugation (5.000 rpm, 4 °C, 10 min) and the pellet was flash frozen in liquid nitrogen and subsequently pestered to powder. After that, the cells were mixed with 100 µl 100 mM Tris pH 8 and centrifuged again (13.000 rpm, 4 °C, 10 min). The obtained supernatant was used in a SDS-PAGE as described in 2.2.5.2.

2.2.4.14 Morphological investigation of *S. macrospora*

The morphological investigation of perithecia and the mycelium growth during the sexual cycle of *S. macrospora* was done with the “Digital Microscope VHX-500F” (Keyence, Germany) or the “AxioImager M1 microscope” (Zeiss, Germany). Therefore, the strains were either plated on solid SWG and BMM medium or for microscopic analysis, inoculated on objective slides coated with 1 – 2 mL SWG medium or on a cellophane layer on solid SWG or BMM medium and incubated at 27 °C (Bloemendal *et al.* 2012). For visualization of asco-rosettes, perithecia were cracked open on object slides into a drop of water, the perithecia hull was removed and asci were covered with a cover slide to evoke asco-rosette formation. The growth velocity of the *S. macrospora* strains was measured as described by Nolting and Pöggeler (2006). To determine germination efficiency of ascospores from deletion and complementation strains a total of 200 spores were isolated from recombinant perithecia and inoculated on BMM supplemented with 0.5% of sodium acetate. Germinated spores were counted after 24 and 48 h. This was repeated at least three times.

2.2.4.15 Light and fluorescence microscopic investigations

For light and fluorescence microscopic analysis, *S. macrospora* strains were grown on solid BMM medium on top of a piece of cellophane (2 x 2 cm) at 27°C for 1 to 2 days. The cellophane sheet with the mycelium was put on a glass slide, covered with water and a cover slip for microscopic analysis. For fluorescence microscopy the “AxioImager M1 microscope” (Zeiss, Germany) was used. Images were captured with a “Photometrix CoolSNAP HQ camera” (Roper Scientific, Germany) and processed with the programs “Metamorph” (version 6.3.1; Universal Imaging) and „GIMP” (GNU Image Manipulation Program, The GIMP Development Team). The “chroma filter set 49002” (exciter ET470/40x, emitter ET525/50m and beamsplitter T495LP) was used to visualize EGFP fluorescence and detection of DsRED was achieved with a “chroma filter set 49005” (excitation/emission filter ET545/30/ET620/60, beam splitter T570lp) and an “X-cite 120 PC lamp” (EXFO).

2.2.4.16 Localization analysis of CAS4 in *S. macrospora*

To analyze the localization of CAS4, DsRED- and EGFP-tagged versions were generated. Plasmids pDS23-CAS4-eGFP, pRSnat-CAS4SS-eGFP and pDS23-CAS4SS-eGFP-KDEL were constructed by homologous recombination in *S. cerevisiae* (Colot *et al.* 2006). Plasmid pDS23-CAS4-eGFP consists of the full-length *cas4* gene C-terminally fused to *egfp* under the control of the constitutive *gpd* promoter. The *cas4* gene (1275 bp) was amplified from wt gDNA with primer pair pDS23cas4eGFP-f/pDS23cas4eGFP-r and cloned into the *HindIII* linearized vector pDS23-eGFP. Plasmid pRSnat-CAS4SS-eGFP consists of 63 bp of the predicted secretion signal of *cas4* fused to *egfp* under the control of the *gpd* promoter. The primer pair cas4ssgfp-f/pRS426GFPprev was used to amplify *egfp* with the secretion signal of *cas4* from plasmid p1783-1. The *gpd* promoter was amplified with overhangs to the pRSnat vector and to *cas4* using primer pair pRS426GPDF2/GPDCAS4-r. Obtained PCR fragments were then cloned into the *XhoI* linearized vector pRSnat. Plasmid pDS23-CAS4SS-eGFP-KDEL contains the coding sequence for the *cas4* secretion signal fused to *egfp* that has an artificial ER-retention signal (KDEL) at the C-terminus. The expression is controlled by the *gpd* promoter and the *trpC* terminator. The secretion signal encoding sequence of *cas4* and *egfp* were amplified with the primer pair CAS4GFP-f/GFP-r from pRSnat-CAS4SS-eGFP and the KDEL motif was attached using the primer pair TrpCKDEL-f/pDS23GFP-r. Both PCR fragments were cloned into the *HindIII* linearized vector pDS23-eGFP. All plasmids were transformed into the *S. macrospora fus1-1* strain. To

localize the fluorescently labeled proteins *in-vivo*, fluorescence microscopy was performed with transformants carrying the described plasmids as well transformants harboring plasmid pDsREDKDEL (Nowrousian *et al.* 2007).

To prove secretion of CAS4, protein extracts of the mycelium and the growth medium were analyzed by Western blotting. For this purpose, all *egfp* expressing strains were grown in 100 mL liquid SWG medium (Elleuche and Pöggeler 2008b) for 7 days at 27 °C. Total protein extracts of the mycelium were isolated according to Nowrousian and Cebula (2005). Proteins from the liquid growth medium were isolated using a “Spin-X UF concentrator” (Corning, Germany). The obtained samples were separated using sodium dodecyl sulfate polyacrylamide gel electrophoresis (SDS-PAGE) and blotted on a “Protran nitrocellulose membrane” (Whatman, Germany) (Laemmli 1970; Towbin *et al.* 1979). The detection of the fusion proteins was performed with a HRP-labelled monoclonal mouse anti-EGFP antibody (1:5000, 1x PBS, 0.5% BSA; Santa Cruz Biotechnology, sc-9996, Germany). The actin protein was detected with a monoclonal anti-mouse anti-actin antibody (1:8000, 1x PBS, 0.5% BSA; Novus, NB100-74340, Germany) and a secondary HRP-linked goat anti-mouse antibody (1:5000, 1x PBS, 0.5% BSA; Dianova, 115-035-003, Germany). The detection of signals was done by using the enhanced chemiluminescent reaction (Haan and Behrmann 2007).

2.2.4.17 Deglycosylation of CAS4-GFP

The deglycosylation of CAS4-GFP isolated from the culture medium was done with the “Protein Deglycosylation Mix” (NEB, Germany) according to the manufacturer’s manual.

2.2.4.18 Overexpression of *cas* genes in *E. coli*

2.2.4.18.1 Construction of *E. coli* overexpression vectors

The ORF of *cas1* (705 bp) was amplified with primer pair CynT1-pQE_f/CynT1_r (Table 3) and cloned into the *Bam*HI/*Sal*I linearized vector pQE30 (Qiagen, Germany). The created plasmid is named pQE30-CAS1 (Table 2) and consists of the *cas1* ORF fused in-frame to an N-terminal RGS-6xHis sequence. The *cas2* ORF (678 bp) was amplified without the coding sequence for the mitochondrial target sequence using primer pair CAS2pET22-f/CAS2pET22-r (Table 3). The ORF of *cas3* (525 bp) was amplified with primer pair Cas3-pet-f/Cas3-pet-r and the *cas4* ORF (1047 bp) was amplified without the

coding sequence for the N-terminal signal peptide for translocation into the endoplasmic reticulum with primer pair Cas4-pet-f/Cas4-pet-r. All PCR fragments were cloned into the pET22b(+) expression plasmid (Novagen, USA) linearized with *NdeI* and *XhoI* to create C-terminal 6xHis fusion proteins. The plasmids were named pET-CAS2, pET-CAS3 and pET-CAS4 (Table 2).

2.2.4.18.2 Expression of *cas* genes in *E. coli*

The production of the proteins was achieved in *E. coli* strains Rosetta (DE3) (Invitrogen, Germany) or BL21 (DE3) (Invitrogen, Germany) (Table 1). Therefore, an overnight pre-culture was used to inoculate 4 × 0.5 LB medium supplemented with 100 mg/L ampicillin and 0.5 mM ZnSO₄ to an OD₆₀₀ of 0.1. The gene expression was induced by the addition of 1 mM IPTG during exponential phase of growth and lasted for 3 – 4 h at 30 °C. Subsequently, the cells were harvested (4000g, 30 min, 4 °C) and flash-frozen with liquid nitrogen and stored at - 20 °C. The completeness of the amino-acids of all four CAS proteins was analyzed by mass spectrometry by Dr. Oliver Valerius (Department of Molecular Microbiology and Genetics, Göttingen) using the “LCQ DecaXP mass spectrometer” (Thermo Scientific, Germany)

2.2.4.18.3 Purification of CAS proteins

Usually, 10 g cells were resuspended in 30 mL lysis buffer (20 mM imidazole, 50 mM NaH₂PO₄ pH 8, 300 mM NaCl, 0.02 mM MgCl₂, 1 “Protease Inhibitor Cocktail” Tablet (Roche, Germany)) and subsequently incubated for 30 min at 4 °C with lysozyme (SERVA, Germany) and DNase I (AppliChem, Germany). After incubation, the cells were disrupted using a “microfluidizer 110S” (Microfluidics, Germany). After centrifugation (50.000 g, 30 min, 4 °C), the clarified lysate was applied on a Ni-NTA agarose (Qiagen, Germany) column equilibrated with lysis buffer. Unbound proteins were removed by washing the column with 3 column volumes (CV) of lysis buffer and bound CAS proteins were eluted with elution buffer containing additionally 250 mM imidazole. The purification protocol of CAS3-His was modified as follows: After applying the lysate containing CAS3-His on the Ni-NTA agarose column, unbound proteins were removed by washing gradually with three CV of lysis buffer containing 40 mM, 60mM, 80 mM and 100 mM imidazole, respectively. Elution fractions were analyzed by SDS-PAGE, pooled, concentrated in a “Spin-X[®] UF 20” (Corning, Germany) and stored at 4 °C.

2.2.5 Proteinchemistry methods

2.2.5.1 Determination of protein concentration

To determine protein concentration a Bradford assay was performed (Bradford 1976). Therefore, 10 μ L of the protein was mixed with 990 μ L of Bradford reagent and incubated for 2 min at RT. Following, the absorption was determined at 595 nm in a “Libra S12” (biochrom, UK) spectrophotometer in a 1 mL cuvette. Prior to this, a calibration line with bovine serum albumin was recorded.

2.2.5.2 Denaturing polyacrylamide gel electrophoresis (SDS-PAGE) and staining of polyacrylamide-gels

SDS-PAGE (Laemmli 1970) was used for separation of proteins according to their size. SDS-gels (Table 5) were casted in a “Mini-PROTEAN[®] Tetra Cell” (Bio-Rad, Germany) and covered with SDS-PAGE-running buffer. The samples were mixed with protein loading dye and incubated for 5 min at 95 °C. After loading, the samples were separated at 130 V for 1 – 2 h. For every run a protein standard (Pageruler[™] Prestained Protein Ladder, SM0671, Thermo Fisher, Germany) was used. For visualization of the proteins after the electrophoresis the gels were incubated for 30 min in SDS-gel staining solution and afterwards in SDS-gel destaining solution for 30 min.

Table 5: Composition of SDS-gels.

| Components | 10% acrylamide separation gel | 5% acrylamide stacking gel | Unit |
|----------------------------------|----------------------------------|-------------------------------|---------|
| Rotiphorese Gel 40 | 1.5 | 0.188 | mL |
| 1.5 M Tris/HCl pH 8.8 | 1.5 | - | mL |
| 0.5 M Tris/HCl pH 6.8 | - | 0.5 | mL |
| 10% (w/v) SDS | 60 | 20 | μ L |
| H ₂ O _{dest} | 2.94 | 1.3 | μ L |
| TEMED | 5 | 1.7 | μ L |
| 10% (w/v) APS | 40 | 13.3 | μ L |

2.2.5.3 Western-blot

The Western-blot technique was used for specific detection of proteins through antigen-antibody reaction. For this purpose, proteins separated in a SDS-PAGE were transferred (200 mA) on the nitrocellulose membrane Protran[®] BA-s (Whatman, Germany) using a semi-dry “Fastblot” device (Biometra, Germany). After the transfer a blocking step with 5% (w/v) milk powder in 1x PBS was performed. After washing three times for 15 min with 1x PBS either a specific horse-radish peroxidase (HRP) coupled His-antibody (Qiagen, Germany, 1:4000, 1x PBS + 0.5% BSA) or a specific anti-eGFP antibody (Santa Cruz Biotechnology, sc-9996, 1:5000, 1x PBS, 0.5% BSA) were applied on the membrane and incubated over night at 4 °C. The antibody was then removed and the membrane washed three times for 15 min. The detection of HRP coupled antibodies was achieved by the enhanced chemiluminescent reaction (Haan and Behrmann 2007).

2.2.5.4 Size-exclusion chromatography and MALLS

Four hundred microliters of CAS1 (3.5 mg/mL) and CAS3 (3 mg/mL) and 260 µL of CAS2 (2 mg/mL) were loaded separately on a 24 ml analytical “Superdex 200 (10/300)” gel filtration column using an “Äkta purifier” coupled to a “miniDAWN MALS” detector (Wyatt Technology, USA). The column was pre-equilibrated with 50 mM NaH₂PO₄ pH 8.0, 250 mM imidazole, 300 mM NaCl. Multi-angle laser light-scattering analysis was performed continuously on the column eluate at 291 K (size-exclusion chromatography coupled with multi-angle laser light scattering, SEC-MALLS). Data analysis was carried out with “Astra software” (Wyatt Technology, USA).

2.2.5.5 Crystallization, data collection and structure determination

CAS1 and CAS2 were crystallized using the sitting-drop vapor diffusion method at 293 K. The droplets were prepared by mixing 1 µl protein solution (CAS1: 15 mg/ml; CAS2: 22 mg/ml) and 1 µl reservoir (CAS1: 0.1 M succinic acid pH 7, 15% PEG 3350; CAS2: 0.1 M Tris-hydrochloride pH 8.5, 25% PEG 4000, 0.2 M CaCl₂ x 2H₂O). Crystals grew within a few days. Prior diffraction experiment, crystals were transferred to cryosolutions containing 10% (v/v) glycerol for CAS1 and 5% (v/v) glycerol for CAS2 in addition to the reservoir solution. The oscillation photographs for the CAS1 crystal were collected at beamline 14.1 at the BESSY II (Berlin, Germany) equipped with a Pilatus 6M detector (Mueller *et al.* 2012). The

diffraction images for CAS2 were collected at beamline P13 equipped with Pilatus 6M detector at the PETRA III (DESY, Hamburg, Germany). The data sets were processed using the XDS package (Kabsch 2010). Both structures were solved by molecular replacement with PHASER (McCoy *et al.* 2005) using the *E. coli* β -CA (PDB: 1DDZ) and the *H. influenzae* β -CA (PDB: 3E3I) as the search models for CAS1 and CAS2 structures, respectively. In both cases initial MR solutions were rebuilt using Rosetta model completion and relaxation (DiMaio *et al.* 2011). Manual model completing was performed with Coot (Emsley *et al.* 2010) alternated with refinement using PHENIX (Adams *et al.* 2010). Data collection and refinement statistics are presented in Table S1. Secondary structure assignment for both structures was done with the DSSP program (Kabsch and Sander 1983). Simulated Annealing omit map has been calculated using the CNS program (Brunger *et al.* 1998; Brunger 2007). Structural figures were generated with PyMOL (<http://www.pymol.org>).

Data collection and structure determination for CAS1 and CAS2 was performed by Dr. Piotr Neumann (Department for Molecular Structural Biology, Göttingen).

2.2.5.6 CA activity and inhibition measurements

An “Applied Photophysics” stopped-flow instrument has been used for assaying the CA catalyzed CO₂ hydration activity (Khalifah 1971). Phenol red (0.2 mM) has been used as indicator (absorbance maximum 557 nm), with 10-20 mM Tris (pH 8.3) as buffer, and 20 mM NaClO₄ for maintaining constant the ionic strength. The initial rates of the CA-catalyzed CO₂ hydration reaction was followed for a period of 10-100 s. The CO₂ concentrations ranged from 1.7 to 17 mM for the determination of the kinetic parameters and inhibition constants. For each inhibitor, at least six traces of the initial 5-10% of the reaction were used for the determination of the initial velocity. The uncatalyzed rates were determined in the same manner and subtracted from the total observed rates. Stock solutions of inhibitors (10 mM) were prepared in distilled, deionized water. These were diluted up to 0.01 μ M with distilled, deionized water. In order to allow for the formation of the E-I complex, inhibitor and enzyme solutions were preincubated together for 15 min at RT prior to the hydration assay. The kinetic parameters for the uninhibited enzymes were determined from Lineweaver-Burk plots. The inhibition constants were obtained by non-linear least-squares methods using PRISM 3 and the Cheng-Prusoff equation (Nishimori *et al.* 2007; Supuran 2010a; De Simone and Supuran 2012; De Luca *et al.* 2012; Monti *et al.* 2013). All values given represent the mean from at least three different determinations. All inhibitors (sodium salts of the anions and the

several small molecules) (Table S2) were commercially available, highest purity compounds from Sigma-Aldrich (Milan, Italy).

The activity and inhibition assays of CAS1 and CAS2 were performed by Dr. Daniela Vullo and Prof. Claudiu T. Supuran (Università degli Studi di Firenze, Sesto Fiorentino (Florence), Italy)

2.3 Measures of safety

Genetic engineering experiments of security level 1 have been conducted according to the guide lines of the genetic engineering law (GenTG) stated on 16.12.1993 (recently altered by Art. 12 G v. 29.7.2009 I 2542).

3. Results

3.1 Characterization of a putative α -class carbonic anhydrase from *S. macrospora*

3.1.1 Identification of the *S. macrospora* α -class carbonic anhydrase CAS4

The first fungal α -class CA (AoCA) was discovered and structurally analyzed in the filamentous ascomycete *A. oryzae* (Bahn and Mühlischlegel 2006; Cuesta-Seijo *et al.* 2011). To isolate a gene encoding a homolog of the *A. oryzae* in *S. macrospora*, a TBLASTN search was performed on the *S. macrospora* genome (Nowrousian *et al.* 2010) with the *A. oryzae* α -CA protein (XP_001827551.1) as a query sequence. The identified ORF *SMAC_03821* (FN178637), encoding a putative *S. macrospora* α -CA, consists of 1278 bp interrupted by two introns of 57 bp and 114 bp. The splicing of the introns was confirmed by cDNA sequencing. The encoded protein consists of 368 amino-acids (aa) with a predicted molecular mass of 39.4 kDa and a theoretical isoelectric point (pI) of 5.84. *In-silico* analyses of *SMAC_03821* using SignalP (Petersen *et al.* 2011) indicated the presence of a 21-aa N-terminal signal sequence for secretion. Therefore, the mature secreted *SMAC_03821* protein consists of 347 aa with a predicted molecular mass of 37.2 kDa and a theoretical pI of 5.55. An amino-acid alignment of the active site of the translated *SMAC_03821* protein with nine other putative or known α -CAs from bacteria, fungi and mammals confirmed that the identified *S. macrospora* protein belongs to the α -class of CAs (Fig. 8A). Three histidine residues at the active center that are conserved in all α -CAs and act as zinc-binding ligands (Supuran 2008a) could also be identified in the *S. macrospora* protein. In addition, the amino acids phenylalanine, glutamic acid and valine within the active site are also conserved in all investigated α -CAs (Fig. 8A). Based on these findings, *SMAC_03821* was named *cas4* (carbonic anhydrase of *Sordaria macrospora*). Comparing the amino-acid sequences of CAS4 at the active center with that of other α -CAs, CAS4 has the highest degree of similarity with fungal α -CAs of *Neurospora crassa* (97%) and *Magnaporthe oryzae* (80%) (Fig. 8B). The α -CA from *A. oryzae* and the putative α -CAs from *Podospira anserina* and *Chaetomium globosum* share 77% identity with CAS4. In contrast, CAS4 shares the lowest sequence identity with α -CAs of mammalian and bacterial origin (Fig. 8B).

A

```

          * ● *
Sma4 : YTLQQFHFHLP-----SEHLDNGTIRAMEMHMVWQ TENQE : 158
Ncr4 : YTLQQFHFHLP-----SEHLDNGTSRAMEMHMVWQ TENQE : 158
Aor  : YTLAQFHFHTP-----SEHNVNEEHFPM EVHFV FQTAAKE : 150
Pan  : FELQQFHFHLP-----SEHLDNGTSQAMEMHMVWQ SAEGE : 158
Cgl  : FELQQFHFHLP-----SEHLDNGTSQAMEMHMV FQSAAQE : 160
Mor  : YDLQQFHFHLP-----SEHLDNGTSMAMEMHMVWQ SAAKE : 158
Afl  : YTLAQFHFHTP-----SEHNVNEEHFPM EVHFV FQTAAKE : 168
Hpy  : YVLDNVHFHAP-----MEFLINNKTRPLSAHFVHKDAKGR : 138
Cre  : AVPTQEFHFHST-----SEHLLAGKIYPLELHIVH QVTEKL : 191
Hsa6 : YIAQQMHHFWGGASSEISGSEHTVDGIRHVIEIHI VHYNSKYK : 225

```

B

| | Sma4 | Ncr4 | Aor | Pan | Cgl | Mor | Afl | Cre | Hpy | Hsa6 |
|------|------|------|------|------|------|------|------|------|------|------|
| Sma4 | 100% | | | | | | | | | |
| Ncr4 | 97% | 100% | | | | | | | | |
| Aor | 77% | 57% | 100% | | | | | | | |
| Pan | 77% | 80% | 51% | 100% | | | | | | |
| Cgl | 77% | 80% | 57% | 91% | 100% | | | | | |
| Mor | 80% | 82% | 60% | 85% | 85% | 100% | | | | |
| Afl | 57% | 57% | 100% | 51% | 57% | 60% | 100% | | | |
| Cre | 42% | 40% | 40% | 42% | 40% | 42% | 40% | 100% | | |
| Hpy | 34% | 34% | 37% | 34% | 31% | 34% | 37% | 34% | 100% | |
| Hsa6 | 30% | 30% | 27% | 27% | 27% | 30% | 27% | 30% | 20% | 100% |

Fig. 8: Multiple sequence alignment of the zinc ion coordinating domain of CAs of the α -class. (A) ClustalW2 amino-acid alignment was created using a part of the following sequences: Sma4 (*Sordaria macrospora*, CAS4 accession number, FN178637), Ncr4 (*Neurospora crassa*, XP_960214.1), Aor (*Aspergillus oryzae*, XP_001827551.1), Pan (*Podospora anserina*, XP_001906308.1), Cgl (*Chaetomium globosum*, XP_001227267), Mor (*Magnaporthe oryzae*, ELQ36827), Afl (*Aspergillus flavus*, XP_002384772.1), Hpy (*Helicobacter pylori*, BAE66646.1), Cre (*Chlamydomonas reinhardtii* CAH1, BAA14232.2), and Hsa6 (*Homo sapiens* CA VI, NP_001206). Amino acids identical in all sequences are shaded black; residues conserved in at least 9 of 10 sequences are shaded in dark grey and residues conserved in at least six sequences are shaded in light grey; histidines important for zinc ion binding are marked with an asterisk. The amino-acids phenylalanine, glutamic acid and valine that are conserved in fungal, algae and mammalian α -CAs are marked with a black dot. (B) Amino-acid identity in % is given for all sequences in pair-wise comparison based on the amino-acid alignment of the conserved region shown in (A).

3.1.2 Analysis of the transcriptional expression of *cas4* during sexual development in ambient air and in 5% CO₂

Since their discovery, no fungal α -CAs have been analyzed on their transcriptional regulation. Therefore, the expression level of *cas4* during sexual and vegetative development of *S. macrospora* was investigated by quantitative real-time PCR (qRT-PCR). The real-time PCR was performed with primer pair *cas4*-RT-f/*cas4*-RT-r that amplified a 159 bp fragment of the *cas4* gene. The life cycle of this fungus is completed in seven days under laboratory conditions. Therefore, expression patterns were surveyed from day 3 (start of ascogonia formation) to day 7 (mature perithecia). To monitor *cas4* expression at different developmental stages in the wt, RNA was isolated from vegetatively grown mycelia from submerged shaking cultures or from floating mycelia grown in non-shaking cultures to induce sexual development. The transcript level of the *cas4* gene was significantly up-regulated early in sexual development and expression was reduced during vegetative growth (Fig. 9A). These results were confirmed by semi-quantitative real-time PCR with 500 ng cDNA of sexually and vegetatively grown wt (Fig. 9B) and a primer pair (*CAS4*-pQE-f/*CAS4*-pQE-r) amplifying the *cas4* gene (1115 bp). Also the semi-quantitative real-time PCR showed that the transcript levels of *cas4* are increased during sexual development but also at later stages (day 5 and day 7) during vegetative growth. As loading control we amplified a part of the actin gene (*SMAC_04416*) (395 bp) which is constitutively expressed at high levels throughout sexual development and vegetative growth of *S. macrospora* with primer pair *Act2In*-f/*Act2In*-r (Fig. 9). Genomic DNA with introns (*cas4*: 1286 bp; actin: 459 bp) was used as purity control.

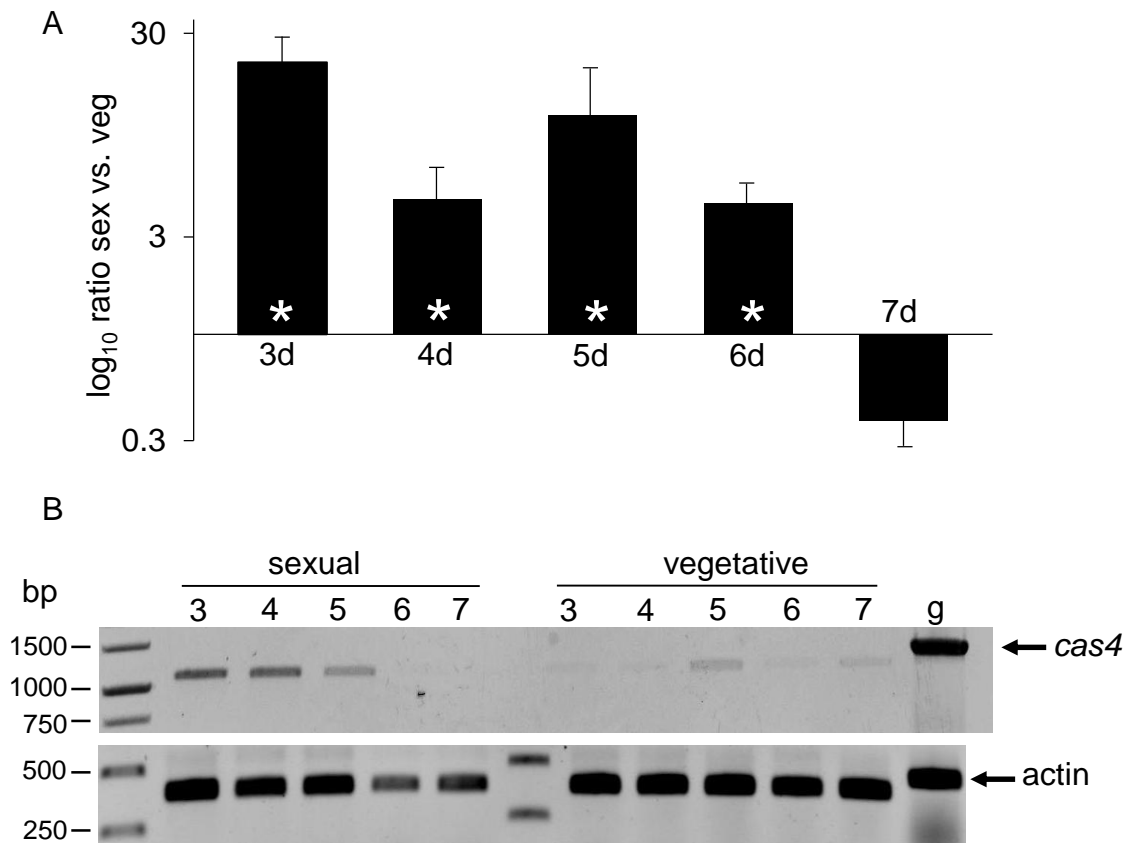


Fig. 9: Expression analysis of the *cas4* gene by quantitative real-time PCR. (A) Quantitative real-time PCR of *cas4* was performed with primer pair *cas4*-RT-f/*cas4*-RT-r on cDNA derived from total RNA isolated from *S. macrospora* wt grown at 27 °C in liquid BMM. Expression of *cas4* was compared between sexually (sex) and vegetatively (veg) grown wt mycelium at the indicated days of development (3-7 days) in ambient air. Values shown represent mean expression ratios of at least three independent biological replicates, each done in triplicates. Standard deviations are indicated. Asterisks indicate significance calculated according to REST (Pfaffl *et al.* 2002). (B) Semi-quantitative RT-PCR was performed with 500 ng of wt cDNA and primer pair (CAS4-pQE-f/CAS4-pQE-r) either for *cas4* (1115 bp) or as loading control a primer pair (Act2In-f/Act2In-r) for the actin gene (395 bp). Genomic DNA (g) containing introns was used as purity control (*cas4*: 1286 bp; actin: 459 bp). The cycle numbers of the PCR was limited to 25.

To investigate the influence of an enriched 5% CO₂ atmosphere on *cas4* expression, growth in ambient air and in 5% CO₂ was analyzed by qRT-PCR. Expression patterns were surveyed on day 3 (start of ascogonia formation), day 5 (large protoperithecia), and day 7 (mature perithecia). Under CO₂-enriched conditions, *cas4* expression was significantly up regulated at day 5 and down regulated at day 7 during sexual development (Fig. 10).

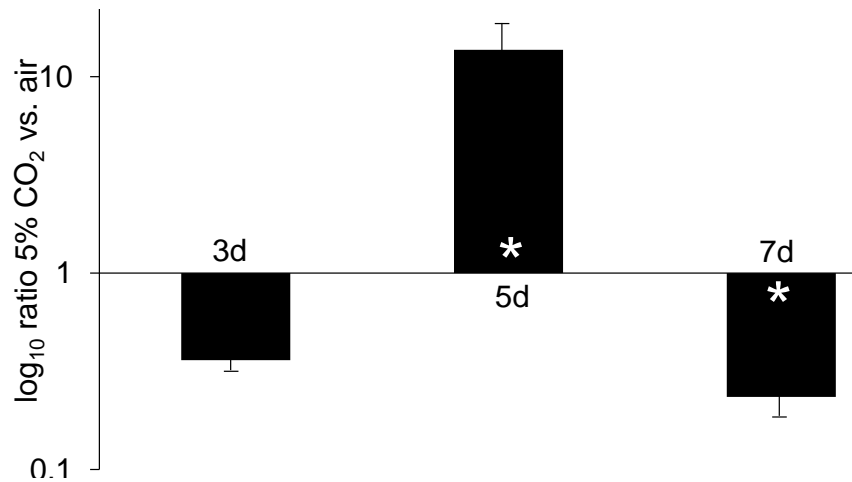


Fig. 10: Expression analysis of the *cas4* gene in ambient air and 5% CO₂ by quantitative real-time PCR. Quantitative real-time PCR of *cas4* was performed with total RNA isolated from *S. macrospora* wt grown at 27 °C in liquid BMM. Expression of *cas4* was compared in wt grown in ambient air and at 5% CO₂ at days 3, 5, and 7. Values shown represent mean expression ratios of at least three independent biological samples, each done in triplicates. Standard deviations are indicated. Asterisks indicate significance calculated according to REST (Pfaffl *et al.* 2002).

3.1.3 Analysis of the N-terminal CAS4 signal peptide and the CAS4 glycosylation pattern

The α -CA AoCA of *A. oryzae* has a functional N-terminal signal peptide for translocation into the endoplasmic reticulum (ER) that was also identified in the *S. macrospora* α -CA CAS4 (Elleuche and Pöggeler 2010; Cuesta-Seijo *et al.* 2011). To verify the secretion of CAS4 via its putative signal sequence (SS), plasmid pDS23-CAS4SS-eGFP-KDEL encoding the *cas4* signal peptide sequence in-frame with *egfp* and the C-terminal ER-retention signal KDEL (Pelham 1990) was constructed and transformed into the *S. macrospora* spore color mutant *fus1-1* strain (Nowrousian *et al.* 2012). The gene was expressed under the control of the constitutive glycerinaldehyde 3-phosphate dehydrogenase promoter (*gpd*) of *A. nidulans*. The fluorescence from the CAS4SS-eGFP-KDEL fusion protein was microscopically analyzed and appeared in net-like structures within the hyphae of transformants (Fig. 11). These structures are typical for the ER in fungal hyphae (Nowrousian *et al.* 2007; Maruyama and Kitamoto 2007). Additional co-localization experiments with ER-localized DsRED (Nowrousian *et al.* 2007) in the *fus1-1* strain expressing the fusion gene coding for CAS4SS-eGFP-KDEL demonstrated that the *cas4* SS mediated translocation into the ER (Fig. 11). Secretion of the full-length CAS4-EGFP fusion protein resulted in fluorescence signals that were not concentrated in the ER but distributed within the hyphae and in the surrounding medium (data not shown). As a control we expressed *egfp* alone in the *S. macrospora fus1-1*

strain. The fluorescence was uniformly distributed within the hyphae and not concentrated to any organelle (Fig. 11) (Pöggeler *et al.* 2003). To analyze whether the predicted signal sequence alone is able to mediate secretion of EGFP, Western-blot analyses of cell-free supernatant and mycelium fractions of *fus1-1* strains carrying plasmids pDS23-CAS4SS-eGFP-KDEL, plasmid pDS23-eGFP that encodes *egfp*, plasmid pRSnat-CAS4SS-eGFP encoding the *cas4* signal sequence fused in frame to *egfp*, and pDS23-CAS4-eGFP encoding full-length *cas4* fused to *egfp* was performed (Fig. 12A).

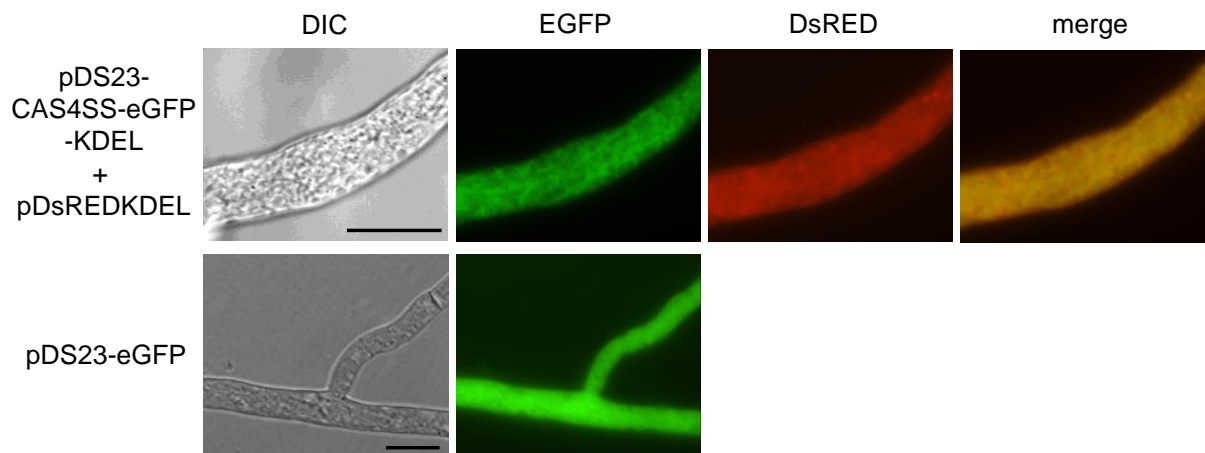


Fig. 11: Fluorescence localization of CAS4SS-EGFP-KDEL and EGFP in *S. macrospora*. Fluorescence microscopy of a *S. macrospora fus1-1* strain carrying plasmids pDS23-CAS4SS-eGFP-KDEL and pDsREDKDEL. The strains were inoculated on solid BMM medium on cellophane sheets overnight. The images illustrate that the fluorescence of the CAS4SS-EGFP-KDEL fusion protein concentrates in a net-like structure resembling the endoplasmic reticulum. CAS4SS-EGFP-KDEL co-localizes with ER-localized DsRED. As a control we expressed *egfp* alone (pDS23-eGFP) in the *S. macrospora fus1-1* strain. The fluorescence was uniformly distributed within the hyphae and not concentrated to any organelle (scale bar: 20 μ m; DIC: Differential interference contrast).

No EGFP signal was detected in cell-free supernatants of strains expressing either EGFP or the CAS4SS-EGFP-KDEL fusion protein. The proteins were not secreted, remained within the hyphae and were detectable only in mycelium fractions (Fig. 12A). In contrast, a single EGFP band at 27 kDa was detected in cell-free supernatants from transformants expressing CAS4SS-EGFP and three bands were detected in cell-free supernatants of transformants expressing full-length CAS4-EGFP. The smaller protein band is equivalent to the size of free EGFP (27 kDa) and was probably a degradation product of the full-length CAS4-EGFP fusion protein that appeared in two forms at about 65 kDa. In the mycelium fraction of the strain expressing CAS4SS-EGFP only a faint 27 kDa EGFP band was observed, while the same fraction of transformants expressing full-length CAS4-EGFP clearly showed a protein

with a size of 27 kDa. Similar to culture medium extracts, this protein appeared to be free EGFP most likely derived from the intracellular degradation of the CAS4-EGFP fusion protein (Fig. 12A). Thus, the signal sequence derived from CAS4 was sufficient to mediate EGFP and CAS4-EGFP secretion.

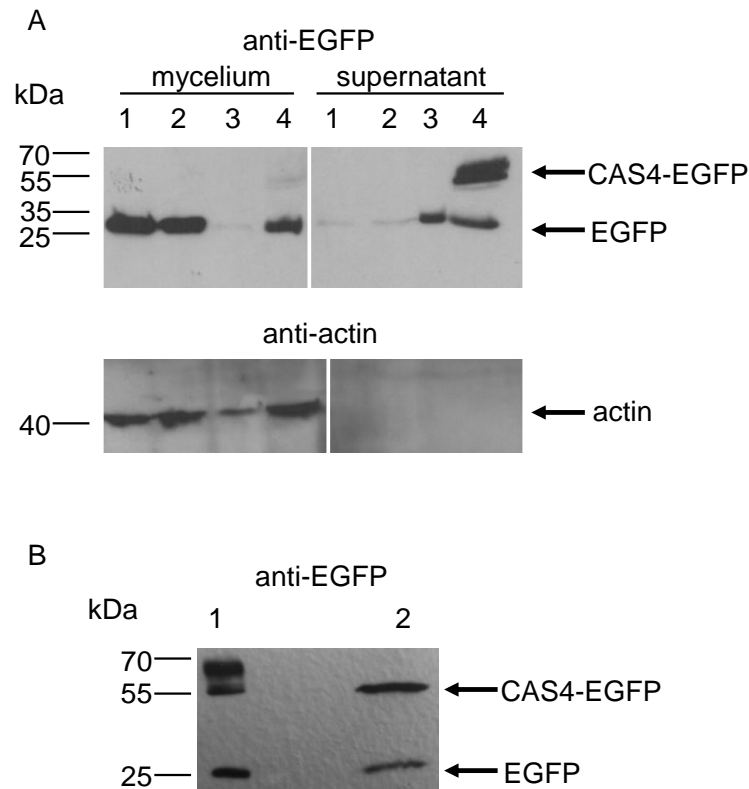


Fig. 12: Western-blot analysis of the localization and glycosylation of CAS4 in *S. macrospora*. (A) Recombinant *S. macrospora fus1-1* strains, expressing either plasmid pDS23-eGFP (1) or plasmid pDS23-CAS4SS-eGFP-KDEL (2) or plasmid pDS23-CAS4SS-eGFP (3) or pDS23-CAS4-eGFP (4), were grown in SWG medium for seven days. Total cellular (mycelium) and total secreted (supernatant) proteins were isolated and subsequently separated by SDS-PAGE and visualized by Western-blotting using an anti-EGFP antibody. The actin protein was used as loading control and visualized with an anti-Actin antibody. (B) Full-length CAS4-EGFP was isolated from the supernatant analyzed on glycosylation before (1) and after (2) treatment with the protein deglycosylation mix. The proteins were separated by SDS-PAGE and visualized by Western-blotting using an anti-EGFP antibody.

The full-length CAS4-EGFP fusion protein isolated from culture supernatants appeared as a diffuse double band by Western blot which might be caused by glycosylation as the most common posttranslational modification of secreted proteins (Fig. 12B) (Peberdy 1999). Glycosylation of CAS4 was investigated by *in-vitro* deglycosylation of proteins isolated from the culture medium. After the application of deglycosylation enzymes, the diffuse

CAS4-EGFP double band disappeared from SDS-PAGE and Western blots and only a single band remained (Fig. 12B).

3.1.4 Construction of a homokaryotic *cas4* deletion strain

To investigate the role of *cas4* during sexual and vegetative development of *S. macrospora*, we constructed a $\Delta cas4$ strain. Due to the close proximity of a nearby gene (*SMAC_03822*) the 1278 bp *cas4* gene was replaced from base 1 to 798 by the hygromycin resistance-cassette including the catalytically important CA domain (Fig. 13).

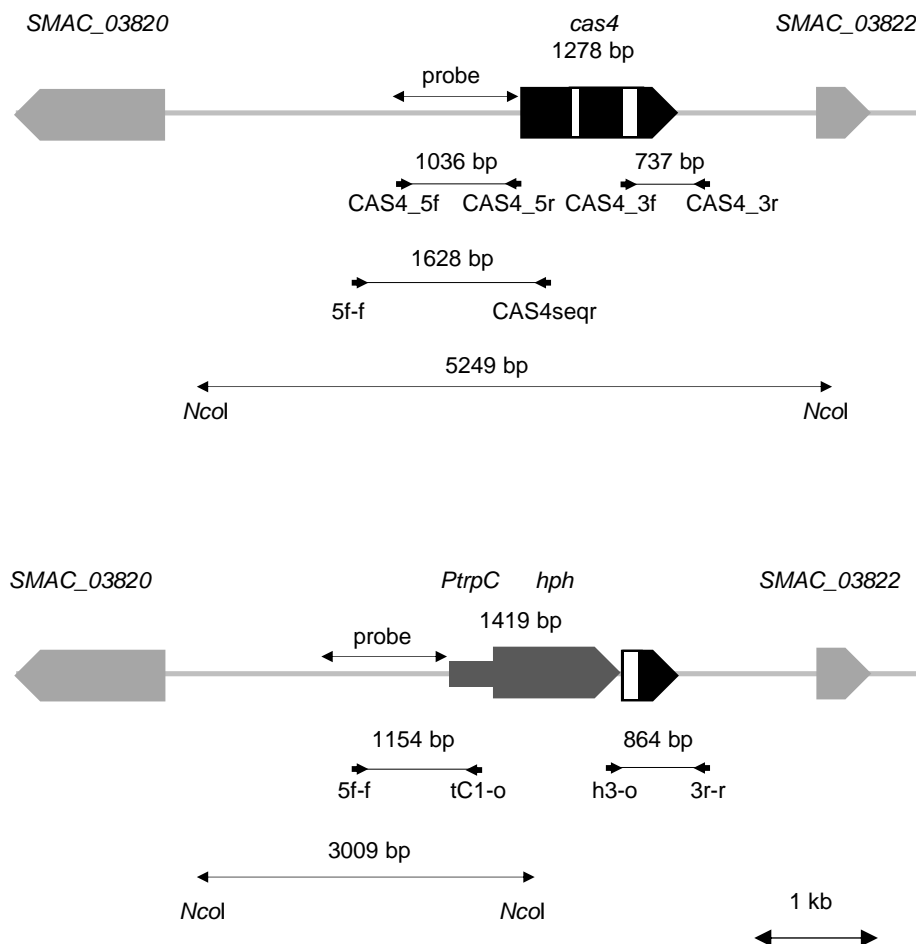


Fig. 13: Construction of a $\Delta cas4$ strain. Schematic illustration of the *cas4* locus (black arrow) and the flanking areas before and after homologous integration of the *hph* cassette (dark grey arrow). Introns are indicated as white boxes. Positions of primer pairs for verification of wild type and knock-out locus are indicated as small arrows. The corresponding PCR fragment sizes for each primer pair are given. The part of the *cas4* locus used as probe for Southern blot is marked. (*hph*, hygromycin resistance; *PtrpC*, tryptophan promoter of *A. nidulans*).

For this purpose, plasmid pRS426- $\Delta cas4$ was constructed as described in 2.2.4.10. The plasmid served as a template in a PCR reaction to amplify the *cas4* deletion-cassette with primer CAS4_5f and CAS4_3r (Table 3). The deletion-cassette consists of the *hph* gene flanked by the 5'- and 3'-region of *cas4* (Fig. 13).

After transformation of the *cas4* deletion-cassette into the *S. macrospora* strain $\Delta ku70::nat$ which is enhanced in homologous recombination (Pöggeler and Kück 2006) we succeeded in isolating three hygromycin (hyg) and nourseothricin (nat) resistant transformants. The partial replacement of the target gene was confirmed by PCR (data not shown). Commonly, these primary deletion strains are heterokaryotic containing mutant ($\Delta cas4::hyg/\Delta ku70::nat$) and wt nuclei (*cas4*/ $\Delta ku70::nat$) and need to be crossed against the spore color mutant *fus1-1* to eliminate the $\Delta ku70::nat$ background and to obtain homokaryotic deletion strains. In summary, twelve hygromycin resistant and nourseothricin sensitive single-spore isolates could be isolated. The integration of the *cas4* deletion-cassette at the desired gene locus and the absence of the wt *cas4* gene were confirmed by PCR (Fig. 14A). Primer pairs used are displayed in Fig. 13. In addition, the successful construction of a $\Delta cas4$ strain was verified by Southern blot using *NcoI* digested gDNA from the wt and $\Delta cas4$ strain. The analysis of the wt *cas4* loci resulted as expected in a 5249 bp fragment while the deletion mutant resulted in a 3009 bp fragment (Fig. 14B).

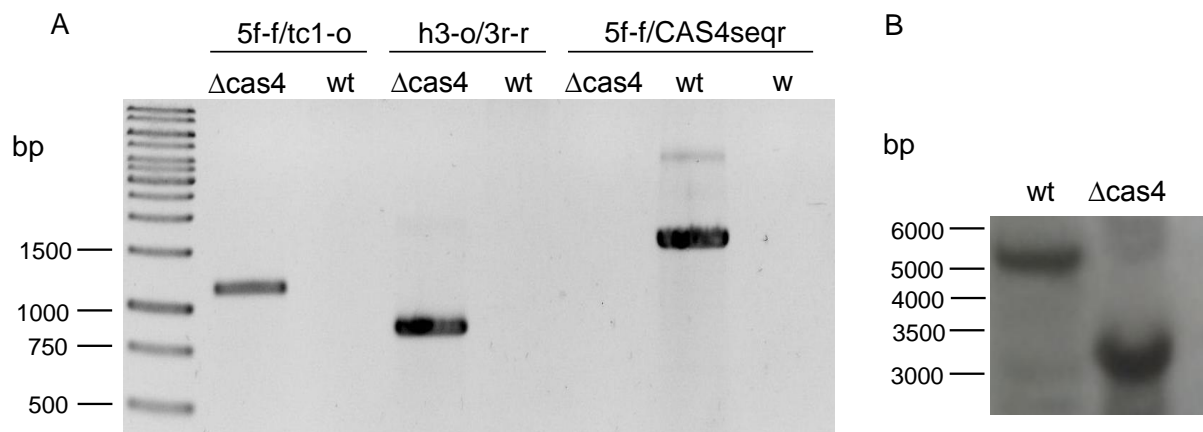


Fig. 14: PCR and Southern blot verification of the successful construction of a $\Delta cas4$ strain. (A) PCR analysis to confirm the integration of the *cas4* deletion-cassette at the desired gene loci by PCR. The expected fragment sizes shown in Fig. 13 could be detected (w, water). (B) Southern hybridization demonstrating the successful integration of the deletion-cassette using a *cas4* locus specific probe. The gDNA of wt and $\Delta cas4$ was digested with *NcoI* and hybridized with the probe as shown in (A). As expected a 5249 bp fragment for the wt and a 3009 bp fragment for the deletion mutant could be detected.

3.1.4.1 Morphological characterization of the *S. macrospora* $\Delta cas4$ strain

The *cas4* deletion mutant was analyzed to elucidate if *cas4* is involved in sexual development, vegetative growth or ascospore germination. The $\Delta cas4$ mutant had no obvious phenotypically alterations compared to the wt. Nevertheless, the deletion mutant was delayed in fruiting-body formation (Fig. 15) that might be a result from a non-significant reduction in the vegetative growth rate of 4% compared to the wt (Fig. 16A). The wt strain completed the sexual life cycle after 7 days on solid cornmeal medium and formed fruiting bodies in ambient air conditions; however, the $\Delta cas4$ deletion strain required 9 days to form mature fruiting bodies with a wt shape and with a normal number of ascospores.

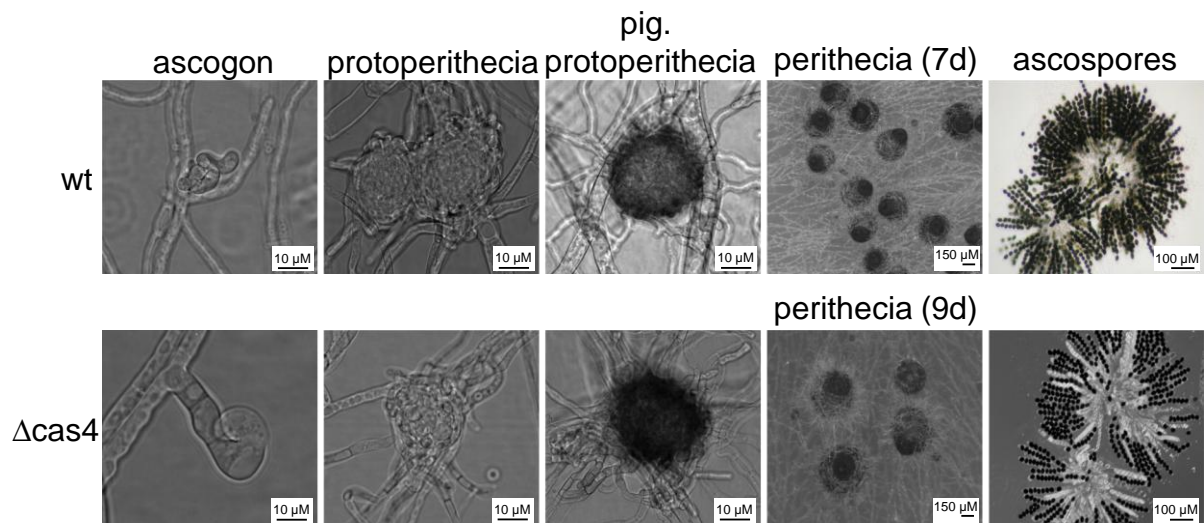


Fig. 15: Phenotypic analysis of wild type and the $\Delta cas4$ strain. Microscopic analysis of the sexual development of $\Delta cas4$ compared to the wt. No obvious morphological changes could be observed in the $\Delta cas4$ strain. Due to the reduced vegetative growth rate the $\Delta cas4$ strain required 9 days to complete the sexual life cycle (pig.: pigmented). The strains were inoculated on solid BMM at 27 °C on a cellophane sheet and sexual development was microscopically investigated after 3,4,5,6, and 7 days. Mature perithecia were opened and the ascospores were separated from the shell.

However, the germination rate of the ascospores from the $\Delta cas4$ mutant was significantly reduced by 15% compared to the wt (Fig. 16B). Incubation at 5% CO₂ did not rescue the germination deficiency. Compared to the wt the phenotype of $\Delta cas4$ was not changed by osmotic stress induced by 5 M sodium chloride, oxidative stress induced by 0.02% H₂O₂, or cell wall stress induced by addition of 0.003% sodium dodecyl sulfate (SDS) to the medium.

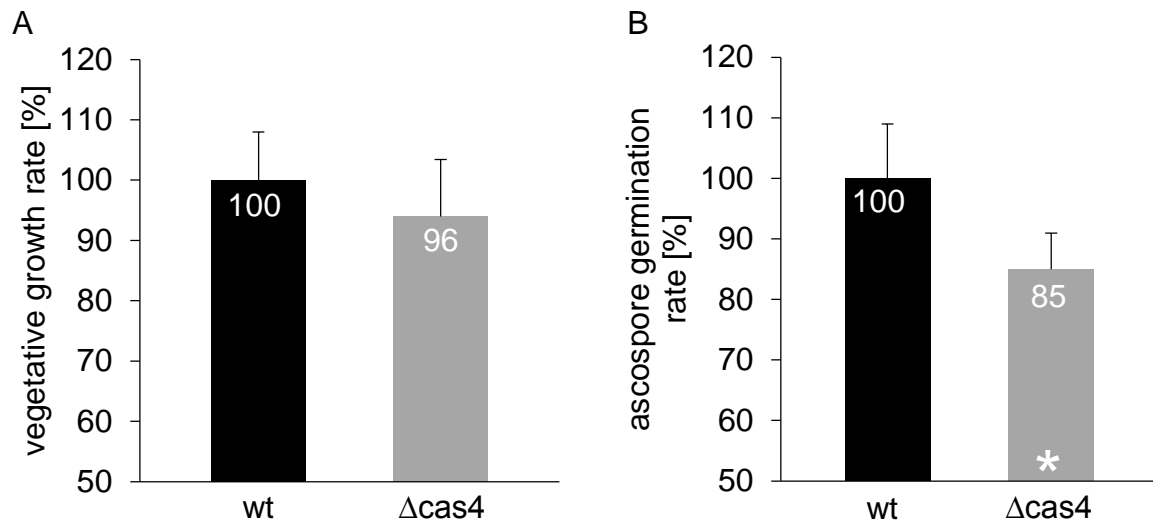


Fig. 16: Comparison of vegetative growth and ascospore germination rate of wild type and the $\Delta cas4$ strain. (A) Comparison of the vegetative growth rate of wt and $\Delta cas4$. Strains were grown for seven days on solid fructification medium (SWG) in ambient air and the growth rate was calculated as cm/d and the wild type was defined as 100%. Growth rates are the average from seven measurements of three independent experiments. Error bars are given as indicated. (B) Analysis of the germination efficiency of $\Delta cas4$ compared to wt. One hundred ascospores were isolated and placed on BMM plates supplemented with 0.5% sodium acetate. Total germinated spores were counted after one, two and three days and the wild type was defined as 100%. This experiment was done in triplicates. Error bars as indicated. The asterisk indicates significance according to Student's t-test.

3.2 Construction of double *cas* gene deletion mutants

To determine if interaction between *cas4* and other *cas* genes is required for proper *S. macrospora* development, we constructed double deletion mutants $\Delta cas1/4$, $\Delta cas2/4$ and $\Delta cas3/4$ by crossing the respective single deletion mutants as described under 2.2.3. Phenotypes of strains $\Delta cas1/4$ and $\Delta cas3/4$ were not different from phenotypes of the $\Delta cas4$ single mutant (Fig. 17). Similar to the wt, all mutants were able to complete the sexual life cycle and form wt shaped fruiting bodies with a normal number of mature ascospores in ambient air. Compared to wt, the vegetative growth rate of $\Delta cas2/4$ was significantly reduced by 30% while the growth rate of $\Delta cas1/4$ and the $\Delta cas3/4$ strains was only slightly reduced (Fig. 18A). Because of the reduced growth rate, all double-deletion mutants needed nine days to form mature fruiting bodies. The double-deletion strain $\Delta cas2/4$ reflect the phenotype of the $\Delta cas2$ and the $\Delta cas1/2$ strains whose growth rates were reduced by 35% and 50%, respectively (Fig. 18A) (Elleuche and Pöggeler 2009b).

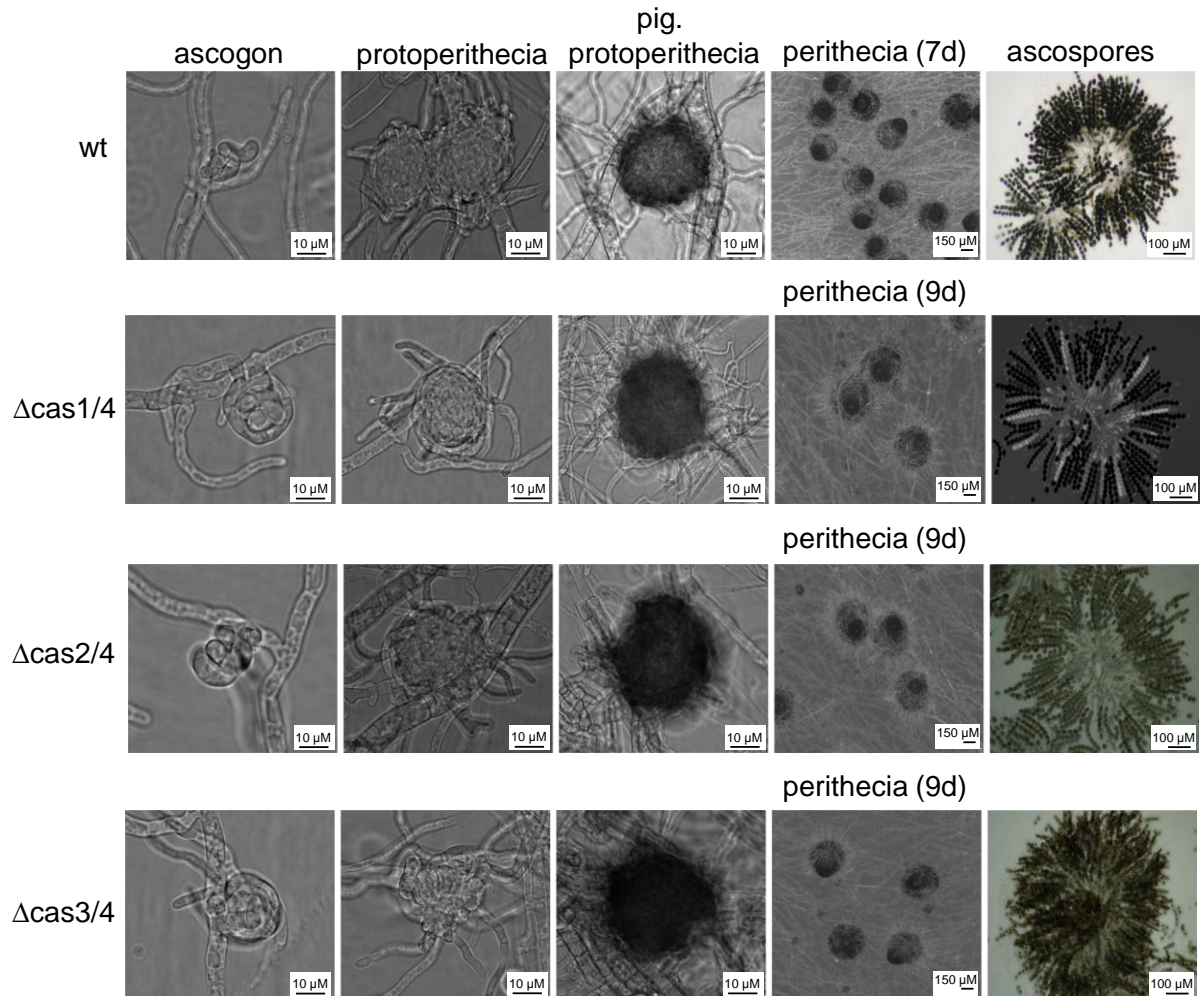


Fig. 17: Comparison of the sexual development of wt and double knock outs. Microscopic analysis of the sexual development of double knock outs compared to the wt. No obvious morphological changes could be observed in the analyzed mutants. Due to the reduced vegetative growth rate all mutant strains required 9 days to complete the sexual life cycle. The strains were inoculated on solid BMM at 27 °C on a cellophane sheet and sexual development was microscopically investigated after 3,4,5,6, and 7 days. Mature perithecia were opened and the ascospores were separated from the shell. The wt is shown as in Fig. 15.

Comparing the ascospore germination rate of the wt with the double-deletion mutants only the $\Delta cas2/4$ strain showed a significant reduction in ascospore germination by 35% similar to the $\Delta cas2$ mutant (Elleuche and Pöggeler 2009b) (Fig. 18). As shown for the $\Delta cas2$ mutant (Elleuche and Pöggeler 2009b), incubation at 5% CO_2 did not rescue the ascospore germination deficiency of $\Delta cas2/4$ (data not shown). The germination rate of $\Delta cas3/4$ was slightly reduced while the germination rate of $\Delta cas1/4$ was not reduced (Fig. 18). In contrast to other fungi, all *S. macrospora* single and double CA deletion-mutants were viable and grew under ambient air conditions (Elleuche and Pöggeler 2009b) (Fig. 15, Fig. 16A, Fig. 17, and Fig. 18A).

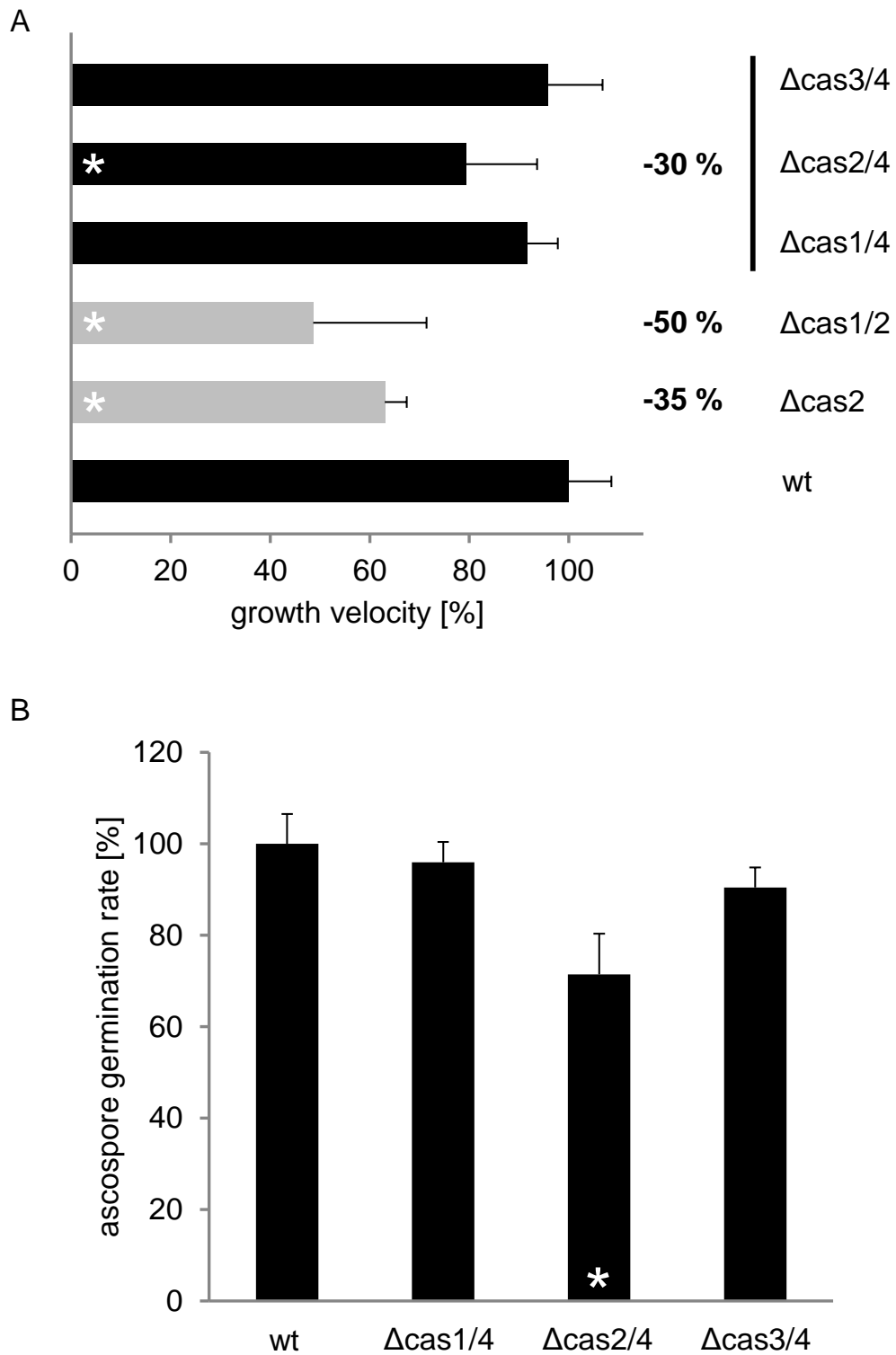


Fig. 18: Comparison of vegetative growth and ascospore germination rate of wt and double-deletion mutants.

(A) Comparison of vegetative growth rate of wt and $\Delta cas1/2$ and $\Delta cas2$ with double knock outs. Strains were grown for seven days on solid minimal medium (SWG) in ambient air and the growth rate was calculated as cm/d and the wt was defined as 100%. Growth rates are the average from seven measurements of three independent experiments. Error bars are given as indicated. Data for grey bars are taken from Elleuche and Pöggeler (2009b) (B) One hundred ascospores were isolated and incubated on BMM plates supplemented with 0.5% sodium acetate. Total germinated spores were counted after one, two and three days and the wt was defined as 100%. This experiment was done in triplicates. Error bars as indicated. The asterisk indicates significance according to Student's t-test.

To further investigate the ability of *S. macrospora* to live without CAs, we constructed triple-deletion strains ($\Delta cas1/2/3$, $\Delta cas1/2/4$, $\Delta cas2/3/4$ and $\Delta cas1/3/4$) and the quadruple deletion mutant ($\Delta cas1/2/3/4$) with no *cas* genes.

3.3 Generation of triple *cas* gene-deletion mutants

Triple mutants were generated by crossing two double deletion mutants differing in spore color and sharing at least one identical gene deletion. All constructed triple-deletions are viable and could grow in ambient air. However, only the triple deletion mutants $\Delta cas1/3/4$ and $\Delta cas2/3/4$ formed mature fruiting bodies and ascospores in ambient air (Fig. 19). The phenotype of the mutant strains $\Delta cas1/2/3$ and $\Delta cas1/2/4$ was similar to that of the $\Delta cas1/2$ mutant (Elleuche and Pöggeler 2009b). After twelve days of incubation these two strains produced neither fruiting bodies nor ascospores (Fig. 19). After extended incubation of 20 days under normal CO₂ conditions both mutants strains formed a few perithecia that were devoid of mature ascospores (data not shown). The analysis of the $\Delta cas1/3/4$ triple mutant revealed an increased number of white, premature ascospores (Fig. 19).

Compared to wt, the vegetative growth rate of the $\Delta cas1/2/4$ strain was significantly reduced by 90%, the $\Delta cas1/2/3$ strain by 70%, and $\Delta cas2/3/4$ strain by 50% (Fig. 20). While the growth rate of the $\Delta cas1/2$ strain was reduced by 50% the growth rate of $\Delta cas1/3/4$ was slightly increased by 4%. Similar to the $\Delta cas2$ strain, the $\Delta cas2/3/4$ strain showed a significant reduction in ascospore germination rate, while the $\Delta cas1/3/4$ strain was not impaired in ascospore germination (Fig. 21). The ascospore germination rate of the triple knock outs $\Delta cas1/2/3$ and $\Delta cas1/2/4$ could not be analyzed because their fruiting bodies were only formed after extended incubation under normal air conditions and devoid of ascospores similar to the $\Delta cas1/2$ mutant (Elleuche and Pöggeler 2009b). When incubated in 5% CO₂ the phenotype of the latter two triple mutants could be partially restored. The few formed perithecia contained only some mature ascospores.

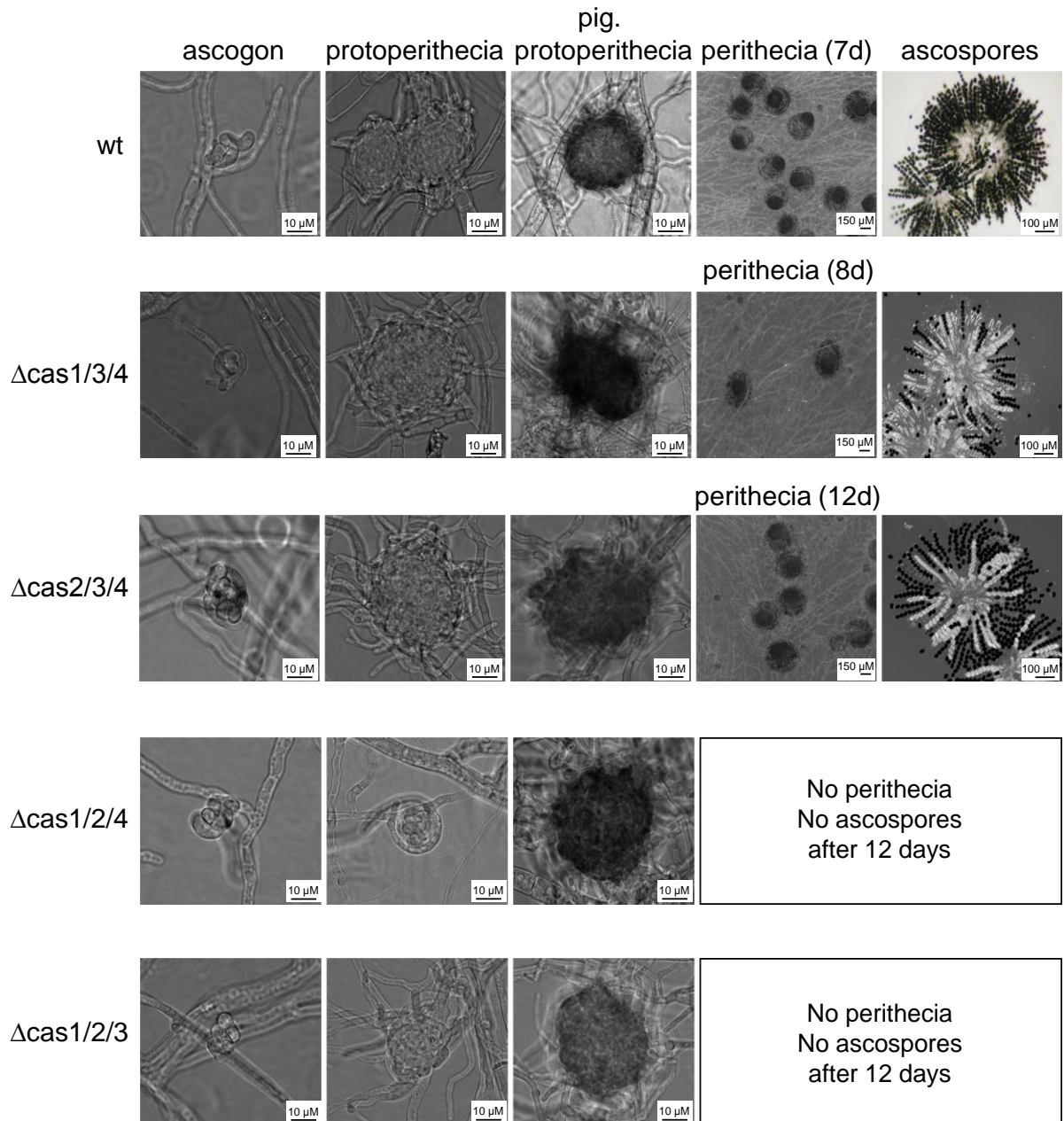


Fig. 19: Microscopic analysis of the sexual development of triple knock outs compared to the wt. Only mutants $\Delta cas1/3/4$ and $\Delta cas1/3/4$ were fertile and able to produce mature ascospores. The $\Delta cas1/3/4$ triple mutant exhibited an unnatural number of white, premature ascospores. Due to the reduced vegetative growth rate (Fig. 20) the mutant strain $\Delta cas1/3/4$ required 9 days to complete the sexual life cycle while $\Delta cas2/3/4$ needed 12 days. The sexual development of $\Delta cas1/2/3$ and $\Delta cas1/2/4$ stopped at the stage of pigmented protoperithecia. The strains were inoculated on solid BMM at 27 °C on a cellophane sheet and sexual development was microscopically investigated after 3,4,5,6, and 7 days. Mature perithecia were opened and the ascospores were separated from the shell. The wt is shown as in Fig. 15.

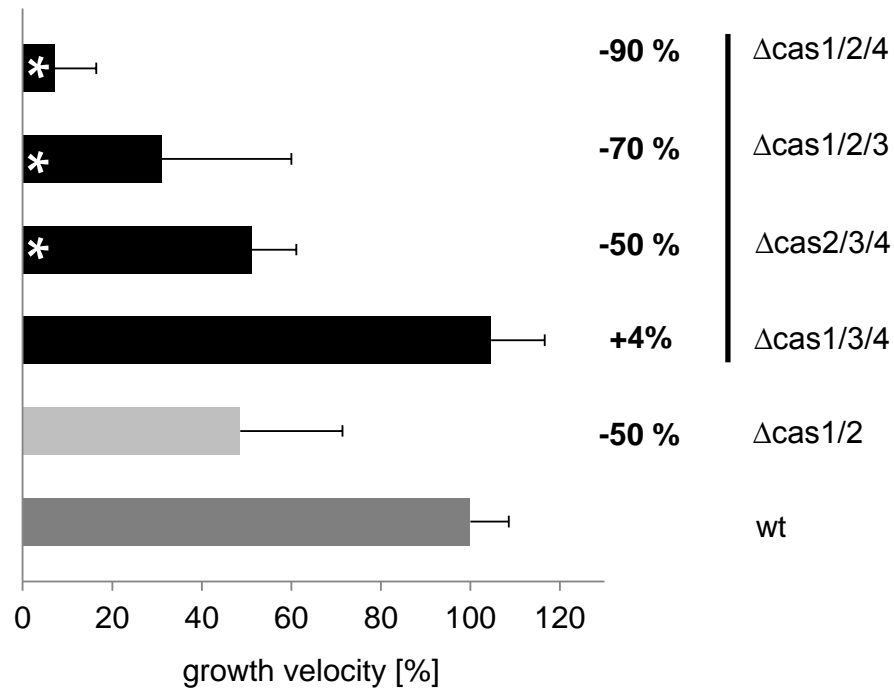


Fig. 20: Comparison of the vegetative growth rate of wt with $\Delta cas1/2$ and triple knock outs. Strains were grown for seven days on solid minimal medium (SWG) in ambient air and the growth rate was calculated as cm/d and the wt was defined as 100%. Growth rates are the average from seven measurements of three independent experiments. Error bars are given as indicated. The asterisks indicate significance according to Student's t-test.

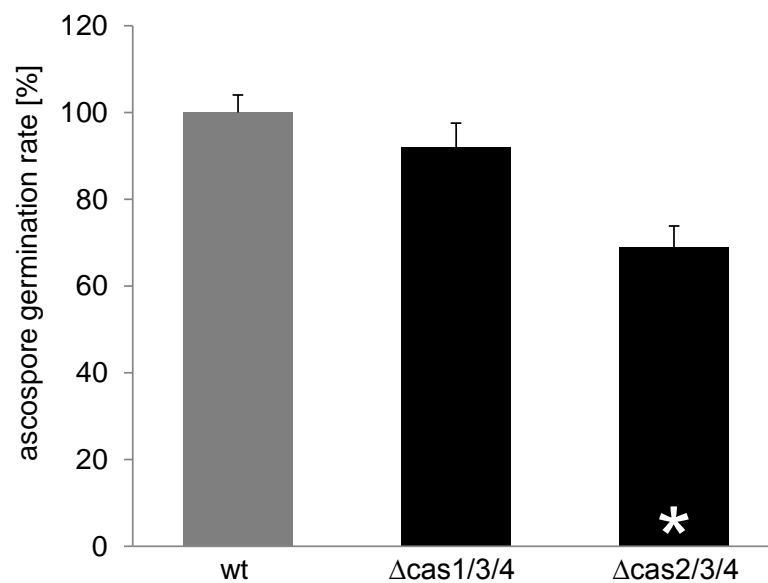


Fig. 21: Analysis of the germination efficiency of triple knock outs compared to wt. One hundred ascospores were isolated and incubated on BMM plates supplemented with 0.5% sodium acetate. Total germinated spores were counted after one, two and three days and the wt was defined as 100%. This experiment was done in triplicates. Error bars as indicated. The asterisk indicates significance according to Student's t-test.

3.4 Construction of a quadruple *cas* gene-deletion mutant

The quadruple mutant was constructed by crossing two triple deletion mutants, differing in spore color that had at least two gene deletions in common. The constructed quadruple deletion mutant was genetically analyzed for the disruption of all four *cas* genes and the integration of the *hph*-cassette at the desired gene loci by PCR with gDNA as a template (Fig. 22A and Fig. 22B). The $\Delta cas1$ and $\Delta cas2$ strains were generated by replacing the regions encoding the catalytic centers with the *hph* cassette (Elleuche and Pöggeler 2009b). Therefore, the PCR product in the quadruple deletion mutant using *cas1*- and *cas2*-specific primers was increased compared to wt (Fig. 22A). The *cas3* gene was completely replaced by the resistance cassette (Elleuche and Pöggeler 2009b) and the *cas4* gene was disrupted except for 480 bp at the C-terminus (Fig. 13). The presence of the *hph* cassette at all four *cas* gene loci was confirmed by PCR (Fig. 22B). In addition, Southern blot with an *hph* cassette-specific probe demonstrated likewise the presence of four deletion-cassettes (Fig. 22C). No PCR fragment was generated for the tested genes when cDNA was the PCR template, indicating that no *cas* gene transcripts were present in the quadruple mutant (Fig. 22A).

The *S. macrospora* quadruple deletion mutant was able to grow without any *cas* gene expression (Fig. 23 and Fig. 24). However, the vegetative growth rate was drastically reduced under ambient air conditions. Compared to wt, the growth rate of the quadruple mutant was significantly reduced by 95% on fructification medium (SWG) in ambient air, and significantly by 40% on complete medium (BMM) (Fig. 23). In both cases, growth rates were partially restored (by 65% on SWG and 20% on BMM compared to growth in ambient air) in a CO₂-enriched atmosphere (Fig. 23).

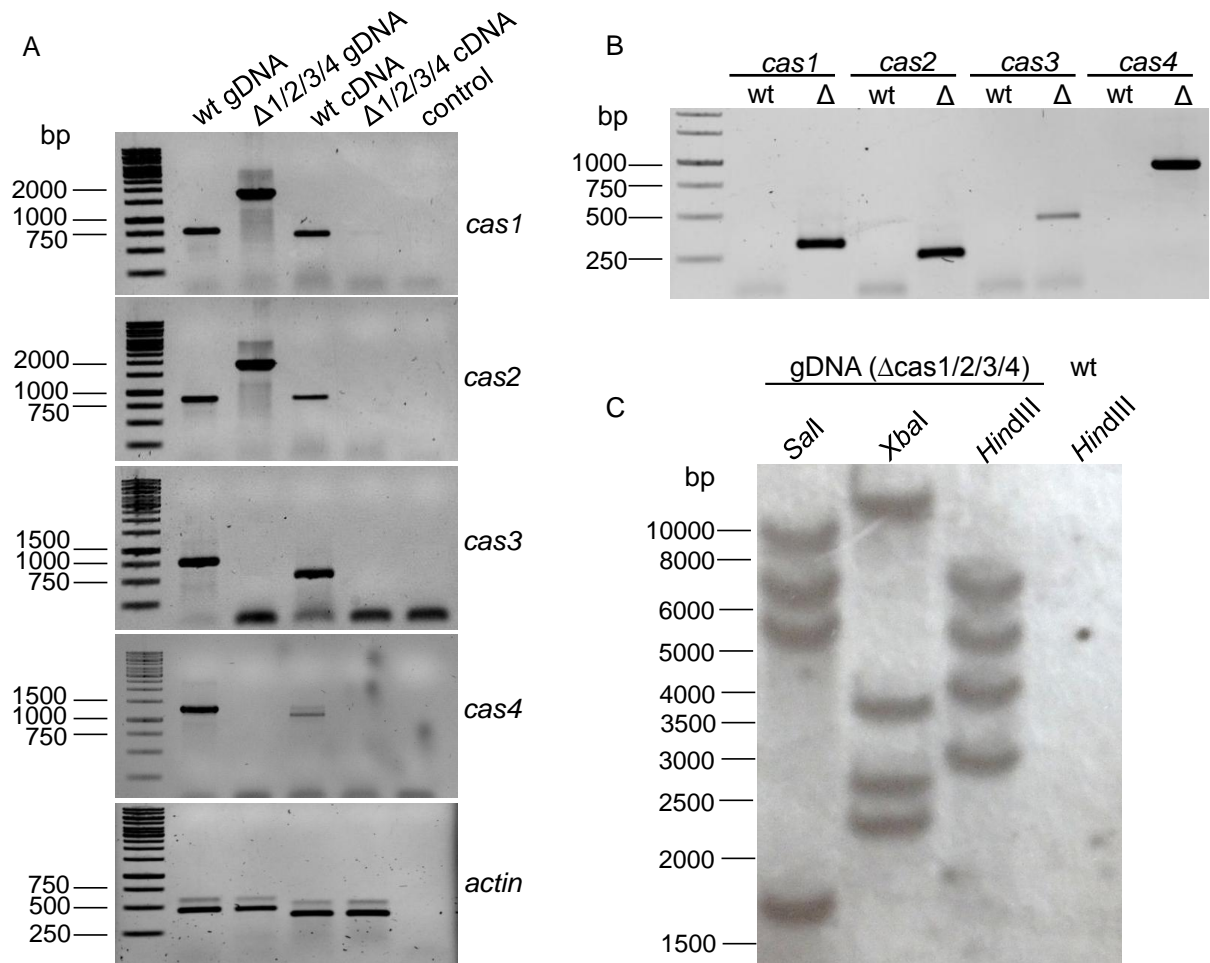


Fig. 22: Genetic analysis of the quadruple knockout strain to confirm the gene deletion. (A) PCR and RT-PCR analysis of wt and quadruple knock out strain ($\Delta cas1/2/3/4$) gDNA and cDNA to confirm deletion of all four *cas* genes. To confirm the absence of the *cas* gene transcripts, cDNA of the wt and the $\Delta cas1/2/3/4$ deletion strain was used. Part of the *actin* gene was amplified and served as an internal control. (B) PCR analysis of gDNA of wt and the quadruple knock out strain to confirm replacement of each *cas* gene by the *hph*-cassette. Primers used for the PCR verification of *cas1*, *cas2* and *cas3* deletions are taken from Elleuche and Pöggeler (2009b) and listed in Table 3. Localization of *cas4* specific primers are shown in Fig. 13 and listed in Table 3. (C) Confirmation of the quadruple knock out strain by Southern blot using gDNA of the $\Delta cas1/2/3/4$ mutant digested with *HindIII*, *Sall* and *XbaI* and a probe against a part of the *hph*-cassette. The expected fragment sizes for *HindIII* (*cas1*: 3009 bp, *cas2*: 6753 bp, *cas3*: 4723 bp and *cas4*: 3869 bp), *Sall* (*cas1*: 10828 bp, *cas2*: 1703 bp, *cas3*: 5806 bp and *cas4*: 6731 bp) and *XbaI* (*cas1*: 3924 bp, *cas2*: 16503 bp, *cas3*: 2716 bp and *cas4*: 1954 bp) could be detected. Wt gDNA, digested with *HindIII*, served as negative control.

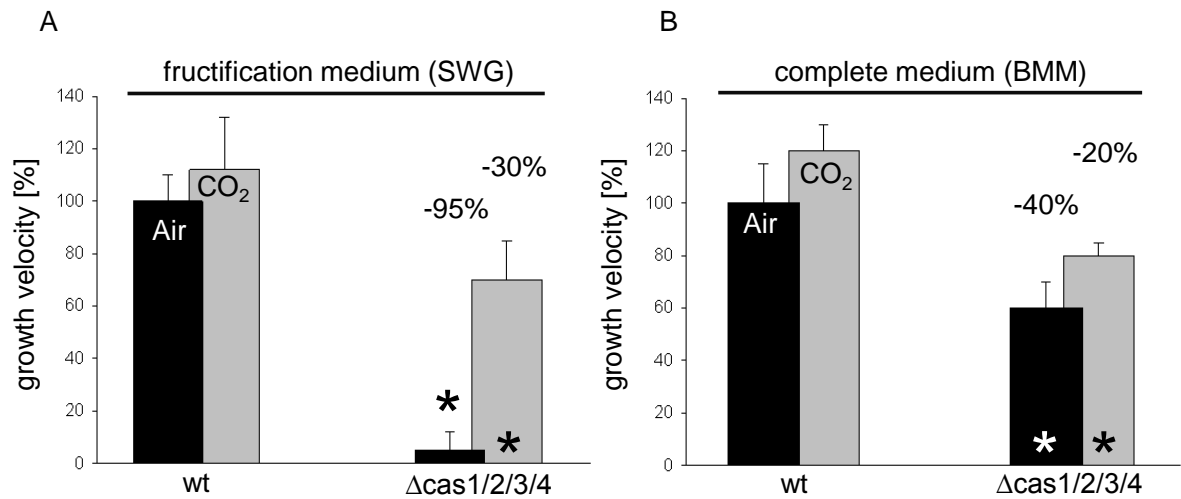


Fig. 23: Vegetative growth rate of *S. macrospora* wild type and quadruple mutant compared on fructification (SWG) and complete medium (BMM) in ambient air and at 5% CO₂ (CO₂). Strains were grown on SWG (A) and BMM (B) for seven days and the growth rate was calculated in cm/d. The growth velocity of the wt in ambient air was defined as 100%. Growth rates are the average from seven measurements of three independent experiments. Error bars are given as indicated. Asterisks indicate significance according to Student's t-test.

Growth in ambient air on BMM supplemented with 30 mg/L fatty acids restored the vegetative growth of the quadruple mutant as well. The mutant was able to grow on the surface again but nevertheless, the mutant did not form fruiting bodies after 7 days of development (data not shown). The addition of 50 mM sodium hydrogen carbonate impaired wt growth and did not restore the phenotype of the quadruple mutant (data not shown).

Furthermore, the quadruple deletion mutant did not grow on the surface of solid agar medium. The mycelium invaded the agar and formed fruiting bodies only after 20 days (Fig. 24). The wt formed perithecia at the air/agar interface, whereas perithecia of the quadruple mutant remained in the agar and did not generate mature ascospores (Fig. 24). When incubated at elevated 5% CO₂ conditions, the quadruple mutant grew on the surface and produced a few fruiting bodies at the air/agar interface, although, these contained no ascospores even after prolonged incubation times (Fig. 24).

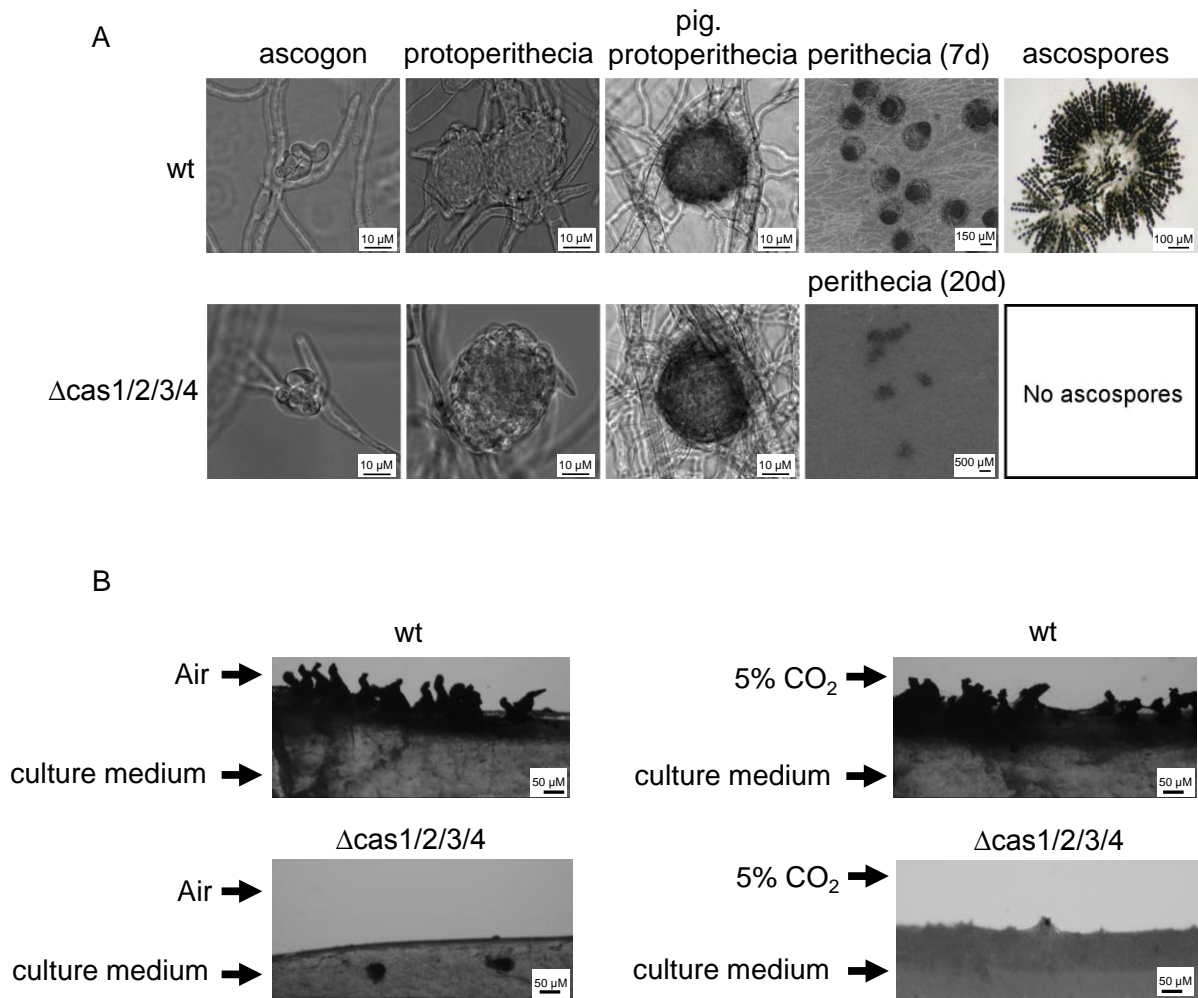


Fig. 24: Comparison of the fruiting-body development of the quadruple knock out strain and wt. (A) Microscopic analysis of the sexual development of $\Delta cas1/2/3/4$ in comparison to the wt. In contrast to the wt, perithecia were formed by the mutant only after 20 days and never contained any mature ascospores. The strains were inoculated on solid BMM on a cellophane sheet and sexual development was microscopically investigated after 3,4,5,6, and 7 days. The wt is shown as in Fig. 15. Mature perithecia were opened and the ascospores were separated from the shell. (B) Side view of quadruple knock out strain and wt. The quadruple mutant formed perithecia embedded in the agar of the culture medium at normal air and but on the agar of the culture medium at 5% CO₂. The wt formed perithecia on the agar under both conditions. The wt and the quadruple knock out strain were inoculated on solid BMM medium at 27 °C. The solid medium was sliced into thin strips that were microscopically investigated.

To analyze the growth phenotype of the agar-embedded *cas* quadruple mutant in more detail, the agar medium was covered with cellophane. The growth phenotype on the cellophane was investigated for the wt, the triple deletion-mutants and the quadruple mutant. Hyphae of triple *cas* mutants and wt grew over the cellophane and wt, $\Delta cas1/3/4$, and $\Delta cas2/3/4$ hyphae even produced fruiting bodies on the cellophane. In contrast, the triple mutants $\Delta cas1/2/4$ and

$\Delta cas1/2/3$ produced few perithecia around the cellophane (data not shown). Hyphae of the $\Delta cas1/2/3/4$ mutant did not grow on the surface of the cellophane sheet but grew and produced immature perithecia under the cellophane (Fig. 25A). When incubated in an enriched 5% CO_2 atmosphere, the quadruple mutant strain grew on the surface of the cellophane again and produced a few perithecia on the surface that did not contain ascospores (Fig. 25B).

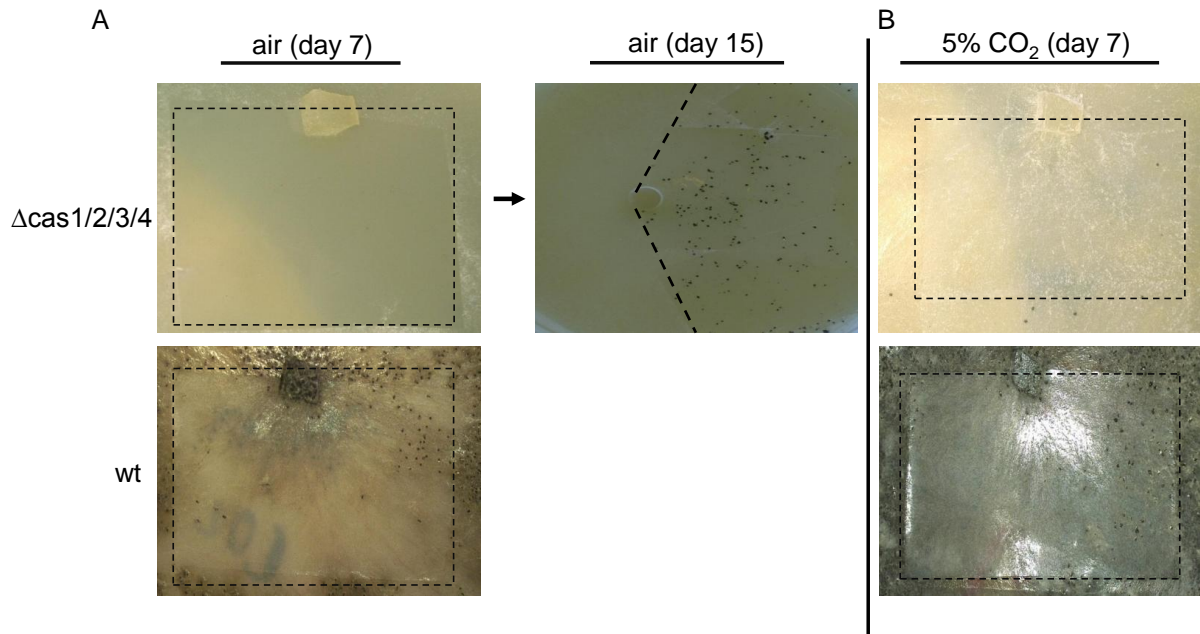


Fig. 25: Investigation of the vegetative growth of wild type and quadruple knock out strain in air and in 5% CO_2 atmosphere. (A) The pictures illustrate that the wt was able to grow over a cellophane sheet while the quadruple mutant was thereto unable under normal air conditions. After fifteen days the mutant starts forming fruiting bodies on the part of the plate covered with cellophane. (B) The growth defects of the quadruple mutant can be unspecifically restored at 5% CO_2 and the mutant regains the ability to grow slowly over the cellophane again. The strains were inoculated on solid BMM medium that was partially covered with cellophane indicated by dashed lines at 27 °C.

3.5 Functional characterization of CAS1, CAS2, CAS3 and CAS4

3.5.1 Complementation of a CA-deficient *S. cerevisiae* $\Delta nce103$ deletion mutant

The budding yeast *S. cerevisiae* contains only the single cytoplasmic plant-like β -CA NCE103p. The respective haploid deletion mutant $\Delta nce103$ exhibits a HCR phenotype and cannot grow in ambient air. Heterologous expression of CA genes can rescue the *S. cerevisiae* $\Delta nce103$ deletion mutant (Götz *et al.* 1999), with complementation depending on carbonic anhydrase activity of the heterologous enzyme (Clark *et al.* 2004). The cDNA of all four *cas* genes was expressed in the yeast mutant. The native CAS2 protein exhibits an N-terminal signal peptide (MTS) for translocation into mitochondria (Elleuche and Pöggeler 2009b). To enable cytoplasmic localization of *cas2* in *S. cerevisiae*, the nucleotides of the *cas2* cDNA encoding the MTS were removed. The CAS4 protein exhibits an N-terminal signal sequence (SS) for translocation into the endoplasmic reticulum that was removed for expression in *S. cerevisiae*. To demonstrate the ability of CAS1, CAS3, and of the truncated CAS2 and CAS4 to functionally restore the CA-deficient yeast strain, the corresponding four genes were expressed in the haploid deletion strain CEN.HE28-h ($\Delta nce103$) (Table 1) (Fig. 26).

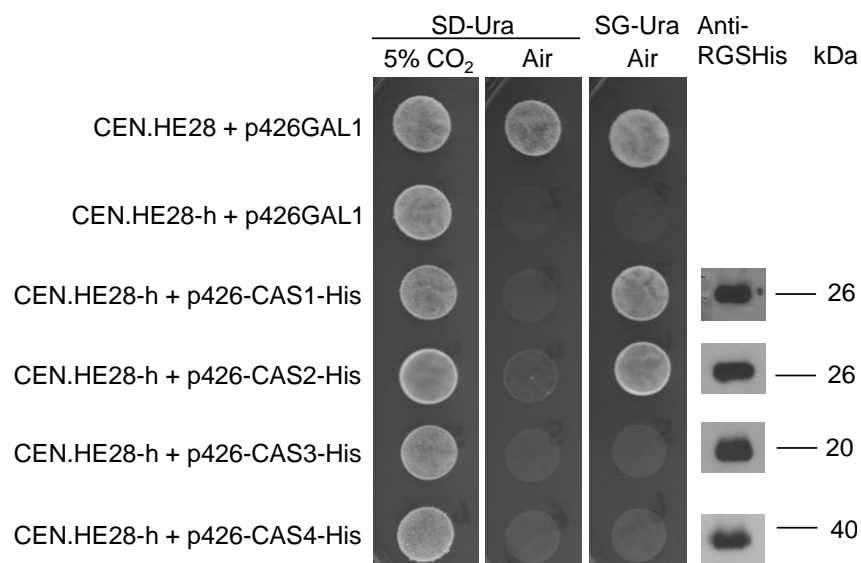


Fig. 26: Functional complementation of the haploid *S. cerevisiae* CA deletion mutant $\Delta nce103$ with *cas1*, *cas2*, *cas3* and *cas4* of *S. macrospora*. The haploid yeast deletion strain CEN.HE28-h ($\Delta nce103$) is only able to grow under high CO₂ levels. It was transformed with galactose-inducible plasmids p426-CAS1-His, p426-CAS2-His, p426-CAS3-His and p426-CAS4-His. Recombinant strains were grown three days at 30 °C in a 5% CO₂ enriched atmosphere as viability control and at 30 °C in ambient air on SD-Ura and SG-Ura plates for repression and induction of gene expression. As controls the haploid as well as the heterozygous diploid strain (CEN.HE28) were transformed with the empty vector p426GAL1. Complementation was confirmed when growth occurs in ambient air on SG-Ura plates. Western blotting with an anti-His antibody was performed to confirm the production of the heterologous proteins.

Only the full length cDNA of *cas1* and a truncated version of the *cas2* cDNA lacking the mitochondrial target sequence (MTS) fully complemented the phenotype of the *S. cerevisiae* Δ *nce103* CA mutant, demonstrating the carbonic anhydrase activity of the *S. macrospora* β -CAs CAS1 and CAS2 (Fig. 26). Neither the *cab*-like β -CA CAS3 nor the α -class CA CAS4 could restore the CA-deficient yeast strain (Fig. 26). The haploid deletion strain transformed with the empty vector served as negative control while the heterozygous strain (CEN.HE28) transformed with the empty vector was used as positive control. In addition, all strains were tested for their viability by incubation on SD-Ura at 5% CO₂ (Fig. 26). To verify the production of both proteins, western blotting with anti-His antibody was performed (Fig. 26). The results are in agreement with the expected fragment sizes for all four proteins (CAS1: 26.2 kDa; CAS2: 26.9kDa; CAS3: 20.3 kDa and CAS4: 38.4 kDa)

3.5.2 Analysis of the *in-vitro* activity and inhibition of CAS1 and CAS2

CAS1 is a cytosolic protein composed of 234 aa with a calculated molecular weight of 25.1 kDa. The native CAS2 protein (284 aa) exhibits an N-terminal signal peptide for translocation into mitochondria (Elleuche and Pöggeler 2009b). The MTS is predicted to be cleaved between His59 and Ser60 (Elleuche and Pöggeler 2009a). Therefore, the nucleotides encoding the MTS were removed to enable expression of *cas2* in *E. coli*. The truncated *cas2* gene expressed in *E. coli* encodes a protein of 225 residues with a calculated molecular weight of 25.9 kDa. CAS3 localizes to the cytoplasm and is composed of 174 aa with a calculated molecular mass of 19.2 kDa. The CAS4 protein (368 aa) exhibits an N-terminal signal sequence for translocation into the endoplasmic reticulum. The SS is predicted to be cleaved between Ser21 and Leu22. For expression in *E. coli* the sequence encoding the SS was removed. The mature, secreted CAS4 protein consists of 347 aa with a predicted molecular mass of 37.2 kDa. CAS1, CAS2, CAS3 and CAS4 were synthesized in *E. coli* Rosetta (DE3) cells as N- or C-terminal His-tag fusions. While CAS1 was N-terminally His-tagged, CAS2, CAS3 and CAS4 had been C-terminally His-tagged. The overexpression of all four *cas* genes was successful and beside of CAS4 all CAS proteins could also be purified (Fig. 27). After purification, 5-10 mg of CAS1, 10-20 mg of CAS2 and 5-7.5 mg CAS3 could be obtained per L of culture. The purified enzymes CAS1 and CAS2 were concentrated to 10 mg mL⁻¹ and dialyzed against 50 mM HEPES pH 8.3, 50 mM NaCl, and tested in a stopped-flow CO₂ hydration assay as described in 2.2.5.6.

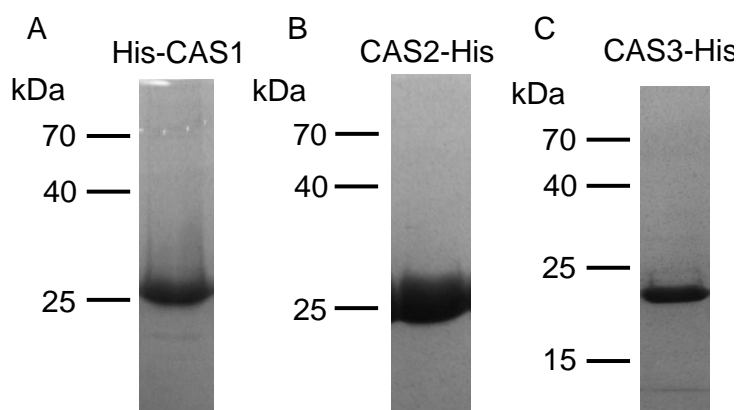


Fig. 27: Purification of His-CAS1 (A), CAS2-His (B) and CAS3-His (C). Coomassie stained, 15% SDS-Gel of purified His-CAS1, CAS2-His and CAS3-His. After washing of unbound proteins the His-tagged enzymes were eluted by addition of 500 μ L elution buffer. 10 μ L of the protein solution were separated in a SDS-PAGE. Expected fragment sizes are 27.34 kDa (CAS1), 26.91 kDa (CAS2) and 20.36 kDa (CAS3).

CAS1 and CAS2 exhibit measurable *in-vitro* CO₂ hydrase activity (k_{cat}/K_m of CAS1: $1.30 \times 10^6 \text{ M}^{-1} \text{ s}^{-1}$; CAS2: $1.21 \times 10^6 \text{ M}^{-1} \text{ s}^{-1}$; Table 6).

In addition, CAS1 and CAS2 were only weakly inhibited by the widely used sulfonamide drug acetazolamide, with inhibition constants of 445 nM and 816 nM against CAS1 and CAS2, respectively (Table 6).

Table 6: Overview about the kinetic parameters of different α - and β -class carbonic anhydrases derived from a CO₂ hydration assay (Khalifah 1971).

| Isozyme | Activity level | k_{cat} (s^{-1}) | k_{cat}/K_m ($\text{M}^{-1} \text{ s}^{-1}$) | K_I (acetazolamide) (nM) |
|---------|----------------|-------------------------------|--|----------------------------|
| hCA I | moderate | 2.0×10^5 | 5.0×10^7 | 250 |
| hCA II | very high | 1.4×10^6 | 1.5×10^8 | 12 |
| Can2 | moderate | 3.9×10^5 | 4.3×10^7 | 10.5 |
| CalCA | high | 8.0×10^5 | 8.0×10^5 | 132 |
| SceCA | high | 9.4×10^5 | 9.8×10^7 | 82 |
| FbiCA 1 | low | 1.2×10^5 | 7.5×10^6 | 27 |
| CAS1 | low | 1.2×10^4 | 1.30×10^6 | 445 |
| CAS2 | low | 1.3×10^4 | 1.21×10^6 | 816 |

The human cytosolic isozymes hCA I and II (α -class CAs), measured at 20 °C and pH 7.5 in 10 mM HEPES buffer and 20 mM Na₂SO₄. The β -CAs Can2 (from *C. neoformans*), CalCA (from *C. albicans*). SceCA (from *S. cerevisiae*), FbiCA 1 (from the plant *Flaveria bidentis*) and CAS1 and CAS2 of *S. macrospora* measured at 20 °C, pH 8.3 in 20 mM TRIS buffer and 20 mM NaClO₄. Inhibition data with the clinically used sulfonamide acetazolamide (5-acetamido-1,3,4-thiadiazole-2-sulfonamide) are also provided.

Inhibition by anions was also investigated, as these have been shown to effectively inhibit CA activity (De Simone and Supuran 2012). The majority of the anions tested were ineffective at inhibiting CAS1 and CAS2 (Table S2).

Perchlorate and tetrafluoroborate showed weak inhibition, similarly to several other CAs (Vullo *et al.* 2013b). Nitrite and nitrate anions were also ineffective CAS1 and CAS2 inhibitors with inhibition constants over 100 mM. The halogens bromide and chloride inhibited CAS1 with inhibition constants of 9.3 and 9.2 mM, respectively, while CAS2 was much more weakly inhibited. Conversely, CAS2 was more strongly inhibited by sulfate ($K_I = 4.8$ mM) than was CAS1 ($K_I > 100$ mM). The best anionic inhibitors were sulfamide, sulfamate, phenylboronic acid and phenylarsonic acid, with inhibition constants from 84 to 9 μ M for CAS1 and from 72 to 48 μ M for CAS2 (Table S2).

3.6 Structural characterization of CAS1 and CAS2

3.6.1 Analysis of the oligomerization state of the plant-type β -CAs CAS1, CAS2 and cab-type β -CA CAS3 by SEC-MALLS

To analyze the oligomerization state of His-CAS1, CAS2-His and CAS3-His in solution, size-exclusion chromatography and multi-angle laser light scattering (SEC-MALLS) was performed (Fig. 28). The CAS1 and the CAS2 samples showed a monomodal particle size distribution while the CAS3 sample displayed a bimodal distribution (Fig. 28A and Fig. 28B). The molar mass for CAS1 was calculated to 103 900 g mol⁻¹ ($\pm 2\%$), which corresponds to 3.8 times the molecular weight of the CAS1 monomer (27.37 kDa) (Fig. 28A). The molar mass of CAS2 was calculated to 96 950 g mol⁻¹ ($\pm 0.1\%$), which corresponds to 3.6 times of the CAS2 monomer (26.91 kDa) (Fig. 28B). The calculated molar mass of CAS3 amounts to 38 650 g mol⁻¹ ($\pm 0.1\%$), which corresponds to 1.9 times of the CAS3 monomer (20.36 kDa) (Fig. 28C). These findings suggest that the biological unit of CAS1 and CAS2 consists of a homo-tetramer in solution. CAS3 seems to be in a homo-dimeric oligomerization state in solution.

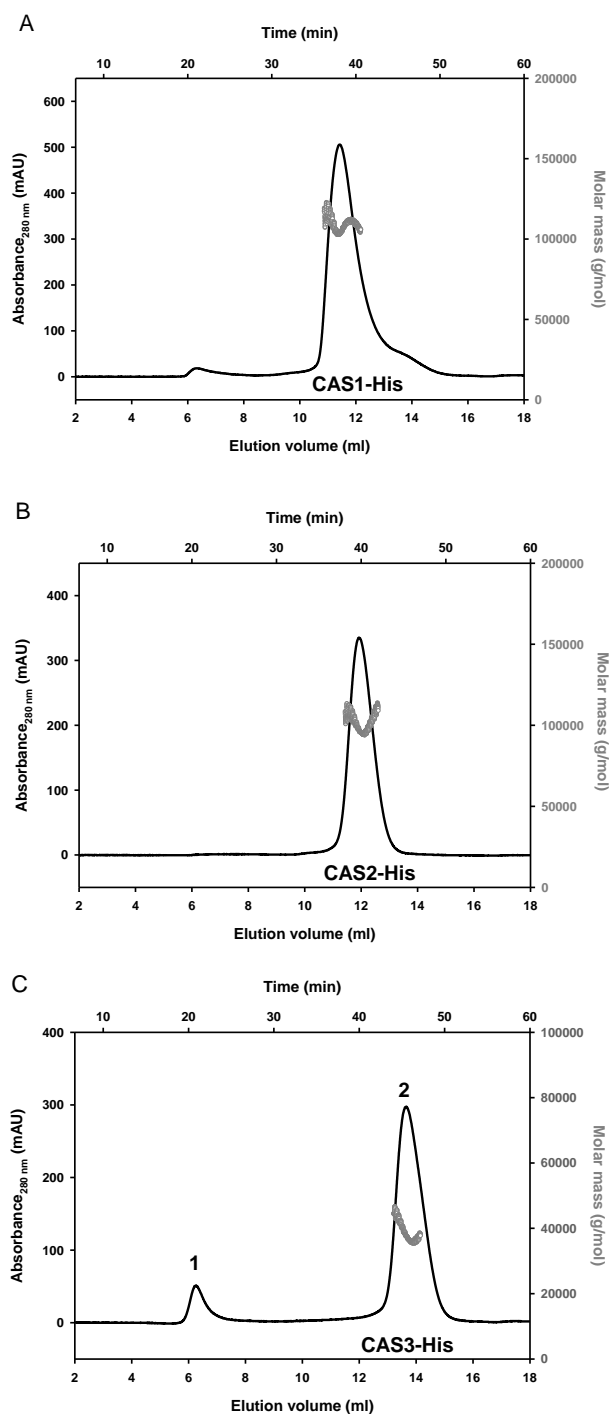


Fig. 28: Size-exclusion chromatography of His-CAS1 (A), CAS2-His (B) and CAS3-His (C) (black lines) on a Superdex 200 10/300 column coupled with multi-angle laser light scattering (grey lines). The reference proteins for SEC had the following elution profile: 670 kDa = 8.16 ml (thyroglobulin), 158 kDa = 12.54 ml (γ -globulin), 44 kDa = 15.08 ml (ovalbumin), 17 kDa = 17.21 ml (myoglobin), 1.35 kDa = 20.46 ml (vitamin B12). The molar mass for CAS1 was calculated to $103\,900\text{ g mol}^{-1}$ ($\pm 2\%$), which corresponds to 3.8 times the molecular weight of the CAS1 monomer (27.37 kDa) (A). The molar mass of CAS2 was calculated to $96\,950\text{ g mol}^{-1}$ ($\pm 0.1\%$), which corresponds to 3.6 times of the CAS2 monomer (26.91 kDa) (B). The calculated molar mass of CAS3 amounts to $38\,650\text{ g mol}^{-1}$ ($\pm 0.1\%$), which corresponds to 1.9 times of the CAS3 monomer (20.36 kDa) (C). Peak 1 in the CAS3 elution profile is very likely due to protein aggregates that eluted close to the void volume of the column. Peak 2 represents the CAS3-His protein.

3.6.2 Analysis of the crystal structure of the plant-like β -CAs CAS1 and CAS2

Despite the large number of fungal β -CAs known, only two have been structurally characterized to date: the N-terminally truncated *S. cerevisiae* CA Nce103p, and the full length CA Can2 from the basidiomycete *C. neoformans* (Teng *et al.* 2009; Schlicker *et al.* 2009). To elucidate the structural details of both enzymes, we crystallized CAS1 and CAS2 and solved their three-dimensional structures (Table S1). CAS1 crystallized in space group $P2_12_12_1$ with two monomers occupying the asymmetric unit. The structure was refined at 2.7 Å to crystallographic R factors of 20.4% and 25.1% for R_{work} and R_{free} , respectively. Analysis of crystal contacts using the PISA software (Krissinel and Henrick 2007) suggested that the biologically active molecule is a homo-tetramer possessing D_2 symmetry (Fig. 29). CAS2 crystallized in the $F222$ space group with one monomer occupying the asymmetric unit, and the structure was refined at 1.8 Å to final R_{work} of 19.1% and R_{free} of 21.1%. Crystal contact analysis indicated an equivalent homo-tetrameric oligomerization state to CAS1 (Fig. 29). The final CAS1 and CAS2 models comprise protein residues 4-213 and 14-224, respectively. The missing residues (CAS1: 1-3, 214-234; CAS2: 1-13, 225) could not be localized in the electron density map and are most likely disordered.

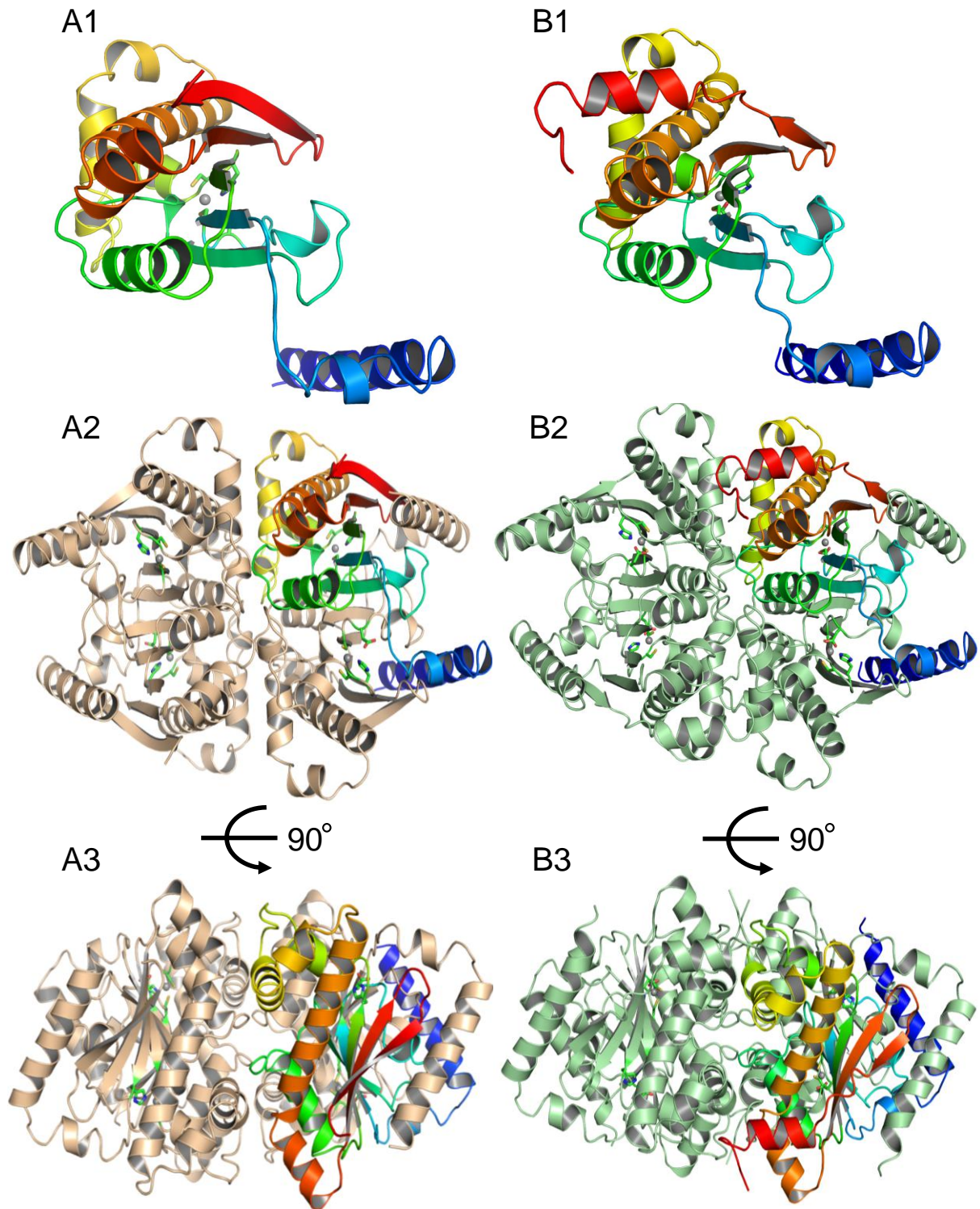


Fig. 29: Crystal structures of carbonic anhydrase CAS1 and CAS2. (A) CAS1 (B) CAS2 A1, B1: Monomers of CAS1 and CAS2 in cartoon representation, rainbow colored. A2, B2: Quaternary structure of CAS1 and CAS2 in cartoon representation illustrating the tetrameric assembly. The rainbow-colored monomers are shown in the same orientation as in A1 and B1, respectively. A3, B3: Tetramer of A2 and B2 rotated by 90° over the x-axis. Zn²⁺ -ions are shown as grey spheres. The side chains of the residues coordinating the Zn²⁺ -ion are depicted as green sticks for CAS1 and CAS2.

3.6.2.1 Structural comparison of CAS1 and CAS2

The monomers of CAS1 and CAS2 are structurally highly similar, the calculated root-mean square deviation (RMSD) amounts to 1.63 Å and has been calculated for 185 matched C α atoms, of which 84 are identical in sequence. The overall structure of each monomer consists of an N-terminal region forming a long arm composed of two perpendicularly oriented α -helices (α 1 and α 2) spanning the adjacent subunit and thus facilitating dimer formation. The central core is made up of a five-stranded mixed β -sheet (β 1- β 5), of which four β -strands (β 2- β 1- β 3- β 4) are in a parallel arrangement and the fifth (β 5) is antiparallel (Fig. 30). The active center is mostly composed of residues located at the tips of β -strands: β 1 (Cys45 of CAS1 and Cys56 of CAS2) and β 3 (His101 of CAS1 and His112 of CAS2) as well as surrounding loops (Asp47 and Cys104 of CAS1, and Asp58 and Cys115 of CAS2) (Fig. 31 and Fig. 32). The C-terminal subdomain is dominated by α -helices flanking on one side the convex surface of the β -sheet while the other side is involved in dimer and homo-tetramer formation.

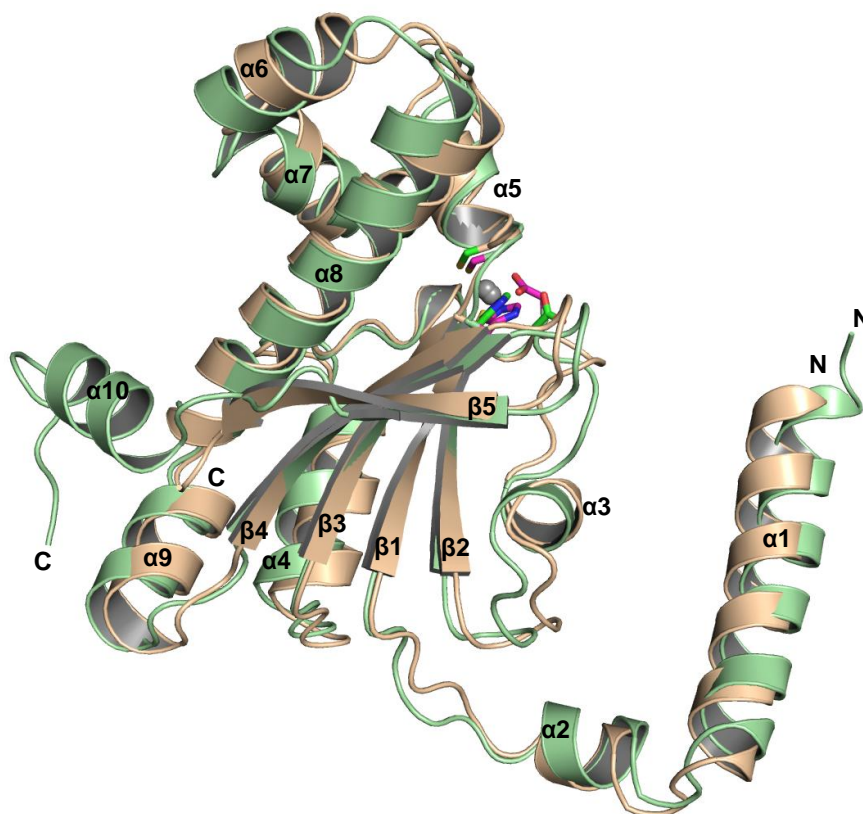


Fig. 30: Superposition of the monomeric ribbon representation for CAS1 (wheat) and CAS2 (pale green). The secondary structure elements are labeled according to the CAS2 monomer. The first and the last residues of each monomer are labeled N and C. The zinc ions are presented as grey spheres and the zinc-coordinating protein residues are depicted as sticks and colored green (CAS1) and purple (CAS2).

3.6.2.2 Analysis of the active site organization of CAS1 and CAS2

The two CAS proteins are closely related isoforms, structurally very similar, and share an overall amino-acid sequence identity of 37% (Fig. 30) (Elleuche and Pöggeler 2009b). Only minor differences were evident between the two compared CAS structures of which the most striking one concerns the coordination of the bound metal ion. In both CAS structures the zinc ion is primarily coordinated by two cysteine and one histidine residues (Cys45, His101 and Cys104 in CAS1; Cys56, His112 and Cys115 in CAS2) (Fig. 31 and Fig. 32). However, the fourth coordination ligand of the zinc ion is a water molecule in CAS1, which is accompanied in the active site of one monomer by two additional water molecules separated with a distance of 2.7 Å from each other (Fig. 31). In contrast, the fourth coordination position of zinc ion in CAS2 is occupied by a carboxylate oxygen atom of the conserved Asp58 (Fig. 32).

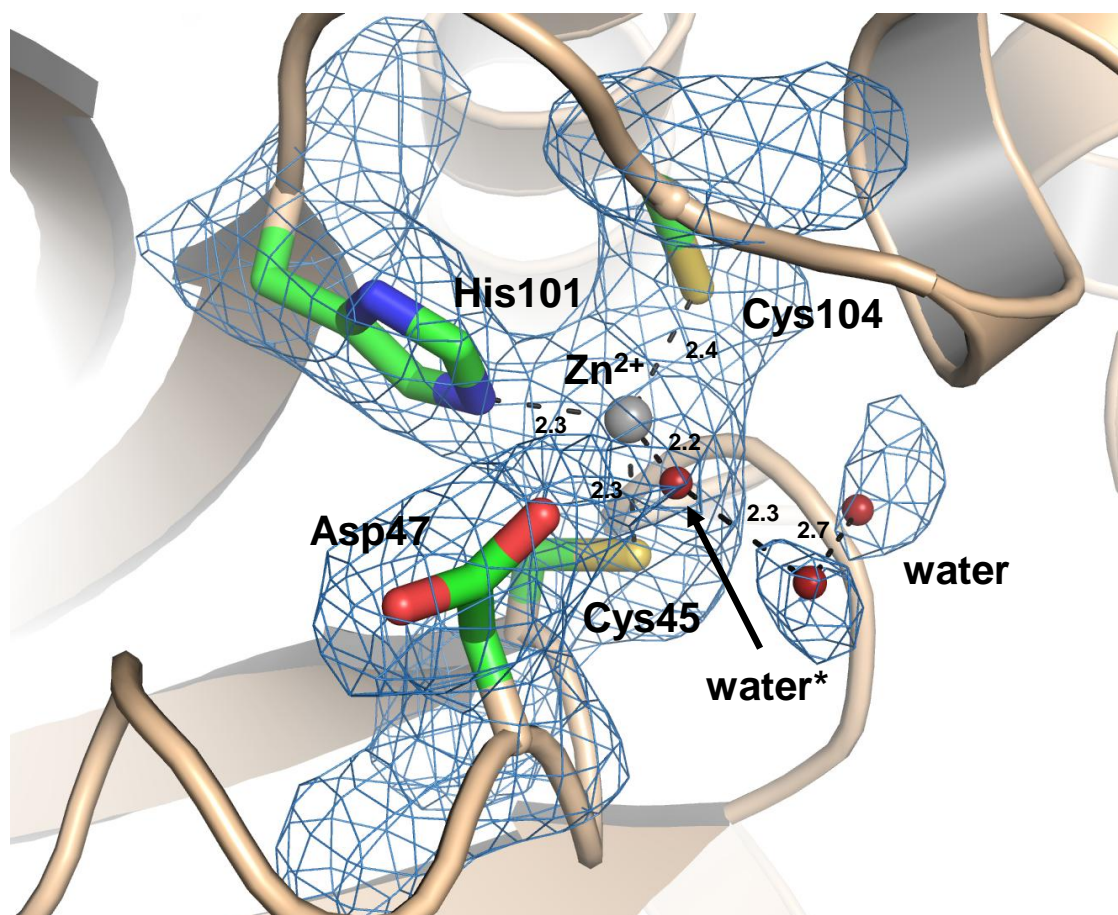


Fig. 31: Illustration of the active center of CAS1. Coordination of the zinc ion at the active site of CAS1 is achieved by side chains of Cys45, His101 and Cys104. Close to the active center three water molecules are located. One of these (marked with an arrow and labelled water*) acts as fourth ligand of the Zn²⁺ -ion. The zinc ion is presented as grey sphere and water molecules as red spheres. Distances are displayed in Å and interactions are marked by dashed lines. Simulated Annealing mFo-DFc omit map is contoured at 3.2 sigma level.

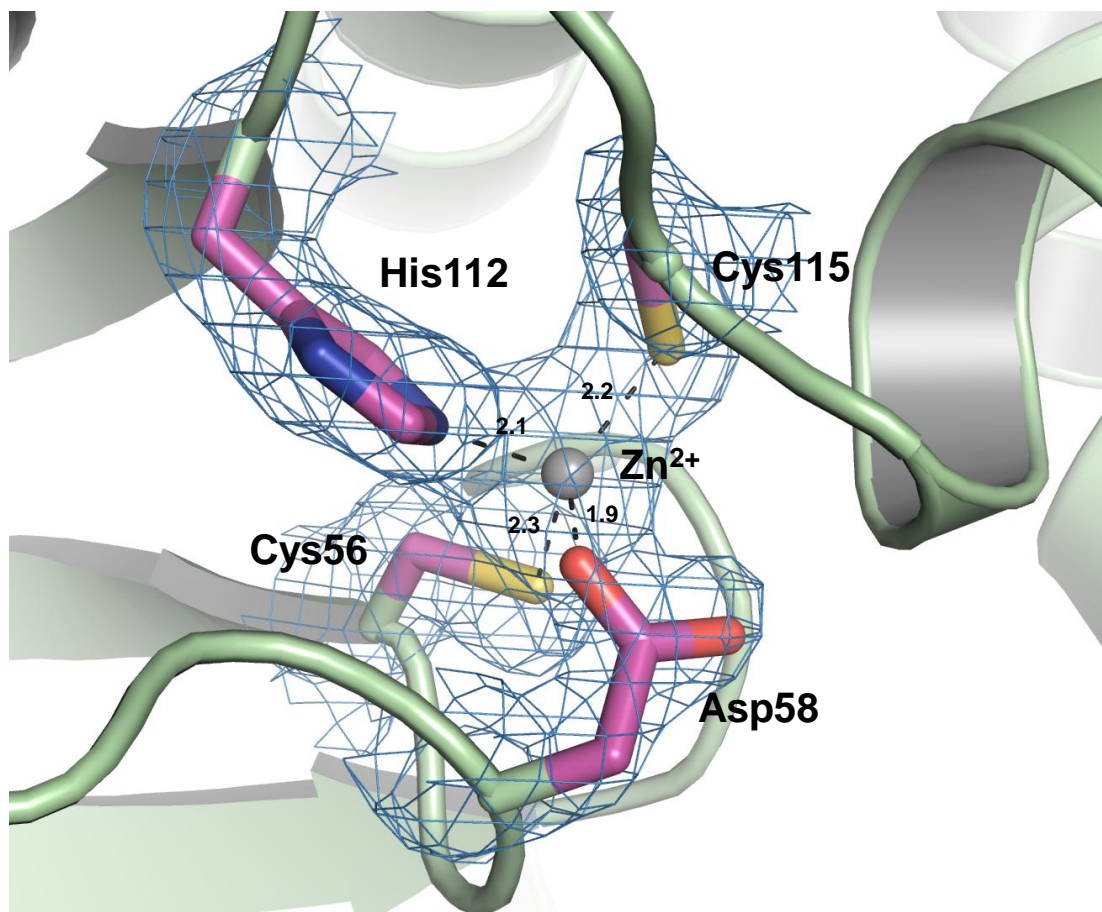


Fig. 32: Illustration of the active center of CAS2. Side chains of Cys56, His112 and Cys115 coordinate the zinc ion in the active center of CAS2. The fourth position is occupied by Asp58. The zinc ion is presented as grey. Distances are displayed in Å and interactions are marked by dashed lines. Simulated Annealing mFo-DFc omit map is contoured at 3.2 sigma level.

The different zinc coordination environments at the active site of CAS1 and CAS2 have been observed previously in CAs and have been termed type-I and type-II (Rowlett 2010; Rowlett 2014). In both enzymes, the conserved aspartic acid is part of an Asp/Arg pair proposed to be involved in proton shuffling (Tripp *et al.* 2001) and catalysis (Kimber and Pai 2000). This amino acid pair is in close proximity to the active core (Fig. 33), and is conserved in all β -CAs analyzed to date (Kimber and Pai 2000; Cronk *et al.* 2001; Schlicker *et al.* 2009; Rowlett 2010). In type-I CAs the arginine and aspartic acid residues are in close contact to each other enabling the proton transfer. In contrast, the Asp/Arg dyad is broken in type-II CAs because to aspartic acid is rotated away from the arginine. This impairs the proton transfer and thereby causing the closed conformation of the enzyme (Fig. 33) (Rowlett 2010).

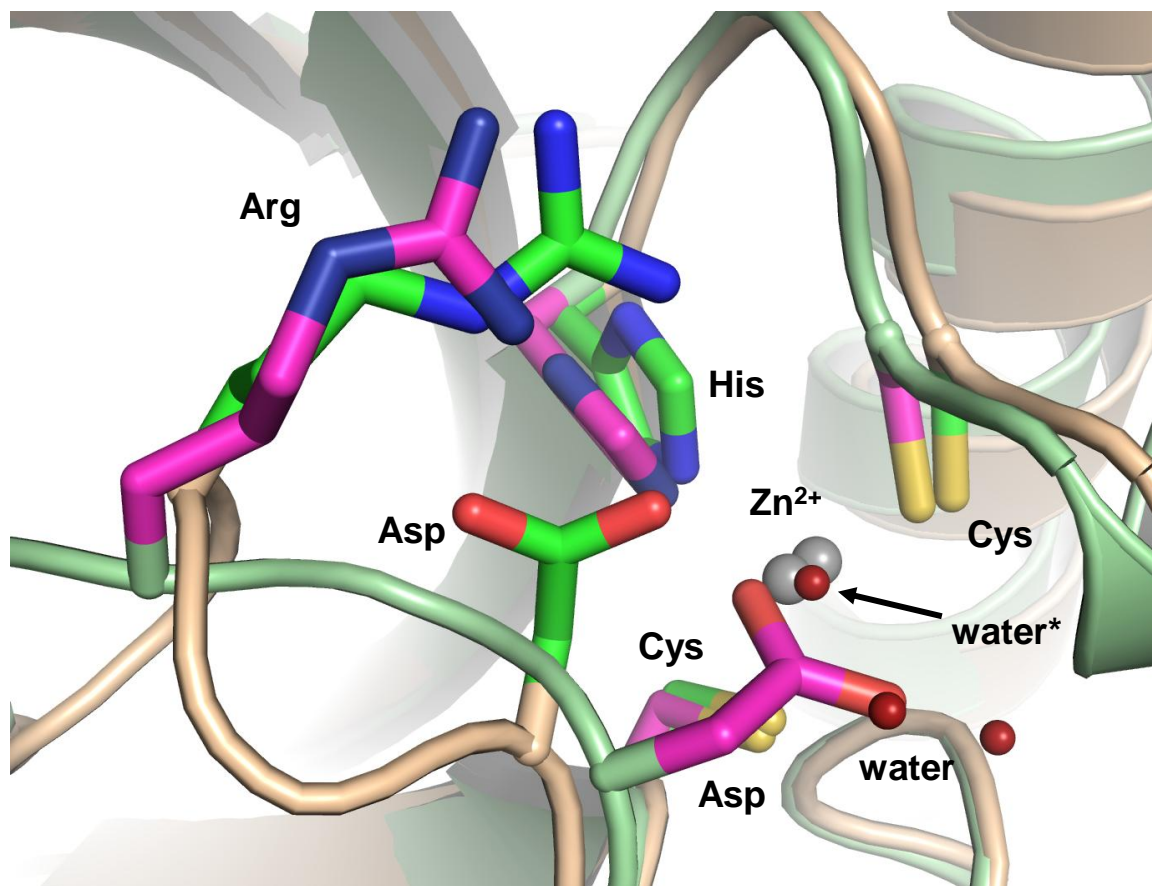


Fig. 33: Overlay of the active site of CAS1 and CAS2. Residues important for zinc binding and catalysis are depicted as sticks and colored green (CAS1) and purple (CAS2). The zinc ions are presented as grey spheres and water molecules in the CAS1 active site as red spheres.

In conclusion, this study demonstrated that CAS1 and CAS2 are tetrameric enzymes in crystal and solution while CAS3 seems to exist as a dimer in solution. CAS1 and CAS2 are active enzymes that can substitute for the yeast β -CA Nce103p. Structurally CAS1 and CAS2 are very similar and differ only in the organization of the active site.

4. Discussion

The genome of *S. macrospora* codes for four CA genes (Elleuche and Pöggeler 2009b) that are designated as *cas1*, *cas2*, *cas3* and *cas4* (Elleuche and Pöggeler 2009a; Elleuche and Pöggeler 2009b; Elleuche 2011). No further CAs could be identified in the genome.

Previously, the functions of the three β -CAs *cas1*, *cas2* and *cas3* have been studied intensively (Fig. 34) (Elleuche and Pöggeler 2009b). One focus of this thesis was to analyze the function of the α -CA *cas4*.

4.1 *S. macrospora* encodes an α -class carbonic anhydrase

Only a single fungal α -class CA (AoCA of *A. oryzae*) has been structurally characterized in detail (Cuesta-Seijo *et al.* 2011). BLAST searches with the α -CA AoCA identified α -CAs in many filamentous fungi such as *M. oryzae*, *P. anserina* or *C. globosum*. Surprisingly, no homologues of AoCA were found in *A. nidulans* and *A. fumigatus* or in yeast species (Elleuche and Pöggeler 2010).

The *S. macrospora* α -class CA CAS4 has high sequence identity with AoCA and other α -CAs from bacteria, plants and mammals. Three conserved histidine residues (His130, His132 and His149 in CAS4) coordinate a zinc ion in the active site of α -CAs (Fig. 8A). In addition, three conserved residues (Gln123, Glu149 and Asn332 in CAS4) hold the three His residues in the correct orientation by hydrogen bonding. Although the protein sequences of AoCA and CAS4 have only an overall amino-acid identity of 26% (data not shown) the identity at the active site is 77% (Fig. 8B). In AoCA, a disulfide bridge is formed between Cys58 and Cys219 (Cuesta-Seijo *et al.* 2011). Amino-acid alignment revealed that these two Cys residues are also conserved in CAS4 and in α -CAs of other fungi (data not shown). Mammalian α -CAs use a His residue (His64 in human CA II) as a proton shuttle for enzyme regeneration. This residue is replaced by phenylalanine in the α -CA of *A. oryzae* and by threonine in the *S. macrospora* CAS4. Cuesta-Seijo *et al.* (2011) have suggested that the absence of a residue that can function as an effective proton shuttle raises the question of whether CO₂ is the preferred substrate of fungal α -CAs.

4.1.1 The *S. macrospora* α -CA is posttranslationally glycosylated and secreted

Analyses of the protein sequence of several fungal α -CAs revealed that most contain an N-terminal signal peptide (Elleuche 2011). In CAS4, a 21-aa signal peptide for secretion was predicted to be cleaved between Ser21 and Leu22 using the program SignalP (Petersen *et al.* 2011). Fusion of the signal peptide-coding sequence to the *egfp* gene mediated secretion of EGFP, confirming the *in-silico* prediction (Fig. 11 and Fig. 12A). The functionality of the N-terminal signal peptide was also shown for the α -class CA AoCA from *A. oryzae* (Cuesta-Seijo *et al.* 2011). The role of secreted α -CAs in fungi is unknown. For a *penicillium* sp. which can produce an extracellular CA as well as for *C. reinhardtii* it was reported that their ability of dissolving limestone to release CO₂ is connected to the enzyme CA (Wu *et al.* 2004; Li *et al.* 2009). Applying extracellular CA inhibitors on the algae and the fungus reduced the rate of CO₂ release dramatically. In the human pathogen *H. pylori*, a periplasmic α -CA was shown to be indispensable for colonization of the gastric environment (Bury-Mone *et al.* 2008). In *S. macrospora*, CAS4 might be involved in adaptation to different environmental conditions during the life cycle and might trigger pH homeostasis or CO₂/HCO₃⁻ interconversion in the extracellular medium (Fig. 34).

Glycosylation is one of the most common posttranslational modification for secreted proteins (Peberdy 1994). Often, glycosylated proteins appear as diffuse bands and have an altered size on SDS-PAGEs (Chen *et al.* 1991; Lara *et al.* 2004). The full-length CAS4-EGFP fusion protein purified from supernatants appeared as a broad, double-band by SDS-PAGE and Western-blot. Deglycosylation removed the upper band, suggesting glycosylation of CAS4 (Fig. 12B). Using the GlycoEP glycosylation prediction program (Chauhan *et al.* 2013), 16 putative O-glycosylation and 3 potential N-glycosylation sites were predicted for CAS4. Glycosylation was also shown for the secreted α -CA AoCA (Cuesta-Seijo *et al.* 2011). For AoCA, N-glycosylation was confirmed by MS analysis prior and after EndoH treatment indicating a mass difference of 1825 Da, corresponding to 11 glycosyl units. Consistent with MS results and bioinformatics predictions, one glycosylation site was observed per monomer in the crystal structure of AoCA (Cuesta-Seijo *et al.* 2011). Glycosylation might increase the stability of secreted CAS4 and protect the enzyme from degradation as shown for a secreted α -D-mannose-1-phosphate guanyltransferase of the *Trichoderma reesei* RutC-30 strain or the protein Msp1/p75 of the probiotic *Lactobacillus rhamnosus* GG for which glycosylation enhances the resistance against proteases (Deshpande *et al.* 2008; Lebeer *et al.* 2012).

Another possible function of glycosylation is to enable enzyme activity or correct folding and efficient secretion. For example, the α -class CA CAH1 of *A. thaliana* is only targeted to the chloroplast when glycosylated (Buren *et al.* 2011). Similarly, the human lysosomal protein CLN5 was only trafficked to its correct destination when glycosylated and remained within the ER without glycosylation (Moharir *et al.* 2013).

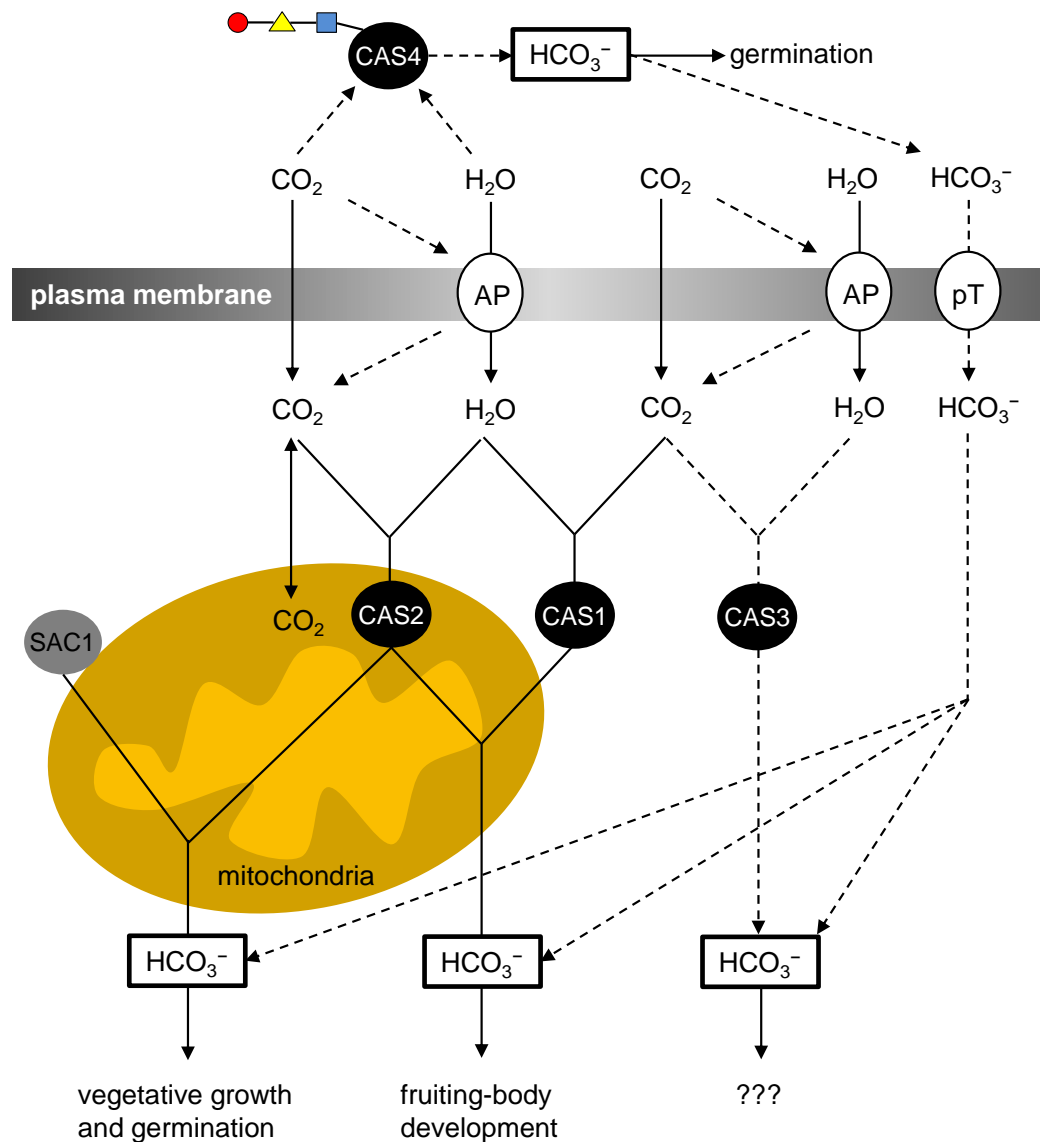


Fig. 34: Schematic illustration of the putative bicarbonate metabolism in *S. macrospora*. CO_2 enters the cell mainly via diffusion and aquaporins or as bicarbonate (HCO_3^-), produced by the glycosylated CAS4, via putative bicarbonate transporters (pT). In the cell CO_2 is quickly and reversibly hydrated to bicarbonate by the mitochondrial CAS2 or the cytoplasmic CAS1 and CAS3. The HCO_3^- produced by CAS1 and CAS2 contributes to vegetative growth and fruiting-body development. The ascospore germination is regulated by HCO_3^- produced in the mitochondria by CAS2 and outside of the cell by CAS4. Whether CAS3 really exhibits CA activity is unclear. By analogy to the adenylyl cyclase of *C. albicans* and *C. neoformans*, the adenylyl cyclase SAC1 of *S. macrospora* might be activated by bicarbonate. Dashed lines indicate putative reactions and pathways. Glycosylation is indicated by the red circle, the blue square and the yellow triangle. (modified from Elleuche and Pöggeler 2010).

4.1.2 The α -CA *cas4* is expressed mainly during sexual development in ambient air and at day five in 5% CO₂

The *S. macrospora* β -CA genes *cas1*, *cas2* and *cas3* were expressed constitutively and differently regulated by elevated 5% CO₂. The transcript level of *cas1* was decreased in ambient air at day 3 and increased at day 5. The *cas3* gene expression was significantly decreased at day 3 in ambient air while *cas2* expression was not regulated by CO₂ (Elleuche and Pöggeler 2009b). The transcript of the β -CA *nce103* of *S. cerevisiae* was increased in low CO₂ (Amoroso *et al.* 2005) while other fungal β -CA genes seem not to be regulated by the CO₂ concentration (Bahn *et al.* 2005; Mogensen and Mühlischlegel 2008).

Anyhow, regulation of fungal α -CA gene expression has not yet been analyzed. The secreted α -CA of *A. oryzae* AoCA was analyzed only structurally but not functionally or genetically (Bahn and Mühlischlegel 2006; Cuesta-Seijo *et al.* 2011). In *S. macrospora*, the *cas4* gene is continuously expressed (Fig. 9). However, it was significantly up regulated during early sexual development. Elevated CO₂ concentrations increased transcript levels at day 5 of fruiting-body development compared to normal air conditions (Fig. 10). This result suggests a specific role for *cas4* during sexual development in ambient air.

The nematode *Caenorhabditis elegans* has two α -class CAs that are constitutively expressed during development and up regulated in a 20% CO₂ atmosphere (Fasseas *et al.* 2011). Similarly, the transcript level of the periplasmic *Chlamydomonas reinhardtii* α -class CA CAH1 increases when the algae are incubated in 5% CO₂ (Fukuzawa *et al.* 1990). In contrast, the α -CA of the human pathogen *H. pylori* is not regulated by CO₂ concentrations and is expressed at the same level under different CO₂ conditions (Chirica *et al.* 2002).

CA activity has been shown to be important for pathogenicity in *C. albicans* and *C. neoformans*. In *C. albicans*, a bicarbonate dependent adenylyl cyclase, which is homologous to prokaryotic adenylyl cyclases (Chen *et al.* 2000), has been described regulate pathogenicity-related genes (Klengel *et al.* 2005; Mogensen *et al.* 2006; Hall *et al.* 2010). Although, there seems to be an obvious connection between the bicarbonate producing CAs and the adenylyl cyclase, the CA expression in *C. albicans* is not regulated by the adenylyl cyclase (Cottier *et al.* 2012).

By analyzing the complex CA regulation of *C. albicans* the novel bZIP transcription factor Rca1p was discovered and described as the first direct CO₂ dependent regulator of CA genes. The transcription factor Rca1p activates CA gene expression at low CO₂ concentrations and also seems to repress virulence-related genes, confirming the existence of an additional

cAMP-independent CO₂ signaling pathway in *C. albicans* (Cottier *et al.* 2012). Orthologs of Rca1p were also discovered in the yeasts *S. cerevisiae* (Cst6p) and *C. glabrata* (CgRca1p) (Cottier *et al.* 2013). In the deletion mutants of the respective transcription factor genes, CA-gene expression was no longer induced in ambient air. It has been shown that the transcription factor Cst6p in *S. cerevisiae* controls CA-gene expression through a conserved TGACGTCA motif in the promoter of the yeast CA-gene *nce103* (Fig. 6) (Garcia-Gimeno and Struhl 2000; Cottier *et al.* 2012). An identical sequence can also be found in the promoter of the *C. glabrata* CA-gene but not in the promoter of the *C. albicans nce103* gene. Deletion of the TGACGTCA motif in the promoter of both CA genes led to the loss of CA-gene induction at 0.04% CO₂ (Cottier *et al.* 2013).

An additional transcription factor that was shown to be involved in CO₂ sensing was identified in *N. crassa*. The transcription factor is involved in the suppression of early conidiation that was even more evident under elevated CO₂ levels and therefore named CHC1 (conidiation at high carbon dioxide) (Sun *et al.* 2011). Homologous genes of the yeast *Cst6* and *Rca1* could also be identified in *N. crassa* (Colot *et al.* 2006). Deletion of these two bZIP transcription factor genes lead to ascospore lethality in *N. crassa*, thus the encoded genes were named *asl1* (NCU_01345) and *asl2* (NCU_01459) (Colot *et al.* 2006). The fungal bZIP transcription factor family can be divided into two separate clades (Tian *et al.* 2011). Interestingly, the *S. cerevisiae* Cst6p, the *C. albicans* Rca1p and the *N. crassa* ASL1 and ASL2 are included in one clade. Orthologs of all three *N. crassa* genes *chc1*, *asl1* and *asl2* could be identified in *S. macrospora* and were named *Smasl1*, *Smasl2* and *Smchc1* (Schütter 2013). The heterokaryotic deletion mutants of these genes exhibited no alterations of the phenotype compared to the wt at 5% CO₂ or in ambient air (Schütter 2013). Based on their sequence identity to the *N. crassa* and yeast genes it is conceivable that these three transcription factors might be involved in CA regulation in *S. macrospora*. So far no homokaryotic deletions mutants of *Smasl1* and *Smasl2* and *Smchc1* could be generated, indicating their importance for viability of *S. macrospora*. This means that their hypothetical involvement in CA regulation in *S. macrospora* cannot be tested as long as no homokaryotic deletions strains are available.

4.1.3 CAS4 is involved in vegetative growth and ascospore germination

Similar to the strains $\Delta cas1$, $\Delta cas2$ and $\Delta cas3$, the strain $\Delta cas4$ exhibits no growth inhibition under regular CO₂ conditions (Elleuche and Pöggeler 2009b) (Fig. 15 and Fig. 16A). The

$\Delta cas4$ strain exhibited a reduced growth rate and a slight delay in fruiting-body formation. HCO_3^- production in mitochondria by CAS2 is required for optimal vegetative growth of *S. macrospora* (Elleuche and Pöggeler 2009b). HCO_3^- produced by the secreted CAS4 might be transported into hyphae to contribute to an intracellular HCO_3^- pool (Cordat and Casey 2009) (Fig. 34). However, medium supplemented with 50 mM HCO_3^- did not complement the reduced vegetative growth of $\Delta cas4$. Interestingly, the addition of 50 mM HCO_3^- equally impaired the growth of wt and $\Delta cas4$ (data not shown).

Similar to the $\Delta cas2$ strain, the $\Delta cas4$ strain showed a significantly reduced ascospore germination rate (Fig. 16B). Therefore, *S. macrospora* either requires a sufficient amount of HCO_3^- in the culture medium for proper ascospore germination or depletion of the internal HCO_3^- pool leads to the same ascospore germination phenotype as the $\Delta cas2$ strain (Elleuche and Pöggeler 2009b) (Fig. 34). Alternatively, by catalyzing the production of protons, the secreted α -class CAS4 might lower the pH to create an environment optimal for germination. *S. macrospora* ascospores display an optimal germination efficiency only on BMM medium supplemented with 0.5% sodium acetate, which results in pH 6.0 (Esser and Kuenen 1967).

4.2 *S. macrospora* survives in ambient air without CA

Fungal mutants without a functional CA cannot grow under standard CO_2 conditions (Elleuche and Pöggeler 2010). In *S. macrospora*, the $\Delta cas1/2$ mutant is unable to form fruiting bodies in ambient air after 7 days but still grows vegetatively (Elleuche and Pöggeler 2009b). To investigate the *cas* genes required for *S. macrospora* growth in normal air conditions, double and triple mutants in all possible combinations and a quadruple mutant were constructed. All mutants grew vegetatively, although, some mutants showed greatly reduced growth rates (Fig. 16A, Fig. 18A, Fig. 20, Fig. 23 and Fig. 24A). Growth of the quadruple mutant improved more on complex BMM medium than on SWG medium (Fig. 23). The complex BMM medium probably provided *S. macrospora* with external substances or end products of CA-dependent metabolic pathways. The vegetative growth defect but not the deficiency to produce fruiting bodies was fully restored by the addition of 30 mg/L fatty acids to the culture medium in the quadruple mutant (data not shown). Similarly, the addition of fatty acids complemented the growth defects in *C. neoformans* $\Delta can2$ and *S. macrospora* $\Delta cas2$ strains (Bahn *et al.* 2005; Elleuche and Pöggeler 2009b). In contrast, the addition of 50 mM HCO_3^- to the culture medium did not restore vegetative growth or perithecia

formation in the quadruple mutant. Regardless of medium or supplements, vegetative growth of $\Delta cas1/2/3/4$ was partially restored by an enriched 5% CO₂ atmosphere (Fig. 23).

At 0.04% CO₂ on solid medium, $\Delta cas1/2/3/4$ hyphae grew invaded into the agar and never grew on the surface of the agar medium (Fig. 24 and Fig. 25). It might be possible that CO₂ produced by respiration was spontaneously converted to HCO₃⁻ and accumulated in the medium. In ambient air, after 20 days, the mycelium of the quadruple mutant embedded in the agar formed a limited number of immature perithecia with no ascospores (Fig. 24). Covering the solid culture medium with a cellophane sheet enhanced the formation of perithecia, possibly because the cellophane impeded the diffusion of CO₂ from the medium and increased the spontaneous formation of HCO₃⁻ (Fig. 25). After 15 days, an increased number of empty fruiting bodies were formed below the cellophane. However, the spontaneous formation of fruiting bodies still seems not to allow the production of mature ascospores. In an atmosphere of 5% CO₂ the $\Delta cas1/2/3/4$ mutant grew on the surface of the cellophane, but formed only a limited number of perithecia that contained no mature ascospores (Fig. 25). In contrast, the $\Delta cas1/2$ mutant produced a reduced number of ascospores at 5% CO₂ (Elleuche and Pöggeler 2009b).

4.3 The plant-type β -CAs CAS1 and CAS2 are active enzymes

The genome of the filamentous ascomycete *S. macrospora* encodes four carbonic anhydrases. Two β -CAs, named CAS1 and CAS2, have been shown to be the major CAs involved in sexual development and ascospore germination (Elleuche and Pöggeler 2009b). Both proteins were able to restore growth in a β -CA *S. cerevisiae* deletion mutant in ambient air, demonstrating their *in-vivo* activity (Fig. 26). CAS1 and CAS2 were heterologously expressed in *E. coli* for structural and functional studies. Purified CAS1 and CAS2 exhibited hydration activity, which was low compared with α - and β -CAs from other organisms (Table 6). Filamentous fungi, such as *S. macrospora*, have evolved a redundant system comprising multiple CAs that can replace each other if needed (Elleuche and Pöggeler 2009b; Elleuche and Pöggeler 2009a; Han *et al.* 2010; Elleuche 2011). In contrast, most bacteria and ascomycetous yeasts have to maintain the supply of bicarbonate with a single CA. Therefore, individual CAs from multi-enzyme organisms may exhibit low *in-vitro* activity, but overall activity may be higher than that of bacteria or yeast with a single CA enzyme. In support of this, *S. macrospora* single CA deletion mutants are still able to grow in ambient air, while deletion mutants of bacteria and yeasts encoding only a single CA cannot grow under these

conditions (Götz *et al.* 1999; Kusian *et al.* 2002; Hashimoto and Kato 2003; Klengel *et al.* 2005; Elleuche and Pöggeler 2009b). Compared to CAs of other organisms, CAS1 and CAS2 are only weakly inhibited by anions and the sulfonamide drug acetazolamide (Table 6 and Table S2). The natural habitat of *S. macrospora* is the dung of herbivores, which is an environment rich in carbon, nitrogen and minerals. High levels of resistance against anionic inhibitors such as nitrite and nitrate might be due to an adaption of *S. macrospora* to its ecological niche in which ions and trace elements are found at high concentrations (Madejón *et al.* 2012). Such an adaption has been proposed for bicarbonate resistance of the α -CA VchCA from *Vibrio cholerae* (Vullo *et al.* 2013a).

Recently, there has been an increased interest in utilizing CAs for industrial applications such as CO₂ sequestration and biofuel production (González and Fisher 2014). Often, biocatalysts used for such applications do not resist the harsh industrial conditions. In particular, the presence of SO_x and NO_x, that can be present in flue gases can pose a problem for enzyme activity (Bond *et al.* 2001). The resistance of *S. macrospora* CAS1 and CAS2 to anionic inhibitors observed in this study, coupled with their efficient expression in *E. coli*, makes them good candidates for industrial applications (Table S2).

4.4 The plant-type β -CAs CAS1 and CAS2 are tetrameric enzymes in crystal and solution

The monomeric structure of both β -CAs from *S. macrospora* closely resembles that of other β -CAs, with the three core elements (N-terminal arm, α/β core and a C-terminal extension) being present in all β -CA structures (Rowlett 2010). Three amino acids, conserved only in plant-like β -CAs (Gln151, Phe179, Tyr205; numbering according to the *Pisum sativum* CA), confirm that CAS1 and CAS2 belong to the plant-like sub class of β -CAs (Elleuche and Pöggeler 2009a). The search for the closest structural neighbors of CAS1 using PDBeFold (Krissinel and Henrick 2004) identified β -CAs from *S. cerevisiae* (RMSD: 1.68 Å, 184 matched C α , 30% sequence identity) and *P. sativum* (RMSD: 1.64 Å, 187 matched C α , 32% sequence identity). For CAS2, the *S. cerevisiae* (RMSD: 1.7 Å, 180 matched C α , 27% sequence identity) and *E. coli* (RMSD: 1.46 Å, 184 matched C α , 53% sequence identity) β -CAs showed highest degree of structural similarity.

Despite their importance for fungal growth and pathogenicity, only two fungal β -CAs and one α -CA have been structurally characterized to date (Schlicker *et al.* 2009; Teng *et al.* 2009; Cuesta-Seijo *et al.* 2011). Although, similar in structure and sequence, the fungal β -CAs

CAS1 and CAS2 structures determined in this work revealed unexpected differences to the structures of the β -CAs from *C. neoformans* and *S. cerevisiae*. The *S. macrospora* CAS1 and CAS2 are tetrameric (Fig. 29), whereas *S. cerevisiae* and *C. neoformans* β -CAs form dimeric assemblies (Teng *et al.* 2009; Schlicker *et al.* 2009). Nevertheless, tetrameric assemblies of β -CAs have been reported from bacteria and algae as well (Cronk *et al.* 2001; Huang *et al.* 2011).

In detail, the N-termini of CAS1 and CAS2 are composed of two perpendicularly oriented α -helices (Fig. 30). Similarly, the N-terminus of *S. cerevisiae* Nce103 is made up of two α -helices shown to be important for activity but not for dimerization (Teng *et al.* 2009). In contrast, the N-terminus of *C. neoformans* Can2 is composed of four antiparallel α -helices that interact with a channel crossing the active-site entrance. Schlicker *et al.* (2009) assumed that this N-terminal extension may be involved in internal regulatory mechanisms, or may mediate interaction with another protein. The N-terminus of the *C. albicans* β -CA is even more extended than that of Can2, which was only capable of partially complementing the *C. albicans* CA mutant strain (Fig. 35). This led to the assumption that the length of the N-terminus was particularly important for activity (Schlicker *et al.* 2009). The conformation of the N-terminal region of CAS1 and CAS2 is structurally similar to that of *S. cerevisiae* CA Nce103, and unsurprisingly, the phenotype of the $\Delta nce103$ yeast mutant was completely restored by heterologous expression of *cas1* and *cas2* (Fig. 26).

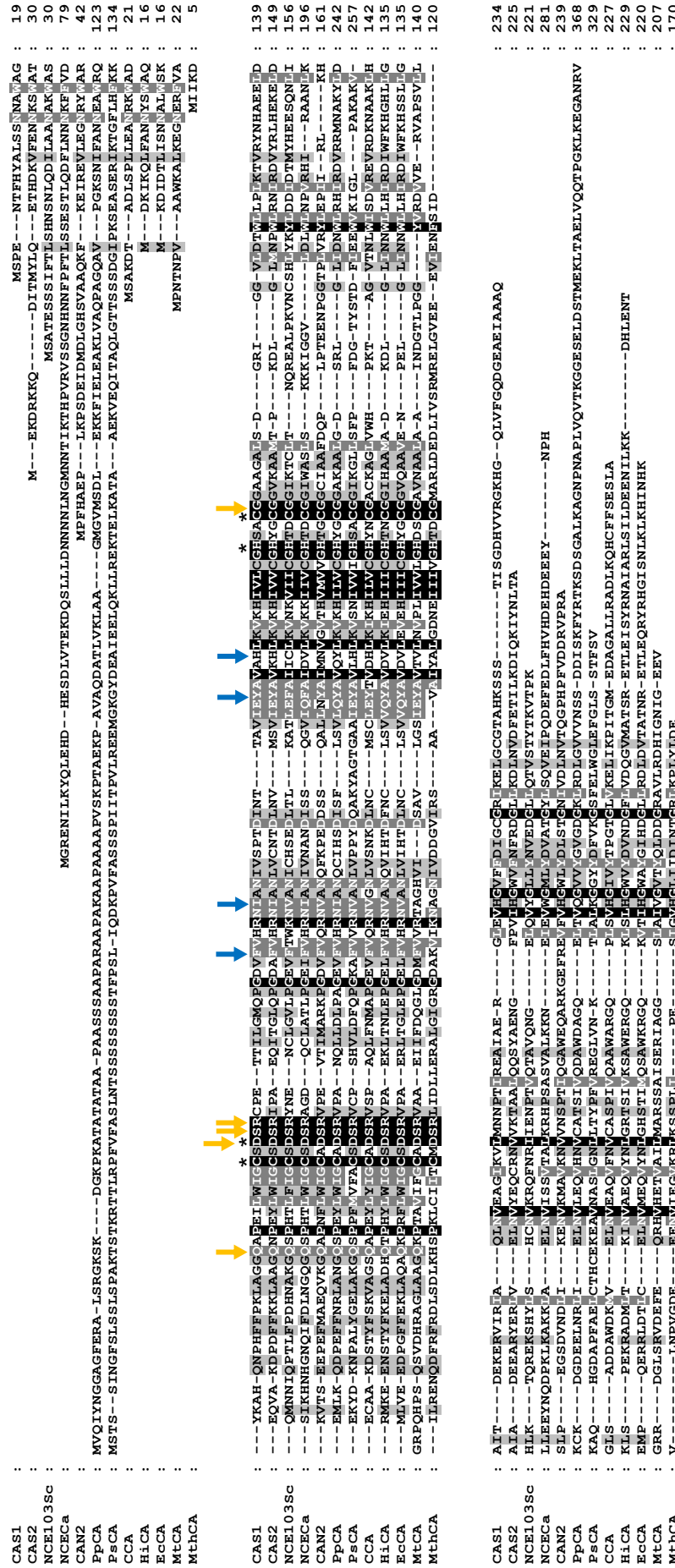


Fig. 35: Amino-acid sequence alignment of β -CAs from different species. The alignment was created with ClustalOmega (Sievers *et al.* 2011) using the following sequences: CAS1 (*S. macrospora*, PDB ID: 4O1J), CAS2 (*S. macrospora*, 4O1K), NCE103Sc (*S. cerevisiae*, 3EYX), NCECa (*C. albicans*, Acc. No. Q5AJ71), CAN2 (*C. neoformans*, PDB ID: 2W3Q), PpCA (*P. purpureum*, 1DDZ), PsCA (*P. sativum*, 1EKJ), CCA (*Cocomyxa spec.*, 3UCJ), HiCA (*H. influenzae*, 2A8C), EcCA (*E. coli*, 1I6P), MtCA (*M. tuberculosis*, 1YLK), MthCA (*M. thermoautotrophicum*, 1G5C). Black asterisks indicate amino acids involved in zinc ion binding (Asp47 of CAS1 and functional equivalent Asp residues in the other sequences are involved in zinc ion binding only in CAs of the type-II active core). Conserved amino acids at the active site are marked by yellow arrows and amino acids at the active site cleft are highlighted with blue arrows (classification of conserved amino acid residues according to Rowlett 2010). Residues are colored black, dark grey and light grey indicating decreasing conservation grades among the sequences. The amino-acid sequence of PpCA has been shortened and lacks the residues 369 to 571.

In the electron density map of CAS1, Cys47, His101 and Cys104 can be clearly seen coordinating the zinc ion. Additionally, three water molecules were observed in the close vicinity of the active site of one monomer occupying the asymmetric unit. One water molecule is positioned 2.3 Å away from the metal ion and occupies the fourth coordination position (Fig. 31) while the other two are spaced 2.7 Å apart, the distance which is about 0.4 Å longer than the spacing between two oxygen atoms in a CO₂ molecule. The distance of 2.3 Å between the water molecule coordinating the zinc ion and one of the water molecules separated by 2.7 Å suggests that the latter two could mimic the oxygen atoms of the substrate CO₂ molecule.

A water molecule acting as the fourth ligand coordinating the zinc ion has been already reported for several plant and yeast β-CAs, e.g.: the *P. sativum*, *C. neoformans* and *S. cerevisiae* β-CAs (Kimber and Pai 2000; Schlicker *et al.* 2009; Teng *et al.* 2009). Those structures and the structure of CAS1 reported here represent the so-called open conformation of the enzyme, also named type-I, (Fig. 36A) (Kimber and Pai 2000; Schlicker *et al.* 2009; Teng *et al.* 2009; Rowlett 2010). In contrast, no water molecules could be localized in the close vicinity of the active site of CAS2. The coordination sphere of the zinc ion in CAS2 is instead completed by a carboxylate oxygen atom of a conserved Asp58 located on a loop connecting β-strands β1 and β2 in the close proximity to the active site (Fig. 36B). An Asp side chain occupying the fourth position of the zinc coordination sphere has been reported previously for structures of the β-CA from the red alga *P. purpureum* and bacterial β-CAs from *E. coli*, *H. influenza* and *M. tuberculosis* (Rv3588c) (Mitsuhashi *et al.* 2000; Cronk *et al.* 2001; Covarrubias *et al.* 2005; Cronk *et al.* 2006). The accompanying structural changes of the loop harboring conserved Asp residue cause active site closure and represent the closed (type-II) conformation of the enzyme, which has been shown to be inactive (Covarrubias *et al.* 2006) (Fig. 36B). However, the closed conformation of the loop harboring the Asp58 in CAS2 is stabilized by crystal contacts. Therefore it is anticipated that the observed closed state may convert to an open state when a water molecule replaces the Asp residue at higher pH, such as pH 8.3, at which the kinetic measurements were performed. This phenomenon was demonstrated for the *M. tuberculosis* enzyme Rv1284 (Covarrubias *et al.* 2005).

In addition to differences in conformation of the loop responsible for changing the state of the active site (opening and closing), less pronounced differences were observed at the C-termini of *S. macrospora* CAS1 and CAS2.

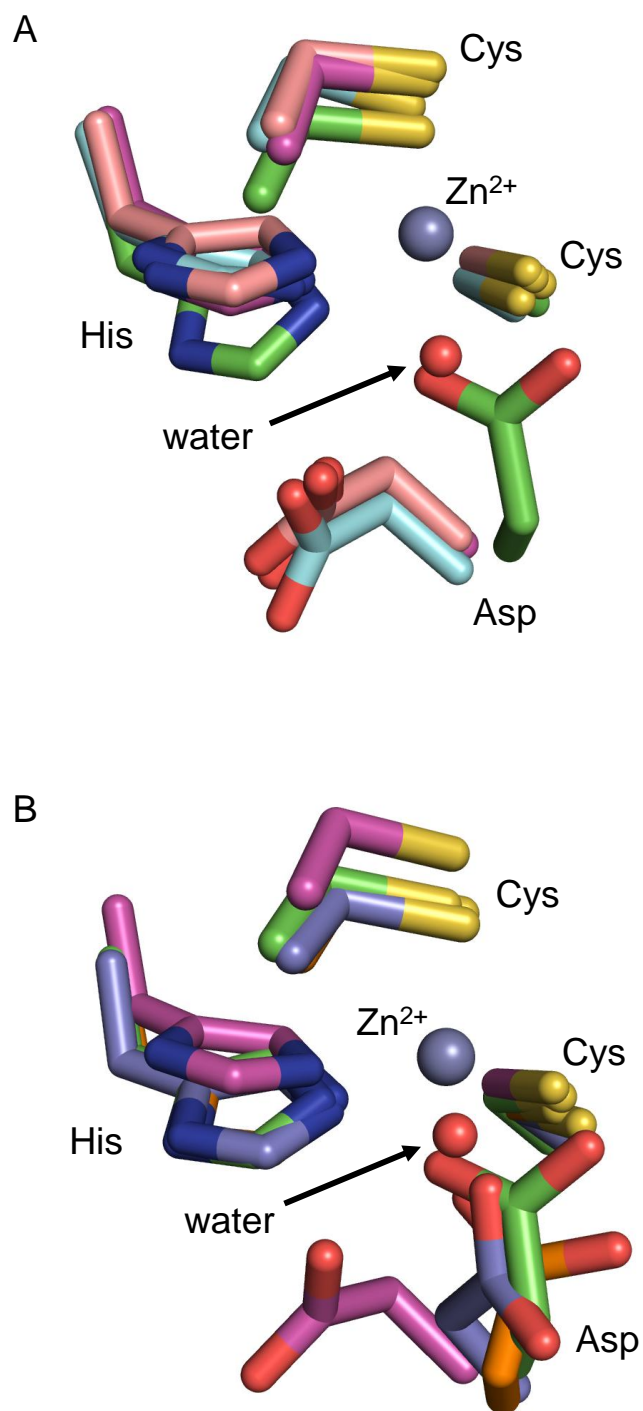


Fig. 36: Superposition of the active site of type-I and type-II plant-like β -CAs. (A) Overlay of the “open” active site of representative type-I plant β -CAs (*P. sativum* (cyan), *C. neoformans* (pink) with CAS1 (purple) and CAS2 (green). (B) Overlay of the “closed” active site of representative type-II plant β -CAs (*E. coli* (blue), *P. purpureum* (orange) with CAS1 (purple) and CAS2 (green). The zinc ions are shown as grey spheres. The water molecule in the active center of CAS1 is indicated as a red sphere.

Although CAS1 is nine amino acid longer than CAS2, its C-terminal 21 residues could not be localized in the electron density map. In contrast, the C-terminus of CAS2 is almost completely resolved and forms a loop-helix-loop extension, establishing several polar contacts to the adjacent monomer which appear to be important for the tetramer formation (Fig. 37).

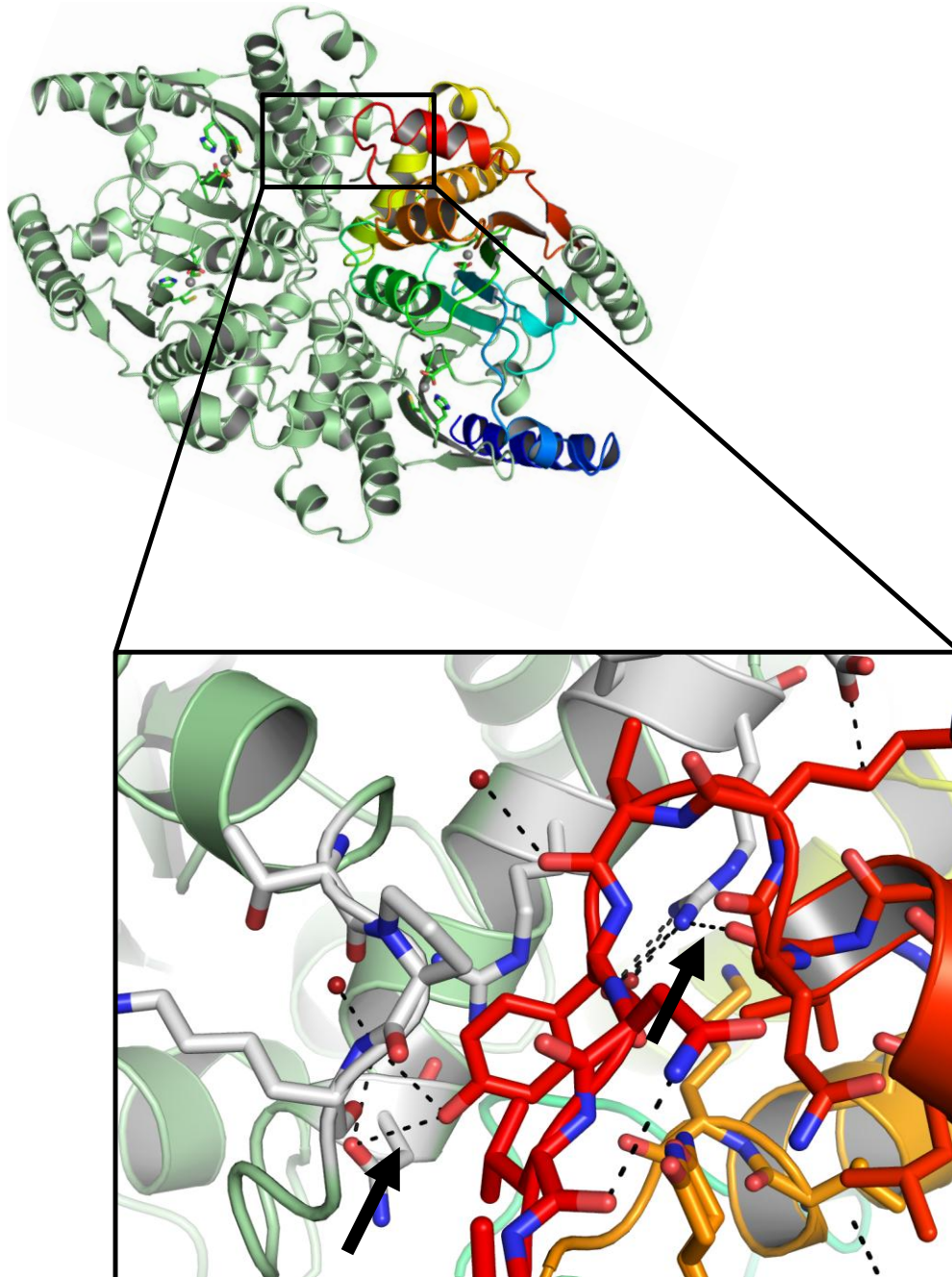


Fig. 37: Detailed view on the C-terminal loop-helix-loop extension of CAS2 and polar contacts to the adjacent subunit. The C-terminal loop-helix-loop extension is colored in red and the adjacent subunit in pale green. Important residues are displayed as sticks. Dashed lines indicate polar contacts and polar contacts between the subunits are highlighted with black arrows. Water molecules are displayed as red spheres.

This observation can be further confirmed by a structure-based sequence alignment of CAS2 with other dimeric, tetrameric and octameric forms of β -CAs (DALI, Holm and Rosenström 2010) revealing the presence of the loop-helix-loop C-terminal motif only in tetrameric β -CAs (Fig. 38).



Fig. 38: Structure-based sequence alignment of CAS2 with nine other β -CAs. The alignment was created with the DALI server (Holm and Rosenström 2010) using the following sequences: CAS2 (*S. macrospora*, PDB ID: 4O1K), 3eyxA (*S. cerevisiae*, NCE103Sc, dimeric), 2w3qA (*C. neoformans*, Can2, dimeric), 1ddzA (*P. purpureum*, PpCA, tetrameric), 1ekjA (*P. sativum*, PsCA, octameric), 3ucjA (*Cocomyxa spec.*, CCA, tetrameric), 2a8cD (*H. influenzae*, HiCA, tetrameric), 1i6pA (*E. coli*, EcCA, tetrameric), 1ylkD (*M. tuberculosis*, MtCA, dimeric) and 1g5cA (*M. thermoautotrophicum*, MthCA, dimeric). The upper part shows the amino-acid sequences of the selected neighbors. The lower part shows the secondary structure assignments by DSSP (*Define Secondary Structure of Proteins*) (H: helix, E: strand, L: coil). The most frequent amino-acid type is colored in each column. Tetrameric proteins are marked with a T, dimeric with a D and octameric with an O. The C-terminal helix domain characteristic for tetrameric β -CAs is marked by a red square.

The dimeric β -CAs have either a short few amino acid long C-terminal tail or like cab-type CAs from *M. thermoautotrophicum* and *M. tuberculosis* Rv1284 terminate with the 5th β -strand of the central β -sheet (Strop *et al.* 2001; Covarrubias *et al.* 2005; Schlicker *et al.* 2009) (Fig. 38).

In conclusion, this work elucidated the interplay of all four CAs in *S. macrospora* that unlike other fungi does not require CAs to grow in ambient air. The major CAs CAS1 and CAS2 are active enzymes with an tetrameric oligomerization state in crystal and solution and exhibit features that qualify them for putative industrial applications.

5. References

- Adams, P. D., Afonine, P. V., Bunkoczi, G., Chen, V. B., Davis, I. W., Echols, N., Headd, J. J., Hung, L. W., Kapral, G. J., Grosse-Kunstleve, R. W., McCoy, A. J., Moriarty, N. W., Oeffner, R., Read, R. J., Richardson, D. C., Richardson, J. S., Terwilliger, T. C. and Zwart, P. H. (2010) PHENIX: a comprehensive Python-based system for macromolecular structure solution. *Acta Crystallogr D Biol Crystallogr* **66**: 213-221.
- Aguilera, J., Van Dijken, J. P., De Winde, J. H. and Pronk, J. T. (2005) Carbonic anhydrase (Nce103p): an essential biosynthetic enzyme for growth of *Saccharomyces cerevisiae* at atmospheric carbon dioxide pressure. *Biochem J* **391**: 311-316.
- Akurathi, V., Dubois, L., Celen, S., Lieuwes, N. G., Chitneni, S. K., Cleynhens, B. J., Innocenti, A., Supuran, C. T., Verbruggen, A. M., Lambin, P. and Bormans, G. M. (2014) Development and biological evaluation of ^{99m}Tc-sulfonamide derivatives for *in-vivo* visualization of CA IX as surrogate tumor hypoxia markers. *Eur J Med Chem* **71**: 374-384.
- Alterio, V., Di Fiore, A., D'Ambrosio, K., Supuran, C. T. and De Simone, G. (2012) Multiple binding modes of inhibitors to carbonic anhydrases: how to design specific drugs targeting 15 different isoforms? *Chem Rev* **112**: 4421-4468.
- Alterio, V., Hilvo, M., Di Fiore, A., Supuran, C. T., Pan, P., Parkkila, S., Scaloni, A., Pastorek, J., Pastorekova, S., Pedone, C., Scozzafava, A., Monti, S. M. and De Simone, G. (2009) Crystal structure of the catalytic domain of the tumor-associated human carbonic anhydrase IX. *Proc Natl Acad Sci USA* **106**: 16233-16238.
- Altschul, S. F., Gish, W., Miller, W., Myers, E. W. and Lipman, D. J. (1990) Basic local alignment search tool. *J Mol Biol* **215**: 403-410.
- Amoroso, G., Morell-Avrahov, L., Müller, D., Klug, K. and Sültemeyer, D. (2005) The gene *NCE103* (YNL036w) from *Saccharomyces cerevisiae* encodes a functional carbonic anhydrase and its transcription is regulated by the concentration of inorganic carbon in the medium. *Mol Microbiol* **56**: 549-558.
- Bahn, Y. S., Cox, G. M., Perfect, J. R. and Heitman, J. (2005) Carbonic anhydrase and CO₂ sensing during *Cryptococcus neoformans* growth, differentiation, and virulence. *Curr Biol* **15**: 2013-2020.
- Bahn, Y. S. and Mühlischlegel, F. A. (2006) CO₂ sensing in fungi and beyond. *Curr Opin Microbiol* **9**: 572-578.
- Banerjee, A. L., Swanson, M., Mallik, S. and Srivastava, D. K. (2004) Purification of recombinant human carbonic anhydrase-II by metal affinity chromatography without incorporating histidine tags. *Protein Expres Purif* **37**: 450-454.
- Becker, D. M. and Lundblad, V. (2001) Introduction of DNA into yeast cells. *Curr Protoc Mol Biol* **13**: 13-17.

- Benson, S. M. and Surles, T.** (2006) Carbon dioxide capture and storage: An overview with emphasis on capture and storage in deep geological formations. *Proc IEEE* **94**: 1795-1805.
- Bertini, I., Luchinat, C. and Scozzafava, A.** (1982) Structure and Bonding: Carbonic anhydrase: An insight into the zinc binding site and into the active cavity through metal substitution in *Biochemistry* **48** pp. 45-92, Springer Berlin Heidelberg.
- Birnboim, H. C. and Doly, J.** (1979) A rapid alkaline extraction procedure for screening recombinant plasmid DNA. *Nucleic Acids Res* **7**: 1513-1523.
- Bloemendal, S., Bernhards, Y., Bartho, K., Dettmann, A., Voigt, O., Teichert, I., Seiler, S., Wolters, D. A., Pöggeler, S. and Kück, U.** (2012) A homologue of the human STRIPAK complex controls sexual development in fungi. *Mol Microbiol* **84**: 310-323.
- Bond, G. M., Stringer, J., Brandvold, D. K., Simsek, F. A., Medina, M.-G. and Egeland, G.** (2001) Development of integrated system for biomimetic CO₂ sequestration using the enzyme carbonic anhydrase. *Energy & Fuels* **15**: 309-316.
- Boone, C., Pinard, M., McKenna, R. and Silverman, D.** (2014) Carbonic anhydrases: Ancient but relevant: Catalytic mechanism of α -class carbonic anhydrases: CO₂ hydration and proton transfer in *Carbonic anhydrase: Mechanism, regulation, links to disease, and industrial applications (Subcellular Biochemistry 75)* (S. C. Frost and R. McKenna, eds) pp. 31-52, Springer Netherlands.
- Bradford, M. M.** (1976) A rapid and sensitive method for the quantitation of microgram quantities of protein utilizing the principle of protein-dye binding. *Anal Biochem* **72**: 248-254.
- Brunger, A. T.** (2007) Version 1.2 of the Crystallography and NMR system. *Nat Protoc* **2**: 2728-2733.
- Brunger, A. T., Adams, P. D., Clore, G. M., DeLano, W. L., Gros, P., Grosse-Kunstleve, R. W., Jiang, J. S., Kuszewski, J., Nilges, M., Pannu, N. S., Read, R. J., Rice, L. M., Simonson, T. and Warren, G. L.** (1998) Crystallography & NMR system: a new software suite for macromolecular structure determination. *Acta Crystallogr D Biol Crystallogr* **54**: 905-921.
- Buren, S., Ortega-Villasante, C., Blanco-Rivero, A., Martinez-Bernardini, A., Shutova, T., Shevela, D., Messinger, J., Bako, L., Villarejo, A. and Samuelsson, G.** (2011) Importance of post-translational modifications for functionality of a chloroplast-localized carbonic anhydrase (CAH1) in *Arabidopsis thaliana*. *PLoS One* **6**: e21021.
- Burnell, J. N., Gibbs, M. J. and Mason, J. G.** (1990) Spinach chloroplastic carbonic anhydrase: nucleotide sequence analysis of cDNA. *Plant Physiol* **92**: 37-40.
- Bury-Mone, S., Mendz, G. L., Ball, G. E., Thibonnier, M., Stingl, K., Ecobichon, C., Ave, P., Huerre, M., Labigne, A., Thiberge, J. M. and De Reuse, H.** (2008) Roles of α - and β -carbonic anhydrases of *Helicobacter pylori* in the urease-dependent response to acidity and in colonization of the murine gastric mucosa. *Infect Immun* **76**: 497-509.

- Carroll, A. M., Sweigard, J. A. and Valent, B.** (1994) Improved vectors for selecting resistance to hygromycin. *Fungal Genet Newslett* **41**: 22.
- Carta, F., Temperini, C., Innocenti, A., Scozzafava, A., Kaila, K. and Supuran, C. T.** (2010) Polyamines inhibit carbonic anhydrases by anchoring to the zinc-coordinated water molecule. *J Med Chem* **53**: 5511-5522.
- Chauhan, J. S., Rao, A. and Raghava, G. P.** (2013) *In silico* platform for prediction of N-, O- and C-glycosites in eukaryotic protein sequences. *PLoS One* **8**: e67008.
- Chen, W. Y., Shen, Q. X. and Bahl, O. P.** (1991) Carbohydrate variant of the recombinant beta-subunit of human choriogonadotropin expressed in baculovirus expression system. *J Biol Chem* **266**: 4081-4087.
- Chen, Y. Q., Cann, M. J., Litvin, T. N., Iourgenko, V., Sinclair, M. L., Levin, L. R. and Buck, J.** (2000) Soluble adenylyl cyclase as an evolutionarily conserved bicarbonate sensor. *Science* **289**: 625-628.
- Chirica, L. C., Elleby, B., Jonsson, B. H. and Lindskog, S.** (1997) The complete sequence, expression in *Escherichia coli*, purification and some properties of carbonic anhydrase from *Neisseria gonorrhoeae*. *Eur J Biochem* **244**: 755-760.
- Chirica, L. C., Elleby, B. and Lindskog, S.** (2001) Cloning, expression and some properties of α -carbonic anhydrase from *Helicobacter pylori*. *Biochim Biophys Acta* **1544**: 55-63.
- Chirica, L. C., Petersson, C., Hurtig, M., Jonsson, B. H., Boren, T. and Lindskog, S.** (2002) Expression and localization of α - and β -carbonic anhydrase in *Helicobacter pylori*. *Biochim Biophys Acta* **1601**: 192-199.
- Christianson, D. W. and Fierke, C. A.** (1996) Carbonic anhydrase: Evolution of the zinc binding site by nature and by design. *Acc Chem Res* **29**: 331-339.
- Christianson, T. W., Sikorski, R. S., Dante, M., Shero, J. H. and Hieter, P.** (1992) Multifunctional yeast high-copy-number shuttle vectors. *Gene* **110**: 119-122.
- Clark, D., Rowlett, R. S., Coleman, J. R. and Klessig, D. F.** (2004) Complementation of the yeast deletion mutant $\Delta NCE103$ by members of the β -class of carbonic anhydrases is dependent on carbonic anhydrase activity rather than on antioxidant activity. *Biochem J* **379**: 609-615.
- Colot, H. V., Park, G., Turner, G. E., Ringelberg, C., Crew, C. M., Litvinkova, L., Weiss, R. L., Borkovich, K. A. and Dunlap, J. C.** (2006) A high-throughput gene knockout procedure for *Neurospora* reveals functions for multiple transcription factors. *Proc Natl Acad Sci USA* **103**: 10352-10357.
- Cordat, E. and Casey, J. R.** (2009) Bicarbonate transport in cell physiology and disease. *Biochem J* **417**: 423-439.
- Cottier, F., Leewattanapasuk, W., Kemp, L. R., Murphy, M., Supuran, C. T., Kurzai, O. and Mühlischlegel, F. A.** (2013) Carbonic anhydrase regulation and CO₂ sensing in the fungal

pathogen *Candida glabrata* involves a novel Rca1p ortholog. *Bioorg Med Chem* **21**: 1549-1554.

Cottier, F., Raymond, M., Kurzai, O., Bolstad, M., Leewattanapasuk, W., Jimenez-Lopez, C., Lorenz, M. C., Sanglard, D., Vachova, L., Pavelka, N., Palkova, Z. and Mühlischlegel, F. A. (2012) The bZIP transcription factor Rca1p is a central regulator of a novel CO₂ sensing pathway in yeast. *Plos Pathog* **8**: e1002485.

Covarrubias, A. S., Bergfors, T., Jones, T. A. and Hogbom, M. (2006) Structural mechanics of the pH-dependent activity of β -carbonic anhydrase from *Mycobacterium tuberculosis*. *J Biol Chem* **281**: 4993-4999.

Covarrubias, A. S., Larsson, A. M., Högbom, M., Lindberg, J., Bergfors, T., Björkelid, C., Mowbray, S. L., Unge, T. and Jones, T. A. (2005) Structure and function of carbonic anhydrases from *Mycobacterium tuberculosis*. *J Biol Chem* **280**: 18782-18789.

Cronk, J. D., Endrizzi, J. A., Cronk, M. R., O'Neill J, W. and Zhang, K. Y. (2001) Crystal structure of *E. coli* β -carbonic anhydrase, an enzyme with an unusual pH-dependent activity. *Protein Sci* **10**: 911-922.

Cronk, J. D., O'Neill, J. W., Cronk, M. R., Endrizzi, J. A. and Zhang, K. Y. (2000) Cloning, crystallization and preliminary characterization of a β -carbonic anhydrase from *Escherichia coli*. *Acta Crystallogr D Biol Crystallogr* **56**: 1176-1179.

Cronk, J. D., Rowlett, R. S., Zhang, K. Y. J., Tu, C., Endrizzi, J. A., Lee, J., Gareiss, P. C. and Preiss, J. R. (2006) Identification of a novel noncatalytic bicarbonate binding site in eubacterial β -carbonic anhydrase. *Biochemistry* **45**: 4351-4361.

Crowley, T. J. (2000) Causes of climate change over the past 1000 years. *Science* **289**: 270-277.

Cuesta-Seijo, J. A., Borchert, M. S., Navarro-Poulsen, J. C., Schnorr, K. M., Mortensen, S. B. and Lo Leggio, L. (2011) Structure of a dimeric fungal α -type carbonic anhydrase. *FEBS Lett* **585**: 1042-1048.

Cummins, E. P., Selfridge, A. C., Sporn, P. H., Sznajder, J. I. and Taylor, C. T. (2013) Carbon dioxide-sensing in organisms and its implications for human disease. *Cell Mol Life Sci* **71**: 831-845.

Dagert, M. and Ehrlich, S. D. (1979) Prolonged incubation in calcium chloride improves the competence of *Escherichia coli* cells. *Gene* **6**: 23-28.

De Luca, V., Vullo, D., Scozzafava, A., Carginale, V., Rossi, M., Supuran, C. T. and Capasso, C. (2012) Anion inhibition studies of an α -carbonic anhydrase from the thermophilic bacterium *Sulfurihydrogenibium yellowstonense* YO3AOP1. *Bioorg Med Chem Lett* **22**: 5630-5634.

De Simone, G. and Supuran, C. T. (2012) (In)organic anions as carbonic anhydrase inhibitors. *J Inorg Biochem* **111**: 117-129.

- Deshpande, N., Wilkins, M. R., Packer, N. and Nevalainen, H.** (2008) Protein glycosylation pathways in filamentous fungi. *Glycobiology* **18**: 626-637.
- DiMaio, F., Terwilliger, T. C., Read, R. J., Wlodawer, A., Oberdorfer, G., Wagner, U., Valkov, E., Alon, A., Fass, D., Axelrod, H. L., Das, D., Vorobiev, S. M., Iwai, H., Pokkuluri, P. R. and Baker, D.** (2011) Improved molecular replacement by density- and energy-guided protein structure optimization. *Nature* **473**: 540-543.
- Dodgson, S. J. and Forster, R. E., 2nd** (1986) Carbonic anhydrase: inhibition results in decreased urea production by hepatocytes. *J Appl Physiol* **60**: 646-652.
- Elleby, B., Chirica, L. C., Tu, C., Zeppezauer, M. and Lindskog, S.** (2001) Characterization of carbonic anhydrase from *Neisseria gonorrhoeae*. *Eur J Biochem* **268**: 1613-1619.
- Elleuche, S.** (2011) Evolution of fungi and fungal-like organisms: Carbonic anhydrases in fungi and fungal-like organisms - functional distribution and evolution of a gene family in *The Mycota 14* (S. Pöggeler and J. Wöstemeyer, eds) pp. 257-274, Springer Berlin Heidelberg.
- Elleuche, S. and Pöggeler, S.** (2008a) A cyanase is transcriptionally regulated by arginine and involved in cyanate decomposition in *Sordaria macrospora*. *Fungal Genet Biol* **45**: 1458-1469.
- Elleuche, S. and Pöggeler, S.** (2008b) Visualization of peroxisomes via SKL-tagged DsRed protein in *Sordaria macrospora*. *Fungal Genetics Reports* **55**: 9-12.
- Elleuche, S. and Pöggeler, S.** (2009a) Evolution of carbonic anhydrases in fungi. *Curr Genet* **55**: 211-222.
- Elleuche, S. and Pöggeler, S.** (2009b) β -carbonic anhydrases play a role in fruiting body development and ascospore germination in the filamentous fungus *Sordaria macrospora*. *PLoS One* **4**: e5177.
- Elleuche, S. and Pöggeler, S.** (2010) Carbonic anhydrases in fungi. *Microbiology* **156**: 23-29.
- Emsley, P., Lohkamp, B., Scott, W. G. and Cowtan, K.** (2010) Features and development of Coot. *Acta Crystallogr D Biol Crystallogr* **66**: 486-501.
- Eng, I., Nowrousian, M. and Kück, U.** (2010) *Sordaria macrospora*, a model organism to study fungal cellular development. *Eur J Cell Biol* **89**: 864-872.
- Esbaugh, A. J. and Tufts, B. L.** (2006) The structure and function of carbonic anhydrase isozymes in the respiratory system of vertebrates. *Respir Physiol Neurobiol* **154**: 185-198.
- Esser, K. and Kuenen, R.** (1967). *Genetics of fungi*. Springer-Verlag.

Falkowski, P., Scholes, R. J., Boyle, E., Canadell, J., Canfield, D., Elser, J., Gruber, N., Hibbard, K., Högberg, P., Linder, S., Mackenzie, F. T., Moore III, B., Pedersen, T., Rosenthal, Y., Seitzinger, S., Smetacek, V. and Steffen, W. (2000) The global carbon cycle: a test of our knowledge of earth as a system. *Science* **290**: 291-296.

Fasseas, M. K., Tsikou, D., Flemetakis, E. and Katinakis, P. (2011) Molecular and biochemical analysis of the α -class carbonic anhydrases in *Caenorhabditis elegans*. *Mol Biol Rep* **38**: 1777-1785.

Fisher, S. Z., Maupin, C. M., Budayova-Spano, M., Govindasamy, L., Tu, C., Agbandje-McKenna, M., Silverman, D. N., Voth, G. A. and McKenna, R. (2007) Atomic crystal and molecular dynamics simulation structures of human carbonic anhydrase II: Insights into the proton transfer mechanism. *Biochemistry* **46**: 2930-2937.

Frost, S. (2014) Carbonic anhydrases: Ancient but relevant: Physiological functions of the alpha class of carbonic anhydrases in *Carbonic anhydrase: Mechanism, regulation, links to disease, and industrial applications (Subcellular Biochemistry 75)* (S. C. Frost and R. McKenna, eds) pp. 9-30, Springer Netherlands.

Fukuzawa, H., Fujiwara, S., Yamamoto, Y., Dionisio-Sese, M. L. and Miyachi, S. (1990) cDNA cloning, sequence, and expression of carbonic anhydrase in *Chlamydomonas reinhardtii*: regulation by environmental CO₂ concentration. *Proc Natl Acad Sci USA* **87**: 4383-4387.

Garcia-Gimeno, M. A. and Struhl, K. (2000) Aca1 and Aca2, ATF/CREB activators in *Saccharomyces cerevisiae*, are important for carbon source utilization but not the response to stress. *Mol Cell Biol* **20**: 4340-4349.

Giordano, M., Norici, A., Forssen, M., Eriksson, M. and Raven, J. A. (2003) An anaplerotic role for mitochondrial carbonic anhydrase in *Chlamydomonas reinhardtii*. *Plant Physiol* **132**: 2126-2134.

González, J. M. and Fisher, S. Z. (2014) Carbonic anhydrases: Ancient but relevant: Carbonic anhydrases in industrial applications in *Carbonic anhydrase: Mechanism, regulation, links to disease, and industrial applications (Subcellular Biochemistry 75)* (S. C. Frost and R. McKenna, eds) pp. 405-426, Springer Netherlands.

Götz, R., Gnann, A. and Zimmermann, F. K. (1999) Deletion of the carbonic anhydrase-like gene *NCE103* of the yeast *Saccharomyces cerevisiae* causes an oxygen-sensitive growth defect. *Yeast* **15**: 855-864.

Guilloton, M. B., Korte, J. J., Lamblin, A. F., Fuchs, J. A. and Anderson, P. M. (1992) Carbonic anhydrase in *Escherichia coli*. A product of the *cyn* operon. *J Biol Chem* **267**: 3731-3734.

Guilloton, M. B., Lamblin, A. F., Kozliak, E. I., Gerami-Nejad, M., Tu, C., Silverman, D., Anderson, P. M. and Fuchs, J. A. (1993) A physiological role for cyanate-induced carbonic anhydrase in *Escherichia coli*. *J Bacteriol* **175**: 1443-1451.

- Haan, C. and Behrmann, I.** (2007) A cost effective non-commercial ECL-solution for Western blot detections yielding strong signals and low background. *J Immunol Methods* **318**: 11-19.
- Hall, R. A., De Sordi, L., MacCallum, D. M., Topal, H., Eaton, R., Bloor, J. W., Robinson, G. K., Levin, L. R., Buck, J., Wang, Y., Gow, N. A. R., Steegborn, C. and Mühlischlegel, F. A.** (2010) CO₂ acts as a signalling molecule in populations of the fungal pathogen *Candida albicans*. *PLoS Pathog* **6**: e1001193.
- Han, K. H., Chun, Y. H., Figueiredo Bde, C., Soriani, F. M., Savoldi, M., Almeida, A., Rodrigues, F., Cairns, C. T., Bignell, E., Tobal, J. M., Goldman, M. H., Kim, J. H., Bahn, Y. S., Goldman, G. H. and Ferreira, M. E.** (2010) The conserved and divergent roles of carbonic anhydrases in the filamentous fungi *Aspergillus fumigatus* and *Aspergillus nidulans*. *Mol Microbiol* **75**: 1372-1388.
- Hashimoto, M. and Kato, J.** (2003) Indispensability of the *Escherichia coli* carbonic anhydrases YadF and CynT in cell proliferation at a low CO₂ partial pressure. *Biosci Biotechnol Biochem* **67**: 919-922.
- Hewett-Emmett, D. and Tashian, R. E.** (1996) Functional diversity, conservation, and convergence in the evolution of the α -, β -, and γ -carbonic anhydrase gene families. *Mol Phylogenet Evol* **5**: 50-77.
- Hoffmann, K. M., Samardzic, D., Heever, K. and Rowlett, R. S.** (2011) Co(II)-substituted *Haemophilus influenzae* β -carbonic anhydrase: spectral evidence for allosteric regulation by pH and bicarbonate ion. *Arch Biochem Biophys* **511**: 80-87.
- Holm, L. and Rosenström, P.** (2010) Dali server: conservation mapping in 3D. *Nucleic Acids Res* **38**: 545-549.
- Huang, S., Hainzl, T., Grundstrom, C., Forsman, C., Samuelsson, G. and Sauer-Eriksson, A. E.** (2011) Structural studies of β -carbonic anhydrase from the green alga *Coccomyxa*: inhibitor complexes with anions and acetazolamide. *PLoS One* **6**: e28458.
- Innocenti, A., Mühlischlegel, F. A., Hall, R. A., Steegborn, C., Scozzafava, A. and Supuran, C. T.** (2008) Carbonic anhydrase inhibitors: inhibition of the β -class enzymes from the fungal pathogens *Candida albicans* and *Cryptococcus neoformans* with simple anions. *Bioorg Med Chem Lett* **18**: 5066-5070.
- James, P., Halladay, J. and Craig, E. A.** (1996) Genomic libraries and a host strain designed for highly efficient two-hybrid selection in yeast. *Genetics* **144**: 1425-1436.
- Jiang, M., Chen, M., Guo, Z.-F. and Guo, Z.** (2010) A bicarbonate cofactor modulates 1,4-dihydroxy-2-naphthoyl-coenzyme a synthase in menaquinone biosynthesis of *Escherichia coli*. *J Biol Chem* **285**: 30159-30169.
- Jones, N. L.** (2008) An obsession with CO₂. *Appl Physiol Nutr Metab* **33**: 641-650.

Jungbluth, M., Mösch, H. U. and Taxis, C. (2012) Acetate regulation of spore formation is under the control of the Ras/cyclic AMP/protein kinase A pathway and carbon dioxide in *Saccharomyces cerevisiae*. *Eukaryot Cell* **11**: 1021-1032.

Kabsch, W. (2010) Xds. *Acta Crystallogr D Biol Crystallogr* **66**: 125-132.

Kabsch, W. and Sander, C. (1983) Dictionary of protein secondary structure: pattern recognition of hydrogen-bonded and geometrical features. *Biopolymers* **22**: 2577-2637.

Karplus, P. A. and Diederichs, K. (2012) Linking crystallographic model and data quality. *Science* **336**: 1030-1033.

Keeling, C. D., Bacastow, R. B., Wahlen, M., Whorf, T. P., Heimann, M. and Meijer, H. A. (2011) Atmospheric CO₂ concentrations (ppm) derived from *in-situ* air measurements at Mauna Loa, Observatory, Hawaii: latitude 19.5 N, longitude 155.6 W, elevation 3397m. Scripps CO₂ Program, Scripps Institution of Oceanography (SIO), University of California, La Jolla.

Khalifah, R. G. (1971) The carbon dioxide hydration activity of carbonic anhydrase I: Stop-flow kinetic studies on the native human isoenzymes B and C. *J Biol Chem* **246**: 2561-2573.

Kimber, M. S. and Pai, E. F. (2000) The active site architecture of *Pisum sativum* β -carbonic anhydrase is a mirror image of that of alpha-carbonic anhydrases. *EMBO J* **19**: 1407-1418.

Kinney, J. N., Salmeen, A., Cai, F. and Kerfeld, C. A. (2012) Elucidating essential role of conserved carboxysomal protein CcmN reveals common feature of bacterial microcompartment assembly. *J Biol Chem* **287**: 17729-17736.

Klengel, T., Liang, W. J., Chaloupka, J., Ruoff, C., Schroppel, K., Naglik, J. R., Eckert, S. E., Mogensen, E. G., Haynes, K., Tuite, M. F., Levin, L. R., Buck, J. and Mühlischlegel, F. A. (2005) Fungal adenylyl cyclase integrates CO₂ sensing with cAMP signaling and virulence. *Curr Biol* **15**: 2021-2026.

Klix, V., Nowrousian, M., Ringelberg, C., Loros, J. J., Dunlap, J. C. and Pöggeler, S. (2010) Functional characterization of MAT1-1-specific mating-type genes in the homothallic ascomycete *Sordaria macrospora* provides new insights into essential and nonessential sexual regulators. *Eukaryot Cell* **9**: 894-905.

Krissinel, E. and Henrick, K. (2004) Secondary-structure matching (SSM), a new tool for fast protein structure alignment in three dimensions. *Acta Crystallogr D Biol Crystallogr* **60**: 2256-2268.

Krissinel, E. and Henrick, K. (2007) Inference of macromolecular assemblies from crystalline state. *J Mol Biol* **372**: 774-797.

Kück, U., Pöggeler, S., Nowrousian, M., Nolting, N. and Engh, I. (2009) Physiology and genetics: *Sordaria macrospora*, a model system for fungal development in *The Mycota 15* (T. Anke and D. Weber, eds) pp. 17-39, Springer Berlin Heidelberg.

- Kumar, R. S. and Ferry, J.** (2014) Carbonic anhydrase: Ancient but relevant: Prokaryotic carbonic anhydrases of earth's environment in *Carbonic anhydrase: Mechanism, regulation, links to disease, and industrial applications (Subcellular Biochemistry 75)* (S. C. Frost and R. McKenna, eds) pp. 77-87, Springer Netherlands.
- Kusian, B., Sültemeyer, D. and Bowien, B.** (2002) Carbonic anhydrase is essential for growth of *Ralstonia eutropha* at ambient CO₂ concentrations. *J Bacteriol* **184**: 5018-5026.
- Laemmli, U. K.** (1970) Cleavage of structural proteins during the assembly of the head of bacteriophage T4. *Nature* **227**: 680-685.
- Lane, T. W. and Morel, F. M. M.** (2000) A biological function for cadmium in marine diatoms. *Proc Natl Acad Sci USA* **97**: 4627-4631.
- Langereis, J. D., Zomer, A., Stunnenberg, H. G., Burghout, P. and Hermans, P. W.** (2013) Nontypeable *Haemophilus influenzae* carbonic anhydrase is important for environmental and intracellular survival. *J Bacteriol* **195**: 2737-2746.
- Lara, M., Servín-González, L., Singh, M., Moreno, C., Cohen, I., Nimtz, M. and Espitia, C.** (2004) Expression, secretion, and glycosylation of the 45- and 47-kDa glycoprotein of *Mycobacterium tuberculosis* in *Streptomyces lividans*. *Appl Environ Microbiol* **70**: 679-685.
- Lebeer, S., Claes, I. J., Balog, C. I., Schoofs, G., Verhoeven, T. L., Nys, K., von Ossowski, I., de Vos, W. M., Tytgat, H. L., Agostinis, P., Palva, A., Van Damme, E. J., Deelder, A. M., De Keersmaecker, S. C., Wuhrer, M. and Vanderleyden, J.** (2012) The major secreted protein Msp1/p75 is O-glycosylated in *Lactobacillus rhamnosus* GG. *Microb Cell Fact* **11**: 15.
- Lecellier, G. and Silar, P.** (1994) Rapid methods for nucleic acids extraction from Petri dish-grown mycelia. *Curr Genet* **25**: 122-123.
- Li, W., Zhou, P. P., Jia, L. P., Yu, L. J., Li, X. L. and Zhu, M.** (2009) Limestone dissolution induced by fungal mycelia, acidic materials, and carbonic anhydrase from fungi. *Mycopathologia* **167**: 37-46.
- Lindskog, S.** (1963) Effects of pH and inhibitors on some properties related to metal binding in bovine carbonic anhydrase. *J Biol Chem* **238**: 945-951.
- Lindskog, S.** (1997) Structure and mechanism of carbonic anhydrase. *Pharmacol Ther* **74**: 1-20.
- Lord, K. M. and Read, N. D.** (2011) Perithecial morphogenesis in *Sordaria macrospora*. *Fungal Genetics and Biology* **48**: 388-399.
- MacAuley, S. R., Zimmerman, S. A., Apolinario, E. E., Evilia, C., Hou, Y.-M., Ferry, J. G. and Sowers, K. R.** (2009) The archetype γ -class carbonic anhydrase (Cam) contains iron when synthesized *in-vivo*. *Biochemistry* **48**: 817-819.

- Madejón, P., Domínguez, M. and Murillo, J.** (2012) Pasture composition in a trace element-contaminated area: the particular case of Fe and Cd for grazing horses. *Environ Monit Assess* **184**: 2031-2043.
- Mandel, M. and Higa, A.** (1970) Calcium-dependent bacteriophage DNA infection. *J Mol Biol* **53**: 159-162.
- Maresca, A., Temperini, C., Pochet, L., Masereel, B., Scozzafava, A. and Supuran, C. T.** (2010) Deciphering the mechanism of carbonic anhydrase inhibition with coumarins and thiocoumarins. *J Med Chem* **53**: 335-344.
- Maresca, A., Temperini, C., Vu, H., Pham, N. B., Poulsen, S. A., Scozzafava, A., Quinn, R. J. and Supuran, C. T.** (2009) Non-zinc mediated inhibition of carbonic anhydrases: coumarins are a new class of suicide inhibitors. *J Am Chem Soc* **131**: 3057-3062.
- Maruyama, J. and Kitamoto, K.** (2007) Differential distribution of the endoplasmic reticulum network in filamentous fungi. *FEMS Microbiol Lett* **272**: 1-7.
- Mayrhofer, S., Weber, J. M. and Pöggeler, S.** (2006) Pheromones and pheromone receptors are required for proper sexual development in the homothallic ascomycete *Sordaria macrospora*. *Genetics* **172**: 1521-1533.
- McCoy, A. J., Grosse-Kunstleve, R. W., Storoni, L. C. and Read, R. J.** (2005) Likelihood-enhanced fast translation functions. *Acta Crystallogr D Biol Crystallogr* **61**: 458-464.
- McKenna, R. and Supuran, C. T.** (2014) Carbonic anhydrase: Ancient but relevant: Carbonic anhydrase inhibitors drug design in *Carbonic anhydrase: Mechanism, regulation, links to disease, and industrial applications (Subcellular Biochemistry 75)* (S. C. Frost and R. McKenna, eds) pp. 291-323, Springer Netherlands.
- Meldrum, N. U. and Roughton, F. J.** (1933a) Carbonic anhydrase. Its preparation and properties. *J Physiol* **80**: 113-142.
- Meldrum, N. U. and Roughton, F. J.** (1933b) The state of carbon dioxide in blood. *J Physiol* **80**: 143-170.
- Mitsuhashi, S., Mizushima, T., Yamashita, E., Yamamoto, M., Kumasaka, T., Moriyama, H., Ueki, T., Miyachi, S. and Tsukihara, T.** (2000) X-ray structure of β -carbonic anhydrase from the red alga, *Porphyridium purpureum*, reveals a novel catalytic site for CO₂ hydration. *J Biol Chem* **275**: 5521-5526.
- Mitsuhashi, S., Ohnishi, J., Hayashi, M. and Ikeda, M.** (2004) A gene homologous to β -type carbonic anhydrase is essential for the growth of *Corynebacterium glutamicum* under atmospheric conditions. *Appl Microbiol Biotechnol* **63**: 592-601.
- Mogensen, E. and Mühlischlegel, F.** (2008) Human and animal relationships: CO₂ sensing and virulence of *Candida albicans* in *The Mycota 6* (A. Brakhage and P. Zipfel, eds) pp. 83-94, Springer Berlin-Heidelberg.

- Mogensen, E. G., Janbon, G., Chaloupka, J., Steegborn, C., Fu, M. S., Moyrand, F., Klengel, T., Pearson, D. S., Geeves, M. A., Buck, J., Levin, L. R. and Mühlischlegel, F. A.** (2006) *Cryptococcus neoformans* senses CO₂ through the carbonic anhydrase Can2 and the adenylyl cyclase Cac1. *Eukaryot Cell* **5**: 103-111.
- Moharir, A., Peck, S. H., Budden, T. and Lee, S. Y.** (2013) The role of N-glycosylation in folding, trafficking and functionality of lysosomal protein CLN5. *PLoS One* **8**: e74299.
- Monti, S. M., De Simone, G., Dathan, N. A., Ludwig, M., Vullo, D., Scozzafava, A., Capasso, C. and Supuran, C. T.** (2013) Kinetic and anion inhibition studies of a β -carbonic anhydrase (FbiCA 1) from the C4 plant *Flaveria bidentis*. *Bioorg Med Chem Lett* **23**: 1626-1630.
- Monti, S. M., Maresca, A., Viparelli, F., Carta, F., De Simone, G., Mühlischlegel, F. A., Scozzafava, A. and Supuran, C. T.** (2012) Dithiocarbamates are strong inhibitors of the β -class fungal carbonic anhydrases from *Cryptococcus neoformans*, *Candida albicans* and *Candida glabrata*. *Bioorg Med Chem Lett* **22**: 859-862.
- Moroney, J., Ma, Y., Frey, W., Fusilier, K., Pham, T., Simms, T., DiMario, R., Yang, J. and Mukherjee, B.** (2011) The carbonic anhydrase isoforms of *Chlamydomonas reinhardtii*: intracellular location, expression, and physiological roles. *Photosynth Res* **109**: 133-149.
- Morotomi, M., Nagai, F. and Watanabe, Y.** (2012) CO₂-dependent growth of *Succinatimonas hippei* YIT 12066T isolated from human feces. *Microbiol Immunol* **56**: 195-197.
- Mueller, U., Darowski, N., Fuchs, M. R., Förster, R., Hellmig, M., Paithankar, K. S., Pühringer, S., Steffien, M., Zocher, G. and Weiss, M. S.** (2012) Facilities for macromolecular crystallography at the Helmholtz-Zentrum Berlin. *J Synchrotron Radiat* **19**: 442-449.
- Mullis, K. B. and Faloona, F. A.** (1987) Specific synthesis of DNA *in-vitro* via a polymerase-catalyzed chain reaction. *Methods Enzymol* **155**: 335-350.
- Mumberg, D., Müller, R. and Funk, M.** (1994) Regulatable promoters of *Saccharomyces cerevisiae*: comparison of transcriptional activity and their use for heterologous expression. *Nucleic Acids Res* **22**: 5767-5768.
- Nair, S. K. and Christianson, D. W.** (1991) Unexpected pH-dependent conformation of His-64, the proton shuttle of carbonic anhydrase II. *J Am Chem Soc* **113**: 9455-9458.
- Neish, A. C.** (1939) Studies on chloroplasts: separation of chloroplasts, a study of factors affecting their flocculation and the calculation of the chloroplast content of leaf tissue from chemical analysis. *Biochem J* **33**: 293-300.
- Nijhout, M. M. and Carter, R.** (1978) Gamete development in malaria parasites - bicarbonate-dependent stimulation by pH *in-vitro*. *Parasitology* **76**: 39-53.
- Nishida, H., Beppu, T. and Ueda, K.** (2009) Symbiobacterium lost carbonic anhydrase in the course of evolution. *J Mol Evol* **68**: 90-96.

- Nishimori, I., Minakuchi, T., Kohsaki, T., Onishi, S., Takeuchi, H., Vullo, D., Scozzafava, A. and Supuran, C. T.** (2007) Carbonic anhydrase inhibitors: the β -carbonic anhydrase from *Helicobacter pylori* is a new target for sulfonamide and sulfamate inhibitors. *Bioorg Med Chem Lett* **17**: 3585-3594.
- Nishimori, I., Minakuchi, T., Maresca, A., Carta, F., Scozzafava, A. and Supuran, C. T.** (2010) The β -carbonic anhydases from *Mycobacterium tuberculosis* as drug targets. *Curr Pharm Des* **16**: 3300-3309.
- Nishimori, I., Onishi, S., Takeuchi, H. and Supuran, C. T.** (2008) The α and β classes carbonic anhydases from *Helicobacter pylori* as novel drug targets. *Curr Pharm Des* **14**: 622-630.
- Nolting, N. and Pöggeler, S.** (2006) A MADS box protein interacts with a mating-type protein and is required for fruiting-body development in the homothallic ascomycete *Sordaria macrospora*. *Eukaryot Cell* **5**: 1043-1056.
- Nowrousian, M. and Cebula, P.** (2005) The gene for a lectin-like protein is transcriptionally activated during sexual development, but is not essential for fruiting-body formation in the filamentous fungus *Sordaria macrospora*. *BMC Microbiol* **5**: 64.
- Nowrousian, M., Frank, S., Koers, S., Strauch, P., Weitner, T., Ringelberg, C., Dunlap, J. C., Loros, J. J. and Kück, U.** (2007) The novel ER membrane protein PRO41 is essential for sexual development in the filamentous fungus *Sordaria macrospora*. *Mol Microbiol* **64**: 923-937.
- Nowrousian, M., Stajich, J. E., Chu, M., Engh, I., Espagne, E., Halliday, K., Kamerewerd, J., Kempken, F., Knab, B., Kuo, H. C., Osiewacz, H. D., Pöggeler, S., Read, N. D., Seiler, S., Smith, K. M., Zickler, D., Kück, U. and Freitag, M.** (2010) *De novo* assembly of a 40 Mb eukaryotic genome from short sequence reads: *Sordaria macrospora*, a model organism for fungal morphogenesis. *PLoS Genet* **6**: e1000891.
- Nowrousian, M., Teichert, I., Masloff, S. and Kück, U.** (2012) Whole-genome sequencing of *Sordaria macrospora* mutants identifies developmental genes. *G3 (Bethesda)* **2**: 261-270.
- Pace, N. R.** (2009) Mapping the tree of life: Progress and prospects. *Microbiol Mol Biol Rev* **73**: 565-576.
- Peberdy, J. F.** (1994) Protein secretion in filamentous fungi-trying to understand a highly productive black box. *Trends Biotechnol* **12**: 50-57.
- Pelham, H. R.** (1990) The retention signal for soluble proteins of the endoplasmic reticulum. *Trends Biochem Sci* **15**: 483-486.
- Petersen, T. N., Brunak, S., von Heijne, G. and Nielsen, H.** (2011) SignalP 4.0: discriminating signal peptides from transmembrane regions. *Nat Methods* **8**: 785-786.

- Pfaffl, M. W., Horgan, G. W. and Dempfle, L.** (2002) Relative expression software tool (REST) for group-wise comparison and statistical analysis of relative expression results in real-time PCR. *Nucleic Acids Res* **30**: e36.
- Pilka, E. S., Kochan, G., Oppermann, U. and Yue, W. W.** (2012) Crystal structure of the secretory isozyme of mammalian carbonic anhydrases CA VI: implications for biological assembly and inhibitor development. *Biochem Biophys Res Commun* **419**: 485-489.
- Pocker, Y. and Joan, S. Y. N.** (1973) Plant carbonic anhydrase. Properties and carbon dioxide hydration kinetics. *Biochemistry* **12**: 5127-5134.
- Pöggeler, S. and Kück, U.** (2006) Highly efficient generation of signal transduction knockout mutants using a fungal strain deficient in the mammalian *ku70* ortholog. *Gene* **378**: 1-10.
- Pöggeler, S., Masloff, S., Hoff, B., Mayrhofer, S. and Kück, U.** (2003) Versatile EGFP reporter plasmids for cellular localization of recombinant gene products in filamentous fungi. *Curr Genet* **43**: 54-61.
- Pöggeler, S., Nowrousian, M., Ringelberg, C., Loros, J. J., Dunlap, J. C. and Kück, U.** (2006) Microarray and real-time PCR analyses reveal mating type-dependent gene expression in a homothallic fungus. *Mol Genet Genomics* **275**: 492-503.
- Qian, D., Jiang, L., Lu, L., Wei, C. and Li, Y.** (2011) Biochemical and structural properties of cyanases from *Arabidopsis thaliana* and *Oryza sativa*. *PLoS One* **6**: e18300.
- Raven, J. A. and Newman, J. R.** (1994) Requirement for carbonic anhydrase activity in processes other than photosynthetic inorganic carbon assimilation. *Plant, Cell & Environment* **17**: 123-130.
- Read, N. D.** (1983) A scanning electron microscopic study of the external features of perithecium development in *Sordaria humana*. *Can J Bot* **61**: 3217-3229.
- Read, N. D. and Beckett, A.** (1985) The anatomy of the mature perithecium in *Sordaria humana* and its significance for fungal multicellular development. *Can J Bot* **63**: 281-296.
- Rowlett, R. S.** (2010) Structure and catalytic mechanism of the β -carbonic anhydrases. *Biochim Biophys Acta* **1804**: 362-373.
- Rowlett, R. S.** (2014) Carbonic anhydrase: Ancient but relevant: Structure and catalytic mechanism of β -carbonic anhydrases in *Carbonic anhydrase: mechanism, regulation, links to disease, and industrial applications (Subcellular Biochemistry 75)* (S. C. Frost and R. McKenna, eds) pp. 53-76, Springer Netherlands.
- Rowlett, R. S., Tu, C., McKay, M. M., Preiss, J. R., Loomis, R. J., Hicks, K. A., Marchione, R. J., Strong, J. A., Donovan Jr, G. S. and Chamberlin, J. E.** (2002) Kinetic characterization of wild-type and proton transfer-impaired variants of β -carbonic anhydrase from *Arabidopsis thaliana*. *Arch Biochem Biophys* **404**: 197-209.

- Sachs, G., Scott, D. R. and Wen, Y. (2011) Gastric infection by *Helicobacter pylori*. *Curr Gastroenterol Rep* **13**: 540-546.
- Saiki, R. K., Gelfand, D. H., Stoffel, S., Scharf, S. J., Higuchi, R., Horn, G. T., Mullis, K. B. and Erlich, H. A. (1988) Primer-directed enzymatic amplification of DNA with a thermostable DNA polymerase. *Science* **239**: 487-491.
- Sambrook, J. and Russell, D. W. (2001). *Molecular cloning: a laboratory manual*. Cold Spring Harbor Laboratory Press.
- Sawaya, M. R., Cannon, G. C., Heinhorst, S., Tanaka, S., Williams, E. B., Yeates, T. O. and Kerfeld, C. A. (2006) The structure of β -carbonic anhydrase from the carboxysomal shell reveals a distinct subclass with one active site for the price of two. *J Biol Chem* **281**: 7546-7555.
- Schlicker, C., Hall, R. A., Vullo, D., Middelhaufe, S., Gertz, M., Supuran, C. T., Mühlischlegel, F. A. and Steegborn, C. (2009) Structure and inhibition of the CO₂ sensing carbonic anhydrase Can2 from the pathogenic fungus *Cryptococcus neoformans*. *J Mol Biol* **385**: 1207-1220.
- Schütter, M. (2013) Functional analysis of *Sordaria macrospora* transcription factors likely involved in CO₂ sensing. Master Thesis, Georg-August-University Göttingen.
- Sedlakova, O., Svastova, E., Takacova, M., Kopacek, J., Pastorek, J. and Pastorekova, S. (2014) Carbonic anhydrase IX, a hypoxia-induced catalytic component of the pH regulating machinery in tumors. *Front Physiol* **4**: 401-414.
- Shah, G. N., Bonapace, G., Hu, P. Y., Strisciuglio, P. and Sly, W. S. (2004) Carbonic anhydrase II deficiency syndrome (osteopetrosis with renal tubular acidosis and brain calcification): Novel mutations in CA2 identified by direct sequencing expand the opportunity for genotype-phenotype correlation. *Human Mutation* **24**: 272-281.
- Shahidzadeh, R., Opekun, A., Shiotani, A. and Graham, D. Y. (2005) Effect of the carbonic anhydrase inhibitor, acetazolamide, on *Helicobacter pylori* infection *in-vivo*: a pilot study. *Helicobacter* **10**: 136-138.
- Sievers, F., Wilm, A., Dineen, D., Gibson, T. J., Karplus, K., Li, W. Z., Lopez, R., McWilliam, H., Remmert, M., Soding, J., Thompson, J. D. and Higgins, D. G. (2011) Fast, scalable generation of high-quality protein multiple sequence alignments using Clustal Omega. *Mol Syst Biol* **7**: 539.
- Sly, W. S., Hewett-Emmett, D., Whyte, M. P., Yu, Y. S. and Tashian, R. E. (1983) Carbonic anhydrase II deficiency identified as the primary defect in the autosomal recessive syndrome of osteopetrosis with renal tubular acidosis and cerebral calcification. *Proc Natl Acad Sci USA* **80**: 2752-2756.
- Smith, K. S., Cosper, N. J., Stalhandske, C., Scott, R. A. and Ferry, J. G. (2000) Structural and kinetic characterization of an archaeal β -class carbonic anhydrase. *J Bacteriol* **182**: 6605-6613.

- Smith, K. S. and Ferry, J. G.** (1999) A plant-type (β -class) carbonic anhydrase in the thermophilic methanoarchaeon *Methanobacterium thermoautotrophicum*. *J Bacteriol* **181**: 6247-6253.
- Smith, K. S., Jakubzick, C., Whittam, T. S. and Ferry, J. G.** (1999) Carbonic anhydrase is an ancient enzyme widespread in prokaryotes. *Proc Natl Acad Sci USA* **96**: 15184-15189.
- So, A. K., Espie, G. S., Williams, E. B., Shively, J. M., Heinhorst, S. and Cannon, G. C.** (2004) A novel evolutionary lineage of carbonic anhydrase (ϵ -class) is a component of the carboxysome shell. *J Bacteriol* **186**: 623-630.
- Steiner, H., Jonsson, B. H. and Lindskog, S.** (1975) Catalytic mechanism of carbonic anhydrase - hydrogen-isotope effects on kinetic parameters of human C isoenzyme. *Eur J Biochem* **59**: 253-259.
- Sterling, D. and Casey, J. R.** (2002) Bicarbonate transport proteins. *Biochem Cell Biol* **80**: 483-497.
- Strop, P., Smith, K. S., Iverson, T. M., Ferry, J. G. and Rees, D. C.** (2001) Crystal structure of the "cab"-type β -class carbonic anhydrase from the archaeon *Methanobacterium thermoautotrophicum*. *J Biol Chem* **276**: 10299-10305.
- Sun, X. Y., Zhang, H. X., Zhang, Z. Y., Wang, Y. and Li, S. J.** (2011) Involvement of a helix-loop-helix transcription factor CHC-1 in CO₂-mediated conidiation suppression in *Neurospora crassa*. *Fungal Genetics and Biology* **48**: 1077-1086.
- Supuran, C. T.** (2008a) Carbonic anhydrases - an overview. *Curr Pharm Des* **14**: 603-614.
- Supuran, C. T.** (2008b) Carbonic anhydrases: novel therapeutic applications for inhibitors and activators. *Nat Rev Drug Discov* **7**: 168-181.
- Supuran, C. T.** (2010a) Carbonic anhydrase inhibition/activation: trip of a scientist around the world in the search of novel chemotypes and drug targets. *Curr Pharm Des* **16**: 3233-3245.
- Supuran, C. T.** (2010b) Carbonic anhydrase inhibitors. *Bioorg Med Chem Lett* **20**: 3467-3674.
- Supuran, C. T.** (2012a) Inhibition of bacterial carbonic anhydrases and zinc proteases: from orphan targets to innovative new antibiotic drugs. *Curr Med Chem* **19**: 831-844.
- Supuran, C. T.** (2012b) Structure-based drug discovery of carbonic anhydrase inhibitors. *J Enzyme Inhib Med Chem* **27**: 759-772.
- Supuran, C. T., Scozzafava, A. and Conway, J.** (2004).CRC enzyme inhibitors series Carbonic Anhydrase: Its inhibitors and activators 1. 1-363, CRC Press.
- Teng, Y. B., Jiang, Y. L., He, Y. X., He, W. W., Lian, F. M., Chen, Y. and Zhou, C. Z.** (2009) Structural insights into the substrate tunnel of *Saccharomyces cerevisiae* carbonic anhydrase Nce103. *BMC Struct Biol* **9**: 67-75.

- Tian, C., Li, J. and Glass, N. L.** (2011) Exploring the bZIP transcription factor regulatory network in *Neurospora crassa*. *Microbiology* **157**: 747-759.
- Tobal, J. M. and Balieiro, M. E.** (2014) Role of carbonic anhydrases in pathogenic microorganisms: a focus on *Aspergillus fumigatus*. *J Med Microbiol* **63**: 15-27.
- Towbin, H., Staehelin, T. and Gordon, J.** (1979) Electrophoretic transfer of proteins from polyacrylamide gels to nitrocellulose sheets: procedure and some applications. *Proc Natl Acad Sci USA* **76**: 4350-4354.
- Tripp, B. C., Bell, C. B., 3rd, Cruz, F., Krebs, C. and Ferry, J. G.** (2004) A role for iron in an ancient carbonic anhydrase. *J Biol Chem* **279**: 6683-6687.
- Tripp, B. C., Smith, K. and Ferry, J. G.** (2001) Carbonic anhydrase: new insights for an ancient enzyme. *J Biol Chem* **276**: 48615-48618.
- Ueda, K., Nishida, H. and Beppu, T.** (2012) Dispensabilities of carbonic anhydrase in proteobacteria. *Int J Evol Biol* **2012**: 1-5.
- van der Klei, I. J. and Veenhuis, M.** (2006) Yeast and filamentous fungi as model organisms in microbody research. *Biochim Biophys* **1763**: 1364-1373.
- Vullo, D., Isik, S., Del Prete, S., De Luca, V., Carginale, V., Scozzafava, A., Supuran, C. T. and Capasso, C.** (2013a) Anion inhibition studies of the α -carbonic anhydrase from the pathogenic bacterium *Vibrio cholerae*. *Bioorg Med Chem Lett* **23**: 1636-1638.
- Vullo, D., Sai Kumar, R. S., Scozzafava, A., Capasso, C., Ferry, J. G. and Supuran, C. T.** (2013b) Anion inhibition studies of a β -carbonic anhydrase from *Clostridium perfringens*. *Bioorg Med Chem Lett* **23**: 6706-6710.
- Watsuji, T. O., Kato, T., Ueda, K. and Beppu, T.** (2006) CO₂ supply induces the growth of *Symbiobacterium thermophilum*, a syntrophic bacterium. *Biosci Biotechnol Biochem* **70**: 753-756.
- Whittington, D. A., Waheed, A., Ulmasov, B., Shah, G. N., Grubb, J. H., Sly, W. S. and Christianson, D. W.** (2001) Crystal structure of the dimeric extracellular domain of human carbonic anhydrase XII, a bitopic membrane protein overexpressed in certain cancer tumor cells. *Proc Natl Acad Sci USA* **98**: 9545-9550.
- Wu, Y. Y., Wang, B. L. and Liu, C. Q.** (2004) Vulnerability studies: *Chlamydomonas reinhardtii*'s influence on the corrosion of rocks in *Geo-Environment: Monitoring, simulation and remediation of the geological environment 1* (J. F. Martín-Duque, C. A. Brebbia, A. E. Godfrey and J. R. Diaz de Teran, eds) pp. 145-149, WIT Press.
- Zimmerman, S. A., Tomb, J. F. and Ferry, J. G.** (2010) Characterization of CamH from *Methanosarcina thermophila*, founding member of a subclass of the γ -class of carbonic anhydrases. *J Bacteriol* **192**: 1353-1360.

6. Appendix

Table S1: Data collection and refinement statistics.

| | CAS1 | CAS2 |
|--|--|--------------------|
| Data collection | | |
| Space group | <i>P</i> 2 ₁ 2 ₁ 2 | <i>F</i> 222 |
| a (Å) | 70.08 | 83.00 |
| b (Å) | 80.72 | 93.90 |
| c (Å) | 82.35 | 97.13 |
| Wavelength (Å) | 0.91841 | 0.82661 |
| Resolution (Å) | 36.2-2.7 (2.8-2.7) | 33.8-1.8 (1.9-1.8) |
| Observed reflections | 46085 (4718) | 70137 (10481) |
| Unique reflections | 13277 (1344) | 16776 (2441) |
| Multiplicity | 3.5 (3.5) | 4.2 (4.3) |
| Completeness (%) | 98.7 (99.7) | 99.2 (99.6) |
| I/σ (σ I) | 8.2 (2.3) | 18.0 (2.4) |
| Rmergea (%) | 19.1 (71.2) ^d | 3.7 (59.9) |
| CC(1/2) b | 97.7 (72.4) | 100.0/79.3 |
| Refinement | | |
| Resolution (Å) | 36.24-2.69 | 33.77-1.83 |
| Rwork (%) | 20.4 (26.8) | 19.1(32.6) |
| Rfreec (%) | 25.1 (31.3) | 21.1 (34.1) |
| Number of atoms/ B average (Å ²) | 3146/40.1 | 1785/48.7 |
| Protein | 2983/40.50 | 1719/48.8 |
| Solvent | 160/33.10 | 65/45.5 |
| Ions | 3/46.38 | 1/32.7 |
| Rmsd from ideal | | |
| Bond length (Å) | 0.005 | 0.010 |
| Bond angles (°) | 0.960 | 1.362 |
| Ramachandran plot (%) | | |
| Favored | 99.49 | 98.10 |
| Outlier | 0.00 | 0.00 |

| | | |
|---------|------|------|
| Allowed | 0.51 | 1.90 |
| PDB id | 4O1J | 4O1K |

Values in this table given in parentheses refer to the outer shell.

^a $R_{\text{merge}} = \sum_{\text{hkl}} \sum_i |I_i(\text{hkl}) - \langle I(\text{hkl}) \rangle| / \sum_{\text{hkl}} \sum_i I_i(\text{hkl})$.

^b Calculated with XSCALE (Karplus and Diederichs 2012).

^c R_{free} factor calculated for 5% randomly chosen reflections not included in the refinement.

^d The elevated Rmerge value is due to high background level of cryo solution and a very small size of the crystal (7x7x40 micron). For comparison the nylon loop used for crystal mounting is 20 microns in diameter.

Table S2: Inhibition constants of anionic inhibitors against α -CA isozymes as well as β -CAs at 20 °C, pH 8.3, by a stopped flow CO₂ hydrase assay (Khalifah 1971).

| | K_I [mM] [#] | | | | | |
|---|-------------------------|--------------------|--------------------|----------------------|-------------------|-------------------|
| | hCA II ^a | SspCA ^b | HpyCA ^c | FbiCA 1 ^d | CAS1 ^e | CAS2 ^e |
| F ⁻ | >300 | 41.7 | 0.67 | 0.71 | >100 | >100 |
| Cl ⁻ | 200 | 8.30 | 0.56 | 0.74 | 9.2 | >100 |
| Br ⁻ | 63 | 49.0 | 0.38 | 0.67 | 9.3 | >100 |
| I ⁻ | 26 | 0.86 | 0.63 | 0.71 | 8.6 | 7.7 |
| CNO ⁻ | 0.03 | 0.80 | 0.37 | 0.93 | 0.90 | 0.82 |
| SCN ⁻ | 1.60 | 0.71 | 0.68 | 0.83 | 5.4 | 5.6 |
| CN ⁻ | 0.02 | 0.79 | 0.54 | 0.62 | 0.94 | 0.75 |
| N ₃ ⁻ | 1.51 | 0.49 | 0.80 | 0.46 | >100 | 6.1 |
| HCO ₃ ⁻ | 85 | 33.2 | 0.50 | 0.66 | 6.5 | 5.5 |
| CO ₃ ²⁻ | 73 | 39.3 | 0.42 | 0.84 | >100 | 8.8 |
| NO ₃ ⁻ | 35 | 0.86 | 0.78 | 0.78 | >100 | >100 |
| NO ₂ ⁻ | 63 | 0.48 | 0.67 | 0.57 | >100 | >100 |
| HS ⁻ | 0.04 | 0.58 | 0.58 | 0.86 | 0.89 | 8.5 |
| HSO ₃ ⁻ | 89 | 21.1 | 0.63 | 55.3 | 3.3 | 7.3 |
| SnO ₃ ²⁻ | 0.83 | 0.52 | 0.48 | 0.53 | 4.3 | 0.92 |
| SeO ₄ ²⁻ | 112 | 0.57 | 0.65 | 24.5 | 2.4 | 9.2 |
| TeO ₄ ²⁻ | 0.92 | 0.53 | 0.45 | 0.90 | 2.5 | 6.3 |
| P ₂ O ₇ ⁴⁻ | 48.50 | 0.69 | 0.75 | 0.83 | 3.1 | 0.96 |
| V ₂ O ₇ ⁴⁻ | 0.57 | 0.66 | 0.18 | 0.66 | >100 | 1.4 |
| B ₄ O ₇ ²⁻ | 0.95 | 0.67 | 0.68 | 0.86 | 6.7 | 6.9 |
| ReO ₄ ⁻ | 0.75 | 0.80 | 0.82 | 0.52 | 8.2 | >100 |

| | | | | | | |
|---|--------|-------|--------|-------|-------|-------|
| RuO ₄ ⁻ | 0.69 | 0.69 | 1.10 | 26.1 | 3.9 | >100 |
| S ₂ O ₈ ²⁻ | 0.084 | 84.6 | 0.93 | 0.87 | 5.0 | >100 |
| SeCN ⁻ | 0.086 | 0.07 | 0.97 | 0.88 | 2.9 | 9.3 |
| CS ₃ ²⁻ | 0.0088 | 0.06 | 0.21 | 0.06 | 0.79 | >100 |
| Et ₂ NCS ₂ ⁻ | 3.1 | 0.004 | 0.0074 | 0.008 | 0.38 | 0.93 |
| SO ₄ ²⁻ | >200 | 0.82 | 0.57 | 0.62 | >100 | 4.8 |
| ClO ₄ ⁻ | >200 | > 200 | 6.50 | > 200 | > 100 | > 100 |
| BF ₄ ⁻ | >200 | > 200 | > 200 | > 200 | > 100 | > 100 |
| FSO ₃ ⁻ | 0.46 | 0.73 | 0.75 | 0.69 | 0.93 | 8.4 |
| NH(SO ₃) ₂ ²⁻ | 0.76 | 0.75 | 0.70 | 50.9 | 0.88 | 9.2 |
| H ₂ NSO ₂ NH ₂ | 1.13 | 0.009 | 0.072 | 0.004 | 0.084 | 0.048 |
| H ₂ NSO ₃ H | 0.39 | 0.042 | 0.094 | 0.005 | 0.069 | 0.072 |
| Ph-B(OH) ₂ | 23.1 | 0.041 | 0.073 | 0.008 | 0.009 | 0.056 |
| Ph-AsO ₃ H ₂ | 49.2 | 0.005 | 0.092 | 0.006 | 0.035 | 0.054 |

hCA II: human α -CA

SspCA: bacterial α -CA from the thermophilic bacterium *Sulfurihydrogenibium yellowstonense*

HpyCA: β -CA from the bacterium *H. pylori*

FbiCA 1: β -CA from the plant *Flaveria bidentis*

CAS1 and CAS2: β -CAs from *S. macrospora*

#Errors were in the range of 3-5% of the reported values, from three different assays.

^a (Supuran 2010b; De Simone and Supuran 2012); ^b (De Luca *et al.* 2012); ^c (Nishimori *et al.* 2007); ^d (Monti *et al.* 2013); ^e This work.

7. Acknowledgment – Danksagung

An erster Stelle möchte ich mich bei meiner Doktormutter Frau Prof. Dr. Stefanie Pöggeler bedanken, für das mir entgegengebrachte Vertrauen und die damit verbundene Möglichkeit meine Promotion in ihrer Arbeitsgruppe absolvieren zu können. Ihr stetes Interesse am Fortschreiten der Arbeit, sowie die Möglichkeit meinen wissenschaftlichen Horizont auf nationalen wie internationalen Konferenzen sowie im Rahmen von Kollaborationen zu erweitern, haben maßgeblich zum Gelingen der Arbeit beigetragen. Darüber hinaus haben die vielen wissenschaftlichen und privaten Diskussionen, meine Promotion zu einer wissenswerten und wertvollen Zeit gemacht.

Ich danke den Mitgliedern meines *thesis committees*, Prof. Dr. Gerhard Braus und Prof. Dr. Heinz Neumann, für die Unterstützung sowie die vielen Diskussionen und Ratschläge während der *thesis committees meetings*.

Ein ganz besonderer Dank gilt Dr. Piotr Neumann für seine Hilfe beim kristallisieren, dem „fischen“ der Kristalle sowie für die Aufnahme mehrere Datensätze in Berlin und Hamburg und der anschließenden Auswertung der Kristallstrukturen.

In diesem Zusammenhang möchte ich auch Prof. Dr. Ralf Ficner und Prof. Dr. Gerhard Braus für die Möglichkeit danken, Geräte in ihren Arbeitsgruppen nutzen zu dürfen.

Des Weiteren bedanke ich mich bei Prof. Dr. Claudiu T. Supuran und Dr. Daniela Vullo für die Durchführung der Aktivitäts- und Inhibierungsassays.

Für die finanzielle Unterstützung danke ich der DFG sowie der „Göttinger Graduiertenschule für Neurowissenschaften, Biophysik und Molekulare Biowissenschaften“.

Im Besonderen möchte ich Marie Fiedler, Sabine Riedel und Maximilian Schütter danken, die ihm Rahmen von Praktika und Abschlussarbeiten zu dieser Arbeit beigetragen haben.

Für die Korrektur dieser Arbeit bedanke ich mich sehr herzlich bei Dr. Britta Herzog.

Allen ehemaligen und aktuellen Mitgliedern der Abteilung Genetik eukaryotischer Mikroorganismen danke ich für die angenehme Arbeitsatmosphäre, die vielen gemeinsamen Kuchen und den regen wissenschaftlichen wie privaten Austausch. Im Besonderen danke ich Dr. Yasmine Bernhards, deren Unterstützung ich mir, insbesondere in den ersten Monaten, immer gewiss sein konnte. Ich danke auch Dr. Skander Elleuche für das Überlassen von Plasmiden und Protokollen sowie für seine ständige Diskussionsbereitschaft. Ich danke auch Barbara „Bärbel“ Herbst sowie Gertrud Stahlhut für ihre Unterstützung bei praktischen Experimenten. Natürlich möchte ich auch Dr. Oliver Voigt, Dr. Britta Herzog, Stefan Frey, Antonia Jakobshagen und Eva Reschka für die gemeinsame, angenehme Zeit im Labor danken.

Schließlich möchte ich noch meiner Familie und meinen Freunden und ganz besonders Astrid danken. Sie hat mit ihrer uneingeschränkten Hilfsbereitschaft, den vielfältigen praktischen wie wissenschaftlichen Tipps und ihrer ständigen Motivation, diese Arbeit erst möglich gemacht.

8. Curriculum vitae

Ronny Lehneck

Georg-August-University Göttingen

Institute of Microbiology and Genetics

Department of Genetics of Eukaryotic Microorganisms

Grisebachstraße 8

Göttingen, Germany

E-Mail: rlehne@gwdg.de

Date of Birth: August 6th 1982

Place of Birth: Jena

Nationality: German

Education

| | |
|-----------------|--|
| 1993-2001 | Friedrich-Schiller-Gymnasium Eisenberg (Abitur) |
| 10/2002-03/2004 | Physics student, Friedrich-Schiller-University Jena |
| 10/2004-03/2010 | Biology student, Martin-Luther-University Halle-Wittenberg |
| 03/2010 | Diploma examination |
| 05/2009-03/2010 | Diploma thesis, Martin-Luther-University Halle-Wittenberg Department of General Microbiology "Biochemische Charakterisierung eines neuartigen Glycyl-Radikal-Enzyms aus <i>Escherichia coli</i> " |
| 10/2010-04/2014 | PhD student in the GGNB program <i>Molecular Biology of Cells</i> , Georg-August-University Göttingen Department of Genetics of Eukaryotic Microorganisms "Functional and structural analysis of carbonic anhydrases from the filamentous ascomycete <i>Sordaria macrospora</i> " |

Thesis Committee: Prof. Stefanie Pöggeler, Prof. Gerhard Braus,
Prof. Heinz Neumann

Talks

- 03/2011 VAAM 2011
“Characterization of a putative α -carbonic anhydrase from the filamentous ascomycete *Sordaria macrospora*”
- 07/2013 Retreat of the GGNB program *Molecular Biology of Cells*
“Life without carbonic anhydrases - a challenging task”

Poster

- 09/2011 MBF 2011
“Characterization of a putative α -carbonic anhydrase from the filamentous ascomycete *Sordaria macrospora*”
- 11/2011 GGNB Science Day 2011
“Characterization of a putative α -carbonic anhydrase from the filamentous ascomycete *Sordaria macrospora*”
- 03/2013 FGC 2013
“Functional analysis of carbonic anhydrases from the filamentous ascomycete *Sordaria macrospora*”
- 12/2013 GGNB Science Day 2013
“Functional analysis of carbonic anhydrases from the filamentous ascomycete *Sordaria macrospora*”